

UCSF

UC San Francisco Electronic Theses and Dissertations

Title

A genetic analysis of the left-right asymmetric polarizations and migrations of the Q neuroblasts in caenorhabditis elegans

Permalink

<https://escholarship.org/uc/item/1h2248s0>

Author

Williams, Lisa Ellen

Publication Date

2003

Peer reviewed|Thesis/dissertation

A Genetic Analysis of the Left-Right Asymmetric
Polarizations and Migrations of the Q Neuroblasts
in *Caenorhabditis elegans*

by

Lisa Ellen Williams

DISSERTATION

Submitted in partial satisfaction of the requirements for the degree of

DOCTOR OF PHILOSOPHY

in

Genetics

in the

GRADUATE DIVISIONS

of the

UNIVERSITY OF CALIFORNIA SAN FRANCISCO

and

UNIVERSITY OF CALIFORNIA BERKELEY

Date

University Librarian

Degree Conferred:

Copyright 2003

by

Lisa Ellen Williams

To my family.

PREFACE

First and foremost I must thank Cynthia Kenyon. Her enthusiasm and genuine love of science are an inspiration. I am always impressed by how quickly her mind works and have enjoyed many insightful lab meetings over the years. She also possesses a remarkable talent for seeing the big picture in any project, and can see through a myriad of complexities to get to the heart of any problem. Another wonderful gift Cynthia has is the ability to recruit friendly, helpful, and brilliant people to the lab. During my time in Cynthia's lab, I have been astounded by the intellects of all of my labmates. I also extend hearty thanks to my thesis committee members, Gian Garriga and Grae Davis. They have provided great reassurance and encouragement during my thesis work, and never made fun of me for always being 9 months pregnant at committee meetings. Gian graciously made the trek across the Bay Bridge several times to attend all meetings and my thesis talk – I know this is no mean feat, and I am very grateful.

Having come to UCSF with no background in biology, I have profited greatly from the help of many, many people. Lee Honigberg first worked on the early asymmetry of the Q cells, and I am honoured to be following in his rather large footsteps. He also continued to ask about my work long after he left the lab – he, too, fell under the spell of the Q cells. I am especially grateful to Joy Alcedo and Scott Alper for help with practically every experiment I have done in the lab. Their combined experience and intelligence have been invaluable to me, and I could not have finished my project without them. They have also been excellent lunch buddies and comrades over the years, and have endured my whingeing

almost without complaint. Joy has become important to my children, and I thank her for spending so much time playing and hiking with us. It has been a blast, and I will miss all our coffee/carbohydrate breaks. I have been fortunate enough to share a bay with Lucie Yang and Douglas Crawford. Lucie's determination and thorough approach to her work are an inspiration – she is a true scientist. In addition, her laughter has brightened many a day for me. We have also spent many an hour commiserating about not understanding a damn thing about biology – it helped tremendously to be sharing the steep learning curve with her. Douglas brought back to our bay the relentless political discussions that left on Javier Apfeld's departure. Having Scott and Douglas arguing over my head during 95% of my experiments was both entertaining and thought-provoking. I also thank Jen Whangbo for being an excellent rotation advisor and worm instructor. It was thanks to her that I fell in love with that tiny little nematode. She is a meticulous scientist, and a great friend. She also graciously read my thesis at short notice, and gave the kind of perfect comments that only a true Q expert could give. Natasha Libina and Yung Lie have been fabulous colleagues and friends, and I admire their balanced outlook on life. I must also thank QueeLim Ch'ng for all his humour, gastronomic discussions, and general entertainment – QueeLim, I still don't watch TV. He was also amenable to as much teasing as I could provide.

Bella Albinder, Vera Tenburg and Mara Shopshovich not only prevented the lab from dissolving into utter chaos, but also showed a genuine interest in my life, both professional and personal. Their wisdom, kindness and humour will be missed.

Finally, my family has been my source of strength all my life. My parents have always supported every decision I have ever made, whether wise or not. My father instilled in me the importance of education which has been a source of encouragement for me, although I have taken it somewhat to extremes. My mother inspires me with her positive outlook on life, and I always look forward to talking with her. I can only hope to have found such a wonderful balance in my own life one day. My Aunt Janet has been my second mother during my time here. She has provided a home filled with love, laughter and warmth, as well as great food. She has been a grandmother to my children, and I know they will miss her deeply. I am also filled with gratitude for my brother, John, who has entertained me innumerable times with witty emails and long, thoughtful telephone conversations. I would have called many more times than I did if it weren't for the aching homesickness I always felt after talking to him.....and the daunting phone bills. His brilliance always amazes me - his political and scientific insights are always thought-provoking. Finally, I am indebted to him for his incredibly fast, preternaturally detailed reading of my thesis. He found many mistakes in science as well as grammar, even though he has no biology training.

Bryce, my partner and soulmate, has seen me through the best and worst of times, and has been nothing but 100% supportive. I am especially grateful that he wouldn't hear any talk of my quitting the programme. His own Ph. D. experience has helped him to understand mine, and he has accordingly provided invaluable advice, support, sympathy, and love. I must thank him most of all for our beautiful children. They have filled my life with more love and joy than I could have ever imagined possible. Everything else pales by comparison.

ABSTRACT

A Genetic Analysis of the Left-Right Asymmetric Polarizations and Migrations of the Q Neuroblasts in *Caenorhabditis elegans*.

Lisa Ellen Williams

In *C. elegans*, the QL and QR neuroblasts are bilateral homologs that polarize and migrate in opposite directions along the anterior-posterior body axis. QL and its descendants migrate towards the posterior, whereas QR and its descendants migrate towards the anterior. The netrin receptor UNC-40 and the novel transmembrane protein DPY-19 are required for the early asymmetry of the Q cells. The Hox gene *mab-5* is expressed in QL, but not QR, and is necessary and sufficient for the posterior migrations of cells in the QL lineage.

This work describes a genetic screen to identify new genes involved in the migrations of the Q neuroblasts. A set of new mutants is described (*qid-5*, *qid-6*, *qid-7*, *qid-8* and *qid-9*) that primarily disrupt the migrations of the QL descendants. Most of these mutants were defective in *mab-5* expression in the QL lineage, and might identify genes that interact directly or indirectly with the EGL-20/Wnt signaling pathway. In one of these mutants, the migrations in the QL lineage were defective even though *mab-5* was still expressed in these cells; this mutation could identify a candidate *mab-5* target.

The screen also identified mutants with defects in the migrations of both the QL and QR lineages. Two of these genes, *mig-21* and *ptp-3*, were characterized and were found to be required for the asymmetric polarizations

and migrations of the Q cells. *mig-21* was cloned and found to encode a novel transmembrane protein that is specifically expressed in the Q cells during their migrations. Thus, MIG-21 may act as a receptor within the Q cells to guide their migrations. Finally, *mig-15*, a STE20/NIK ortholog, was characterized and found to be required for the migrations, but not the polarizations, of the Q cells. *mig-15* also appears to be required for *mab-5* expression specifically in the QL lineage.

This thesis presents several new components of a genetic pathway for the guidance of Q cell migration, their interactions with previously known components, and suggests a model for how the genes may function in the migrations of the Q cells.

PREFACE	iv
ABSTRACT	vii
TABLE OF CONTENTS.....	ix
LIST OF TABLES	xii
LIST OF FIGURES	xiii
CHAPTER 1: Introduction.....	1
INTRODUCTION.....	1
BACKGROUND	3
Neuronal migration during vertebrate development	3
Border cell migration in <i>Drosophila</i>	5
Sex myoblast migration in <i>C. elegans</i>	8
The role of netrins in axon outgrowth and guidance	10
Rho GTPases: rearranging the actin cytoskeleton	13
The migrations of the Q neuroblasts.....	18
THESIS OVERVIEW.....	21
REFERENCES	23
CHAPTER 2: Identification Of Genes That Regulate A Left-Right Asymmetric Neuronal Migration In <i>Caenorhabditis elegans</i>	33
ABSTRACT	33
INTRODUCTION.....	34
RESULTS.....	36
Screening for mutations that disrupt cell migrations in the Q lineages	36
Identification of new genes that disrupt cell migrations in the QL lineage ..	37

Further characterization of the new mutants with abnormal cell migrations in the QL lineage.....	39
Phenotypes of the mutants with cell migration defects in the QL lineage	42
<i>lin-17</i> /Frizzled is required for normal PLM axonal outgrowth	44
DISCUSSION	45
Genes isolated in this screen for cell migration mutants	46
Possible role(s) of these genes in regulating <i>mab-5</i> expression.....	46
Role of <i>qid-7</i> in potentiating or executing <i>mab-5</i> function	49
Conclusion.....	50
EXPERIMENTAL PROCEDURES	51
ACKNOWLEDGMENTS.....	62
REFERENCES	82
CHAPTER 3: The Roles Of The Genes <i>mig-21</i> , <i>ptp-3</i> , and <i>mig-15</i> In Establishing the Left-Right Asymmetry of Q Neuroblast Migration In <i>C. elegans</i>	87
ABSTRACT	87
INTRODUCTION.....	88
RESULTS	92
<i>mig-21</i> and <i>ptp-3</i> are required for asymmetric Q cell polarization and migration	92
Q cells can change direction of polarization in <i>mig-21</i> and <i>ptp-3</i> mutant animals	93
<i>mig-15</i> is required for Q cell migration but is not required for polarization.	93
The migrations of the Q.pax cells are defective in <i>mig-21</i> , <i>ptp-3</i> , and <i>mig-15</i> mutant animals	94

<i>mab-5</i> is required for the Q descendants to remain in the posterior in <i>mig-21</i> , <i>ptp-3</i> , and <i>mig-15</i> mutants	94
Mutations in <i>mig-21</i> specifically disrupt Q cell migration, whereas mutations in <i>ptp-3</i> affect other neuronal migrations	95
Mutations in <i>unc-40</i> and <i>ptp-3</i> enhance the Q descendant migration phenotype of <i>mig-21</i> mutants	96
<i>mig-21</i> encodes a novel transmembrane protein with thrombospondin type I domains	97
<i>mig-21</i> is expressed in the Q cells at the time of their migrations	98
DISCUSSION	99
<i>mig-21</i> and <i>ptp-3</i> are required for the early asymmetry of the Q cells	99
The role of <i>mig-15</i> in Q cell migration: cell motility and <i>mab-5</i> expression .	103
A model for Q cell polarization and migration.....	106
EXPERIMENTAL PROCEDURES	107
REFERENCES	139
CHAPTER 4: Future Directions	145
OVERVIEW.....	145
FUTURE DIRECTIONS.....	147
What and where is the Q polarization signal?	147
How do MIG-21 and UNC-40 interact?	149
The role of PTP-3 in guiding the Q cells.....	152
<i>mig-15</i> , cellular motility and the control of <i>mab-5</i> expression.....	154
CONCLUDING REMARKS	156
REFERENCES	157

LIST OF TABLES

Table 2-1. New mutations in known QL and QR cell migration genes	75
Table 2-2. New genes involved in the migrations of cells in the QL lineage	76
Table 2-3. Axon outgrowth phenotypes	77
Table 2-4. Male tail phenotypes	78
Table 2-5. Expression of <i>mab-5::lacZ</i> in QL.d.....	79
Table 2-6. Summary of mutant phenotypes	80

LIST OF FIGURES

Figure 2-1. The left-right asymmetric migrations of the QL and QR lineages.....	63
Figure 2-2. The screen for cell migration mutants.	65
Figure 2-3. The distribution of the final positions of the QL and QR descendants in the cell migration mutants.	67
Figure 2-4. The distribution of the final positions of the migratory neurons BDU, ALM, CAN, and HSN in the cell migration mutants.....	69
Figure 2-5. Cell migration mutants with axon outgrowth defects.....	71
Figure 2-6. A genetic pathway for cell migrations in the QL and QR lineages.....	73
Figure 3-1. The Left-Right Asymmetric Migrations of the QL and QR lineages.	113
Figure 3-2. Polarization and migration of a QL neuroblast in early L1 in a <i>muIs57</i> (<i>scm::GFP::CAAX</i>) animal.	115
Figure 3-3. Migrations of the Q nuclei in N2, <i>mig-21(mu238)</i> , <i>ptp-3(mu256)</i> and <i>mig-15(rh80)</i> animals.	117
Figure 3-4. Polarizations of the Q cells in N2, <i>mig-21(mu238)</i> , <i>ptp-3(mu256)</i> , and <i>mig-15(rh80)</i> animals.	119
Figure 3-5. Polarization of a single Q cell can change over time in <i>mig-21</i> and <i>ptp-3</i> animals.	121
Figure 3-6. Mutations in <i>unc-40</i> or <i>ptp-3</i> synergize with <i>mig-21</i> in Q descendant migration, and <i>mab-5</i> is required for the Q descendants to remain in the posterior in <i>mig-21</i> and <i>ptp-3</i> mutants.	126

Figure 3-7. <i>mig-21</i> encodes a novel single-pass transmembrane protein with two thrombospondin type I domains.	130
Figure 3-8. <i>mig-21</i> is expressed in QL and QR at the time of their migrations. ..	133
Figure 3-9. Models for the origin of asymmetry in Q cell migration.	135
Figure 3-10. A Model for the signal transduction pathway that controls Q neuroblast migration.	137

Chapter One: Introduction

INTRODUCTION

Cell migration is a fascinating and exquisitely complex component of animal and neural development, and a critical component of immune system function and wound healing. Abnormalities in cell migrations during embryogenesis can lead to profound developmental defects or disease, and during adult life can lead to cancer metastasis. The proper regulation and guidance of cell migration is therefore of central importance to development. Investigating cell migration generates a number of questions:

- What induces cells to move? What are the signals, external or internal, that instruct cells to migrate?
- How do cells know which way to go? How is the direction of movement determined?
- How do migratory cells respond to migratory signals? What are the signal transduction pathways required for this response?
- How are these signals relayed to the cytoskeleton to generate cell shape change and movement? How is the cytoskeleton then rearranged appropriately?
- Once migrating, how do cells navigate their way along complex trajectories? For example, how do they choose turning points?
- How do migrating cells know when to stop moving? How are intermediate targets and final destinations recognized?

Numerous model systems have provided invaluable insights into the molecular mechanisms underlying cell motility: these include genetic studies in *C. elegans* and *Drosophila melanogaster*, vertebrate development, and *in vitro* studies of cultured cells such as fibroblasts.

The molecular study of axon outgrowth and guidance has also provided many clues into the mechanisms guiding both cells and growth cones in their journeys (Tessier-Lavigne and Goodman, 1996; Yu and Bargmann, 2001). Axons face many of the same obstacles as migrating cells: detecting a directional signal, responding appropriately to that signal, and mediating this information downstream to remodel the actin cytoskeleton to generate movement or outgrowth. Furthermore, many of the molecular components, from signals to receptors to downstream effectors, are conserved between the two processes, demonstrating that the field of growth cone guidance is rich with information relevant to the field of cell migration.

Below are some examples of systems in which a signaling pathway directing migration has begun to be elucidated. While there is no single mechanism that accounts for the guidance of cell migrations in each of the organisms studied, there is nonetheless a great deal of similarity in how these organisms direct migrating cells to their destinations. Some of the molecules are conserved, although often, where the proteins themselves differ, the paradigms of signal detection and transduction are highly similar. The migrations of neuronal cells in the cerebral cortex during vertebrate development, border cells in *Drosophila*, and sex myoblasts in *C. elegans* are outlined. Also, the netrin pathway and its role in cell and axon guidance is described. A common theme emerging in all studies of cell migration is that the Rho family of small GTPases

is ubiquitously involved in the actin cytoskeletal dynamics that allow the cells to move. Therefore, a description of Rho family GTPases and their role in cell motility is also provided. Finally, an overview of the migrations of the Q neuroblasts and the known mechanisms which guide them, is also presented.

BACKGROUND

Neuronal migration during vertebrate development

The developing nervous system is dependent on the migrations of neurons – it is estimated that most neuronal precursors undergo some kind of directed migration from their point of origin (for reviews, see (Park et al., 2002; Rao et al., 2002). Defects in the migrations of neurons during vertebrate development can result in devastating diseases (Gleeson and Walsh, 2000). As an example, lissencephaly (“smooth brain”) is caused by defects in neural positioning. The clinical manifestations of these defects are severe mental retardation and epilepsy, and afflicted individuals usually die in early childhood (Gupta et al., 2002).

Neuronal migration during vertebrate development can be broadly classified into two modes: radial and tangential (Gupta et al., 2002; Hatten, 2002; Park et al., 2002). This classification is based on the relative directions taken by migratory neuronal precursor cells – radial migrations take place in a direction perpendicular to the surface of the developing brain, whereas tangential migrations occur parallel to the surface of the brain. In recent years, some of the molecular mechanisms controlling radial migrations have become known, and those pathways will be briefly discussed here.

The radial migration of neuronal precursor cells during embryogenesis contributes to the formation of layers in the cerebral cortex. Migrating cells travel along a radial glial system - glial cells act as a guide and provide a pathway for postmitotic neuronal migration. The first population of cells, the Cajal-Retzius cells, generates the preplate. As more cells leave the cerebral cortex and migrate along the glial cells, they split the preplate into an outer layer of Cajal-Retzius cells and the subplate. Subsequent populations of migratory cells then migrate past the subplate to a position just underneath the Cajal-Retzius cells in an "inside-out" manner, with the outermost cells being the latest born and *vice versa*.

Insights into the molecular details of these migrations came from studies of mouse mutants in which the formation of layers in the cerebral cortex is disrupted. In particular, *reeler* mice have defects in the early migrations – the migratory cells fail to invade the preplate and subsequent cortical layering is scrambled. The physical manifestation of this defect is a reeling and stumbling gait. Reelin, the protein encoded by the *reeler* gene, is a large, secreted protein. It is synthesized by the earliest migrating neurons, the Cajal-Retzius cells, consistent with the early disruption in cortical layer formation. Reelin binds to the receptors VLDLR (Very Low Density Lipoprotein Receptor) and ApoE2 and initiates a tyrosine kinase cascade via phosphorylation of the intracellular adaptor *Dab1*, the murine ortholog of Disabled in *Drosophila* (D'Arcangelo et al., 1999; Howell et al., 1997; Sheldon et al., 1997; Ware et al., 1997). Mutations in *Dab1* result in a similar *reeler* phenotype as is observed in *reeler* mutants. *Drosophila* Disabled interacts genetically with Abl, a non-receptor kinase, and

Ena, an adaptor protein implicated in axon outgrowth through regulation of actin cytoskeletal dynamics.

Border cell migration in *Drosophila*

The fruit fly *Drosophila melanogaster* and the nematode *C. elegans* are particularly convenient systems in which to study the genetics of cell migration and axon guidance, and some pathways have been genetically dissected in great detail. The study of border cell migration has shed light on many aspects of cell migration: factors required for the specification of migratory cell fate have been identified, as have molecules required for the guidance of the cells, and some of the downstream effectors and cell motility machinery.

The border cells in *Drosophila* consist of a set of six to ten somatic follicle cells which undergo a two-step migration during oogenesis: the first phase is a posteriorly directed migration, and the second is a dorsally directed migration. These cells originate at the anterior tip of the egg chamber and migrate posteriorly through the middle of the germline-derived nurse cell cluster, stopping at the border between the nurse cells and the oocyte (Montell, 1999). After the border cells reach the oocyte, they then migrate a short distance dorsally toward the germinal vesicle.

In order to initiate migration, the pre-migratory follicle cells must be induced to adopt a migratory cell fate. The earliest known signal providing this information is the cytokine-like molecule Unpaired, which activates the JAK-STAT pathway (Beccari et al., 2002; Silver and Montell, 2001) through the cytokine receptor Domeless (Ghiglione et al., 2002) thus inducing border cell fate.

The timing of border cell migration may be controlled by the hormone ecdysone signaling through a nuclear receptor and the co-receptor Usp (Buszczak et al., 1999), and transcriptional co-factor Taiman (Bai et al., 2000).

Once the migratory fate has been specified, the transcription factor C/EBP and its downstream target, the transcription factor jing, are required for the border cells to initiate their migrations (Liu and Montell, 2001). The dynamic regulation of the small GTPase Ras is also required for this initiation step: Ras is downregulated immediately prior to the initiation of the migrations, although Ras activity is required during the migrations. These changes in Ras activity are essential for the border cells to migrate properly (Lee et al., 1996).

The migrations of the border cells to the oocyte are guided by the RTKs PVR, related to vertebrate PDGF and VEGF, and EGFR (Duchek and Rorth, 2001; Duchek et al., 2001). The guidance cue for the migrations is believed to be the ligand PVF1 produced by the oocyte. This guidance cue is thought to be present in a gradient that provides directional information for the posteriorly migrating cells, as uniform misexpression of either receptor or ligand causes the cells to migrate inefficiently. Dominant-negative forms of the receptors also result in inefficient migrations of the border cells, as well as misdirected migrations, suggesting that these factors are required for guidance rather than motility. These guidance cues induce the first visible sign of cell polarity observed in the border cells: shortly before they initiate their migrations, the cells develop a long cellular extension (Fulga and Rorth, 2002). This protrusion requires spatial information provided by the RTKs as well as adhesion to the substratum. That the extension is a response to the gradient of a spatial cue, rather than acting as a pathfinder sampling the environment for guidance cues, is demonstrated by the

fact that dominant-negative forms of the PVR and EGFR receptors compromise the cell's ability to send out this projection.

The guidance information provided by the RTKs is mediated by Mbc/DOCK180/CED-5 and Rac (Duchek et al., 2001). Mbc is required in the border cells for their migrations, and acts downstream of PVF1. Rac is activated by Mbc, and activated forms of Rac block border cell migration. The second, dorsally-directed, phase of the border cell migrations is guided by EGFR, with the ligand Gurken/TGF- α providing the guidance cue (Duchek and Rorth, 2001). The downstream components of this pathway are as yet unidentified.

Mutations in *DE-cadherin*, nonmuscle myosin II and Cofilin/ADF result in defective border cell migrations, presumably by disrupting the basic cellular movement machinery. The role of myosin in border cell migrations is also reflected in the expression pattern of the regulatory light chain (RLC) of nonmuscle myosin II: the border cells extend projections that stain brightly for RLC, and staining for RLC is brighter in border cells than in the adjacent nurse cells (Edwards and Kiehart, 1996). *DE-Cadherin* is required in both the border cells and the substratum in order for the cells to migrate, indicating a role in regulating the strength or turnover of adhesive complexes. Another intriguing possibility is raised by the observation that homophilic cadherin interactions may contribute to actin polymerization. The link to the actin cytoskeleton is demonstrated by the fact that cofilin/ADF is required for border cell migration. Cofilin/ADF is required for the depolymerization of actin, allowing the treadmilling process which is thought to drive actin-based cell motility.

Sex myoblast migration in *C. elegans*

For a number of reasons, the nematode *Caenorhabditis elegans* is an ideal model organism in which to study cell migration: the nematode is transparent at all stages of development, allowing the real time observation of individual cells as they undertake their migrations *in vivo*; the complete cell lineage is precisely known and invariant, and is amenable to extensive genetic analysis, as the genome is fully sequenced, it exists as a self-fertilizing hermaphrodite and has a short generation time. Various cell migrations take place during *C. elegans* embryonic and post-embryonic development. During embryogenesis, the canal associated neurons (CANs) migrate a short distance posteriorly, the BDU cells undergo short anterior migrations, and the hermaphrodite specific neurons (HSNs) migrate anteriorly. Post-embryonic migrations include the asymmetric migrations of the Q neuroblasts during the first larval stage, and the migrations of the sex myoblasts during the second larval stage.

A hierarchy of localization signals guides the migrations of the sex myoblasts (reviewed in (Chen and Stern, 1998)). The sex myoblasts are mesodermal cells that differentiate to form the sex muscles, a set of vulval and uterine muscles that must be positioned properly to allow them to make functional attachments to the uterus, the vulva, and the lateral hypodermis. The sex myoblasts undergo a precisely controlled migration during larval development: they are born in the posterior body of the worm, and migrate anteriorly to well-defined final positions that flank the center of the gonad. These migrations are controlled by several mechanisms: a gonad-independent mechanism required for the broad anterior migration, a gonad-dependent

attractive mechanism that specifies the precise positioning of the cells at the center of the gonad, and an underlying gonad-dependent repulsive mechanism that is revealed in the absence of the gonad-dependent attractive cues. The gonad-independent guidance mechanism is revealed upon laser ablation of the gonad: in these animals, the sex myoblasts are able to undergo an anterior migration towards the center of the animal. In *unc-53*, *unc-71*, or *unc-73*, *mig-2(gf)* mutants however, these migrations are significantly shortened (Chen et al., 1997). The source and nature of the gonad-independent guidance signal is unknown.

The gonad-dependent migrations are guided by the chemoattractant EGL-17/FGF and its receptor EGL-15/FGFR (Burdine et al., 1997; DeVore et al., 1995). Mutations in either of these genes result in severely posteriorly displaced sex myoblasts (Burdine et al., 1997), indicating that the attractive guidance cue from the gonad is no longer interpreted in these mutants. Laser ablation of the gonad in these mutants results in the restoration of the anterior migrations of the myoblasts, thus there is a repulsive cue that is gonad-derived (Stern and Horvitz, 1991). The presence of both attractive and repulsive guidance cues in these cell migrations raises the possibility that a balance between attraction and repulsion is required for the precise positioning of the sex myoblasts. *egl-17* encodes the chemoattractant FGF, and is expressed by the vulval precursor cell P6.p. This cell is positioned precisely at the stopping point of the sex myoblasts, suggesting that EGL-17 in P6.p acts as an attractive cue to guide the sex myoblasts to their final positions. Consistent with this, *egl-17* expression in P6.p is sufficient (although not necessary) for correct positioning of the sex myoblasts (Burdine et al., 1998). The receptor tyrosine kinase EGL-15/FGFR is presumably the receptor for EGL-17. *egl-15* is expressed in the sex myoblasts as they undergo their migrations, thus

it is a strong candidate as the mediator of EGL-17 signaling in sex myoblast migrations.

The Ras signal transduction pathway mediates FGF receptor signaling, and several components of this pathway have been shown to have a role in sex myoblast migration (Sundaram et al., 1996). Specifically, mutations in the Ras pathway components *let-60/Ras*, *ksr-1*, *lin-45 raf*, *let-537/mek-2* or *sur-1/mpk-1* cause the sex myoblasts to adopt a broader range of final positions than in wild-type animals, illustrating a role for the Ras pathway in the control of the precise positioning of the cells.

The role of netrins in axon outgrowth and guidance

Netrins are secreted, laminin-related proteins that can act either as repulsive or attractive cues in axon outgrowth (Ishii et al., 1992; Wadsworth et al., 1996). Mutations in the *unc-6* gene result in the disruption of many dorsally and ventrally directed axon migrations: for example, the ventral guidance of the AVM, PVM, HSN, PDE, amphid and phasmid axons, and the dorsal guidance of the DA, DB and DD motor axons (Hedgecock et al., 1990). In the *C. elegans* embryo, the netrin UNC-6 is secreted along the ventral surface of the animal and serves as a guidance cue for the circumferential growth of axons either towards, or away from, this source. The vertebrate homologs of UNC-6, the Netrins, were originally purified from chick brain extracts as an axon-outgrowth promoting activity. Vertebrate Netrins are also expressed along the ventral midline of the developing embryo, in floor plate cells and the ventral spinal cord (Kennedy et al., 1994). Netrin deficient mice display defects in commissural axon guidance,

further confirming the role of netrins in circumferential axon outgrowth (Serafini et al., 1996). Recombinant netrin-1 can actively re-orient axon growth, again demonstrating that netrins act instructively rather than permissively in axon guidance. Certain classes of axons are repelled by netrins *in vivo* (Colamarino and Tessier-Lavigne, 1995), thus netrins appear to be bifunctional guidance cues: they can either attract or repel axons depending on the environmental and cellular context.

Shortly after netrins were characterized, UNC-40/ DCC was identified as a potential receptor for mediating netrin function. The *C. elegans* netrin receptor, UNC-40, is expressed in motile cells and pioneering axons, and has been shown to be required cell-autonomously for axon attraction (Chan et al., 1996). *unc-40* encodes a single pass transmembrane protein containing 4 Ig and 3 FNIII repeats in the extracellular domain. Mutations in *unc-40* result in phenotypes strikingly similar to those found in *unc-6* mutants and the phenotypes of double mutants are no more severe than either single mutant (Hedgecock et al., 1990; Honigberg and Kenyon, 2000), suggesting that most UNC-6 attractive activity is mediated through the UNC-40 receptor. One striking exception to this general observation is that of Q neuroblast migration. The migrations of the Q neuroblasts are the only longitudinal migration disrupted in *unc-40* mutants (Hedgecock et al., 1990; Honigberg and Kenyon, 2000), and these migrations do not require the netrin UNC-6 (Honigberg and Kenyon, 2000). The vertebrate UNC-40 homolog, DCC, has been shown to have netrin-binding activity (Keino-Masu et al., 1996), and is expressed on axons in the embryonic CNS as well as motor axons in the peripheral nervous system. DCC mutants have defects in axon guidance and

targeting (Fazeli et al., 1997), commensurate with their role in netrin-mediated axon pathfinding.

UNC-40/DCC is also required for the repulsive activities of netrins (Chan et al., 1996; Colavita and Culotti, 1998; Hong et al., 1999). UNC-5 is also required for many dorsal, but not ventral, cell and axon migrations in *C. elegans*. (Hedgecock et al., 1990): ventral migrations are completely unaffected in *unc-5* mutants. *unc-5* encodes a transmembrane protein with 2 immunoglobulin domains and 2 thrombospondin type I repeats in its extracellular domain (Leung-Hagesteijn et al., 1992), and mosaic analysis reveals that it is required within migrating cells and pioneering neurons. Misexpression of *unc-5* in ALM, PLM, AVM, and PVM is sufficient to reorient the ventral migrations to become dorsally directed in an UNC-6-dependent manner (Hamelin et al., 1993), underscoring the instructive role of UNC-5 in UNC-6-mediated dorsal guidance. Homologs of UNC-5 have also been identified in vertebrates and flies, revealing a conserved role in UNC-6-mediated repulsive axon guidance (Ackerman et al., 1997; Keleman and Dickson, 2001). Experiments using cultured *Xenopus* spinal axons revealed that UNC-5 can convert the attractive netrin response to a repulsive response (Hong et al., 1999), suggesting that UNC-5 can act as a switch between attractive and repulsive responses to netrin. This repulsion requires DCC, and the UNC-5 cytoplasmic domain is sufficient to effect the conversion. Genetic interactions between *unc-40* and *unc-5* suggest that either receptor retains partial function in the absence of the other (Merz et al., 2001), indicating the ability of either receptor to signal independently.

The signaling pathways downstream of the UNC-40 and UNC-5 receptors are just beginning to be elucidated. Experiments using cultured *Xenopus* spinal neurons have demonstrated a role for calcium signaling and cAMP in the netrin pathway (Ming et al., 1997). The chemoattractive response of these neurons towards a source of netrin-1 is converted to a chemorepulsive response when cAMP or PKA levels are lowered (Ming et al., 1997). Thus the cytosolic level of cAMP may determine whether the response to a netrin signal is attractive or repulsive, however whether cAMP signaling mediates the netrin response *in vivo* is still unknown. A role for MAPK signaling has also been reported (Forcet et al., 2002): upon netrin binding to DCC, ERK-1 and ERK-2 are recruited to a DCC receptor complex, and inhibition of ERK-1/2 antagonizes netrin-dependent axon outgrowth. Downstream effectors of netrin signaling must ultimately result in the reorganization of the actin cytoskeleton. Recent results suggest that this link is provided by CED-10/Rac and UNC-115/abLIM. CED-10, UNC-115 and UNC-34/Ena were identified as suppressors of a gain-of-function *unc-40* construct (Gitai et al., 2003), indicating that these proteins may play a role downstream of UNC-40 in relaying signaling information. Furthermore, CED-10 and UNC-115 act in one pathway and in parallel to UNC-34 through distinct UNC-40 interaction domains, implying that UNC-40 may act as a molecular scaffold to deliver signals to the actin cytoskeleton.

Rho GTPases: rearranging the actin cytoskeleton

Rho GTPases have been implicated in a vast array of actin-based cellular processes, including cellular morphology and shape changes, single cell

migration and coordinated cell movements, cell contraction, phagocytosis, proliferation, and regulated secretion (Etienne-Manneville and Hall, 2002). An underlying feature of this extraordinary functional complexity is that a single GTPase, acting as a molecular switch, can regulate multiple signaling pathways. Rho GTPases act as molecular switches by alternating between an active, GTP-bound state, and an inactive, GDP-bound state. Switching between these two states is achieved by the regulatory proteins GEFs (activators) and GAPs (inactivators). In the GTP-bound form, the GTPase is activated and able to mediate responses from the external signals until the bound GTP is hydrolyzed to GDP. This hydrolysis is effected by GAPs (GTPase Activating Proteins). The inactive GTPase is reactivated by GEFs (Guanine Nucleotide Exchange Factor), which replace the bound GDP with cytosolic GTP (Etienne-Manneville and Hall, 2002).

There are three classes of Rho GTPases - rho, rac, and cdc42 - and each mediates a distinct actin-based cellular process. Insights into the role of each protein in cellular motility have been provided by mutant forms of the proteins. Mutants in which the GTP hydrolysis step is compromised render the protein constitutively active. Conversely, mutations which prevent GDP exchange act as dominant negatives (Etienne-Manneville and Hall, 2002). *In vitro* studies on mammalian fibroblasts have demonstrated that each Rho GTPase has a specific effect on actin dynamics. Injection of constitutively active rac1 into Swiss 3T3 fibroblasts results in the formation of the actin-rich lamellipodial protrusions believed to be the driving force for cell movement (Ridley et al., 1992).

Furthermore, inhibition of rac in a wounding assay blocks the formation of these

lamellipodia and can completely prevent cell movement, underscoring the importance of rac in fibroblast motility (Nobes and Hall, 1999). Similarly, injection of constitutively active rho into fibroblasts results in the formation of stress fibers and focal adhesions (Ridley and Hall, 1992). Stress fibers and focal adhesions also form in response to stimulation with growth factors, and this response is blocked when endogenous rho function is inhibited. Finally, injection of cdc42 triggers the formation of highly motile filopodia, followed by the rac-dependent formation of lamellipodia, and the rho-dependent formation of stress fibers. Thus, activation of cdc42 leads to the activation of endogenous rac and endogenous rho in a hierarchical signaling cascade (Nobes and Hall, 1995). Cdc42 appears not to be required for cell motility *per se*, but controls polarity signals required for directed migration (Nobes and Hall, 1999). An example of this is the role of cdc42 in the directed migration of macrophage chemotaxis – without cdc42, the macrophage is unable to recognize the signal gradient, although movement itself is not compromised (Allen et al., 1998): rather than moving in response to a gradient of chemoattractant, the cells moved in a random walk. This appears to be a common theme in the role of cdc42 in cell movement: it is not required for motility *per se*, but enables the cell to sense direction – cdc42 helps the cell to stabilize polarization in one direction, thus generating directional movement.

Signals from the rho family GTPases must be transduced to the actin cytoskeleton to effect rearrangements and motility. One protein family with a key role in this process is the Wiscott-Aldrich syndrome protein (WASP) family, which includes WASP, N-WASP, Scar and WAVE. WASP was first identified as

a *cdc42* interactor by a yeast two-hybrid screen (Aspenstrom et al., 1996), and binding to both *cdc42* and *rac* is dependent on the GTPases being in the GTP-bound conformation. Subsequent studies revealed that WASp and its family members are able to nucleate actin polymerization via the Arp2/3 complex (Machesky et al., 1999), and are activated by binding to activated *cdc42* and PI(4,5)P₂ (Higgs and Pollard, 2000; Prehoda et al., 2000; Rohatgi et al., 2000). Arp2/3 is a 7-protein complex with 2 actin-related proteins (for a recent review, see (Weaver et al., 2003). This complex binds to the side of a pre-existing actin filament and activates the nucleation of a new filament at a 70° angle to the original filament. These new filaments contain free barbed ends from which actin polymerization can proceed. An emerging theme from Arp2/3 studies is that this complex may be activated and may function in multicomponent complexes with signaling proteins, phospholipids and cytoskeletal proteins, effecting the rearrangement of cytoskeletal actin in response to external signals.

Rho family GTPases also play a critical role in axon outgrowth – another example of the molecular and mechanistic conservation between cell movement and axon guidance (Dickson, 2001; Luo et al., 1997). Several independent screens identified *Drosophila* Trio, the homolog of the human GEF Trio, as being critical for photoreceptor and motor axon pathfinding in the developing embryo (Awasaki et al., 2000; Bateman et al., 2000; Liebl et al., 2000; Newsome et al., 2000). Trio is expressed in the developing CNS, and is required in the neurons for proper axon outgrowth. Trio was also identified as an enhancer of the Abl tyrosine kinase mutant phenotype, suggesting a genetic interaction between Trio and Abl. Trio is localized to the plasma membranes and in growth cones,

underscoring its role in actively migrating axons (Newsome et al., 2000). Axon migrations depend on the tight regulation of Trio: both loss of function and gain of function mutations disrupt guidance. The signaling downstream of Trio is through Rac, Pak and Dock – Trio stimulates nucleotide exchange on Rac and interacts genetically with Rac, the kinase Pak, and the downstream effector Dock (Newsome et al., 2000). The *C. elegans* GEF, UNC-73, is also required for axon guidance (Steven et al., 1998; Zipkin et al., 1997). Rac and Rho also interact genetically with PlexB, the *Drosophila* semaphorin receptor. Semaphorins have a well-described role in mediating growth cone collapse and axon repulsion. In *Drosophila*, PlexB binds directly to active Rac and to both active and inactive forms of RhoA (Hu et al., 2001). A similar interaction was found for vertebrate PlexinB1 and Rac1 (Vikis et al., 2000). Gene dosage experiments suggest a model in which PlexB mediates repulsion by coordinating opposite effects on the two small GTPases: Rac output is downregulated by binding to PlexB, whereas RhoA output increases upon PlexB binding (Hu et al., 2001). Studies in *C. elegans* and *Drosophila* have also demonstrated a redundancy in the activities of rac proteins in these organisms (Lundquist et al., 2001; Ng et al., 2002) – loss of function of any one rac protein has no visible phenotype, but removal of all rac function results in widespread axon growth and guidance defects in both the fly and the worm. Similarly, while loss-of-function mutants of *mig-2*, the *C. elegans* small GTPase, have no axon guidance phenotype, mutations resulting in a constitutively active protein have a profound effect on many axon guidance and cell migration processes during development (Zipkin et al., 1997). This suggests that cycling of the GTPase between active and inactive states is essential for its proper function in axon outgrowth.

The migrations of the Q neuroblasts

The Q cells are neuroblasts born in bilaterally symmetric positions along the anterior-posterior axis of the worm. Although the cells are born in the same position, between the lateral seam cells V4 and V5, and undergo an identical set of cell divisions and cell deaths, the two lineages migrate in opposite directions: QR and its descendants migrate towards the anterior whereas QL and its descendants migrate towards the posterior (Chalfie and Sulston, 1981; Sulston and Horvitz, 1977). The left-right asymmetry is evident soon after the Q cells are born. Shortly after hatching, the cells extend long cytoplasmic projections in opposite directions: QR to the anterior and QL to the posterior. The nuclei and cell bodies then migrate into these projections. QR migrates dorsally and anteriorly until it is positioned over the seam cell V4, and QL migrates dorsally and posteriorly until it is over the seam cell V5. Shortly after these migrations are completed, a second left-right asymmetry is apparent: the Hox gene *mab-5* is expressed in QL but not QR. After the initial migration and *mab-5* activation, the Q cells divide, and their daughter cells continue to migrate. The daughter cells undergo an identical pattern of cell division and programmed cell deaths to give rise to three neurons: SDQR, AVM (the QR.pax cells), and AQR (QR.ap) on the right, and SDQL, PVM (the QL.pax cells), and PQR (QL.ap) on the left. The Q descendants stop migrating at stereotypical positions not associated with any obvious anatomical landmarks: on the right, SDQR and AVM migrate into the anterior body region and AQR migrates into the head. Whereas on the left, SDQL and PVM remain in the posterior body region and PQR migrates into the tail.

Recently, several genes have been identified that are required for the various steps in the Q cell migrations. The netrin receptor UNC-40 and the multipass transmembrane receptor DPY-19 are both required for the first step in which asymmetry is apparent (Honigberg and Kenyon, 2000). Mutations in either *unc-40* or *dpy-19* result in an apparent randomization of this polarization – either cell, QL or QR, can polarize in either direction. Furthermore, this polarization is dynamic – a single cell can extend and retract a process and polarize in multiple directions over time. By analogy with the role of UNC-40 in axon guidance, it seems likely that UNC-40 acts as a receptor within the Q cells to receive a signal that instructs the cells to polarize and orients them along the anterior-posterior axis. The identity and nature of this signal are yet to be determined, thus it is unknown whether the asymmetry arises from outside the Q cells (such as an asymmetrically localized signal), or inside the Q cells (each cell may respond differently to a symmetric polarizing signal). The role of DPY-19 in Q cell migration is unclear: a *dpy-19::GFP* construct is expressed weakly in the Q cells and more strongly in surrounding tissue, and its subcellular localization is yet to be determined (Honigberg and Kenyon, 2000). The expression of *mab-5* is also randomized in *unc-40* and *dpy-19* mutants: either cell, QL or QR, can express *mab-5*. Whether or not a Q cell expresses *mab-5* determines the migratory fate of its descendants. Thus, the positions of the Q descendants are also randomized in these mutants (Honigberg and Kenyon, 2000).

Once the Q cells have polarized and marked their preferred direction of migration, the nuclei and cell bodies migrate into these protrusions. These migrations require the cell motility genes *mig-2*, which encodes a small GTPase,

and *unc-73*, the putative GEF for *mig-2* (Honigberg and Kenyon, 2000; Steven et al., 1998; Zipkin et al., 1997). Mutations in either of these genes result in shortened migrations of the cells, but have no effect on their polarizations. These motility genes are therefore not required for the directional sense of the Q cells, but are required for their ability to move.

mab-5 is expressed in QL shortly after this initial migration is completed. *mab-5* is necessary and sufficient for posterior migration of the QL descendants: loss of function mutations in *mab-5* result in anterior migration of the QL lineage and ectopic activation of *mab-5* in a single, anteriorly migrating cell by laser-induced heat-shock causes that cell to stop migrating anteriorly, turn around, and migrate towards the posterior (Harris et al., 1996). Expression of the Hox gene *mab-5* in QL is induced by a canonical Wnt signaling pathway. EGL-20/Wnt is expressed left-right symmetrically in a few cells in the tail of the animal, but QL and QR have distinct responses to its signal: QL appears to be more sensitive to EGL-20 than QR (Whangbo and Kenyon, 1999). Dose-response experiments suggest that high levels of EGL-20 activate the canonical Wnt signaling pathway, resulting in expression of *mab-5* in QL in the wild-type animal. Lower levels of EGL-20 result in the activation of an alternate pathway in QR that results in anterior migration (Whangbo and Kenyon, 1999). The nature of this alternate signaling pathway is a mystery, as is the reason for QL being more sensitive to EGL-20 signaling than QR.

The anterior migrations of the QR descendants require the activities of the Hox gene *lin-39* and Hox cofactors *ceh-20* and *unc-62* (Yang et. al., manuscript in preparation). Mutations in any of these genes shorten the migrations of the

QR.pax cells. The anterior migrations of the QR descendants are controlled in part by the cell-nonautonomous function of MIG-13, a transmembrane protein containing a CUB domain and an LDL receptor domain (Sym et al., 1999). MIG-13 appears to act as a guidance cue for many anteriorly directed migrations along the anterior-posterior axis. The stopping points of the Q cells are controlled by the dose of MIG-13: higher levels of MIG-13 promote anterior migration, and lower levels shift the cells towards the posterior (Sym et al., 1999).

THESIS OVERVIEW

The migrations of the Q neuroblasts can be considered from many different angles: as a question of how cells polarize; how directed migration is achieved; the control of Hox gene expression; or a basic problem of left-right asymmetry. This work has principally considered the question of how cells are instructed to polarize, as some of the other asymmetric aspects of Q migration (directed migration, control of Hox gene expression) can be considered as secondary to this polarization, since they occur after the initial left-right asymmetric polarization. The question of left-right asymmetry is intriguing, and is presumably a consequence of the asymmetry established early in the developing embryo. Unfortunately, the work in this thesis has not identified the underlying basis for the left-right asymmetry of the Q cells. Instead, some of the components of the signaling pathway responsible for Q polarization and motility have been determined.

Chapter two of this work describes a genetic screen undertaken by QueeLim Ch'ng and Mary Sym. This screen isolated mutants in which the Q.pax cells are misplaced, presumably as a result of misguided migrations. The

mutants were characterized, mapped and placed into complementation groups in order to identify new Q migration genes. The class of genes whose primary defect is in the migrations of the QL.pax cells is described here.

Chapter three of this work describes the characterization of three genes: *mig-21* and *ptp-3*, isolated in the aforementioned Q descendant migration screen; and a candidate gene *mig-15*. These genes have defects in the positions of the Q.pax cells on both left and right sides of the animal. This apparent randomization suggested that they may play a role in the early asymmetry of the Q cells. The cloning and expression pattern of *mig-21* is also presented in this chapter.

Chapter four describes some of the conclusions of this work, and offers some suggestions for future experiments which may help to elucidate the signaling pathways responsible for Q cell migration.

REFERENCES

- Ackerman, S. L., Kozak, L. P., Przyborski, S. A., Rund, L. A., Boyer, B. B. and Knowles, B. B.** (1997). The mouse rostral cerebellar malformation gene encodes an UNC-5-like protein. *Nature* **386**, 838-842.
- Allen, W. E., Zicha, D., Ridley, A. J. and Jones, G. E.** (1998). A Role for Cdc42 in Macrophage Chemotaxis. *The Journal of Cell Biology* **141**, 1147-1157.
- Aspenstrom, P., Lindberg, U. and Hall, A.** (1996). Two GTPases, Cdc42 and Rac, bind directly to a protein directly implicated in the immunodeficiency disorder Wiskott-Aldrich syndrome. *Current Biology* **6**, 70-75.
- Awasaki, T., Saito, M., Sone, M., Suzuki, E., Sakai, R., Ito, K. and Hama, C.** (2000). The *Drosophila* Trio Plays an Essential Role in Patterning of Axons by Regulating Their Directional Extension. *Neuron* **26**, 119-131.
- Bai, J., Uehara, Y. and Montell, D. J.** (2000). Regulation of Invasive Cell Behavior by Taiman, a *Drosophila* Protein Related to AIB1, a Steroid Receptor Coactivator Amplified in Breast Cancer. *Cell* **103**, 1047-1058.
- Bateman, J., Shu, H. and Van Vactor, D.** (2000). The Guanine Nucleotide Exchange Factor Trio Mediates Axonal Development in the *Drosophila* Embryo. *Neuron* **26**, 93-106.
- Beccari, S., Teixeira, L. and Rorth, P.** (2002). The JAK/STAT pathway is required for border cell migration during *Drosophila* oogenesis. *Mechanisms of Development* **111**, 115-123.

Burdine, R. D., Branda, C. S. and Stern, M. J. (1998). EGL-17(FGF) expression coordinates the attraction of the migrating sex myoblasts with vulval induction in *C. elegans*. *Development* **125**, 1083-93.

Burdine, R. D., Chen, E. B., Kwok, S. F. and Stern, M. J. (1997). egl-17 encodes an invertebrate fibroblast growth factor family member required specifically for sex myoblast migration in *Caenorhabditis elegans*. *Proc Natl Acad Sci U S A* **94**, 2433-7.

Buszczak, M., Freeman, M. R., Carlson, J. R., Michael, B., Cooley, L. and Segraves, W. A. (1999). Ecdysone response genes govern egg chamber development during mid-oogenesis in *Drosophila*. *Development* **126**, 4581-4589.

Chalfie, M. and Susslon, J. (1981). Developmental Genetics of the mechanosensory neurons of *Caenorhabditis elegans*. *Developmental Biology* **82**, 358-370.

Chan, S. S., Zheng, H., Su, M. W., Wilk, R., Killeen, M. T., Hedgecock, E. M. and Culotti, J. G. (1996). UNC-40, a *C. elegans* homolog of DCC (Deleted in Colorectal Cancer), is required in motile cells responding to UNC-6 netrin cues. *Cell* **87**, 187-95.

Chen, E. B., Branda, C. S. and Stern, M. J. (1997). Genetic enhancers of *sem-5* define components of the gonad-independent guidance mechanism controlling sex myoblast migration in *Caenorhabditis elegans* hermaphrodites. *Dev Biol* **182**, 88-100.

Chen, E. B. and Stern, M. J. (1998). Understanding cell migration guidance: lessons from sex myoblast migration in *C. elegans*. *Trends in Genetics* **14**, 322-327.

Colamarino, S. A. and Tessier-Lavigne, M. (1995). The Axonal Chemoattractant Netrin-1 Is Also a Chemorepellent for Trochlear Motor Axons. *Cell* **81**, 621-629.

- Colavita, A. and Culotti, J. G.** (1998). Suppressors of Ectopic UNC-5 growth cone steering identify eight genes involved in axon guidance in *Caenorhabditis elegans*. *Developmental Biology* **194**, 72-85.
- D'Arcangelo, G., Homayouni, R., Keshvara, L., Rice, D. S., Sheldon, M. and Curran, T.** (1999). Reelin is a Ligand for Lipoprotein Receptors. *Neuron* **24**, 471-479.
- DeVore, D. L., Horvitz, H. R. and Stern, M. J.** (1995). An FGF receptor signaling pathway is required for the normal cell migrations of the sex myoblasts in *C. elegans* hermaphrodites. *Cell* **83**, 611-20.
- Dickson, B. J.** (2001). Rho GTPases in growth cone guidance. *Current Opinion in Cell Biology* **11**, 103-110.
- Duchek, P. and Rorth, P.** (2001). Guidance of cell migration by EGF receptor signaling during *Drosophila* oogenesis. *science* **291**, 131-3.
- Duchek, P., Somogyi, K., Jekely, G., Beccari, S. and Rorth, P.** (2001). Guidance of Cell Migration by the *Drosophila* PDGF/VEGF Receptor. *Cell* **107**, 17-26.
- Edwards, K. A. and Kiehart, D. P.** (1996). *Drosophila* nonmuscle myosin II has multiple essential roles in imaginal disc and egg chamber morphogenesis. *Development* **122**, 1499-1511.
- Etienne-Manneville, S. and Hall, A.** (2002). Rho GTPases in cell biology. *Nature* **420**, 629-635.
- Fazeli, A., Dickinson, S. L., Hermiston, M. L., Tighe, R. V., Steen, R. G., Small, C. G., Stoeckli, E. T., Keino-Masu, K., Masu, M., Rayburn, H. et al.** (1997). Phenotype of mice lacking functional *Deleted in colorectal cancer (Dcc)* gene. *Nature* **386**, 796-804.

- Forcet, C., Stein, E., Pays, L., Corset, V., Llambi, F., Tessier-Lavigne, M. and Mehlen, P. (2002).** Netrin-1-mediated axon outgrowth requires deleted in colorectal cancer-dependent MAPK activation. *Nature* **417**, 443-447.
- Fulga, T. A. and Rorth, P. (2002).** Invasive cell migration is initiated by guided growth of long cellular extensions. *Nature Cell Biology* **4**, 715-719.
- Ghiglione, C., Devergne, O., Georgenthum, E., Carballes, F., Medioni, C., Cerezo, D. and Noselli, S. (2002).** The *Drosophila* cytokine receptor Domeless controls border cell migration and epithelial cell polarization during oogenesis. *Development* **129**, 5437-5447.
- Gitai, Z., Yu, T. W., Lundquist, E. A., Tessier-Lavigne, M. and Bargmann, C. I. (2003).** The Netrin Receptor UNC-40/DCC Stimulates Axon Attraction and Outgrowth through Enabled and, in Parallel, Rac and UNC-115/AbLIM. *Neuron* **37**, 53-65.
- Gleeson, J. G. and Walsh, C. A. (2000).** Neuronal migration disorders: from genetic diseases to developmental mechanisms. *Trends in Neurosciences* **23**, 352-359.
- Gupta, A., Tsai, L.-H. and Wynshaw-Boris, A. (2002).** Life is a Journey: A Genetic Look at Neocortical Development. *Nature Reviews Genetics* **3**, 342-355.
- Hamelin, M., Zhou, Y., Su, M. W., Scott, I. M. and Culotti, J. G. (1993).** Expression of the UNC-5 guidance receptor in the touch neurons of *C. elegans* steers their axons dorsally. *Nature* **364**, 327-30.
- Harris, J., Honigberg, L., Robinson, N. and Kenyon, C. (1996).** Neuronal cell migration in *C. elegans*: regulation of Hox gene expression and cell position. *Development* **122**, 3117-31.

- Hatten, M. E.** (2002). New Directions in Neuronal Migration. *science* **297**, 1660-1663.
- Hedgecock, E. M., Culotti, J. G. and Hall, D. H.** (1990). The *unc-5*, *unc-6*, and *unc-40* genes guide circumferential migrations of pioneer axons and mesodermal cells on the epidermis in *C. elegans*. *Neuron* **4**, 61-85.
- Higgs, H. N. and Pollard, T. D.** (2000). Activation by Cdc42 and PIP₂ of Wiscott-Aldrich Syndrome protein (WASP) Stimulates Actin Nucleation by Arp2/3 Complex. *The Journal of Cell Biology* **150**, 1311-1320.
- Hong, K., Hinck, L., Nishiyama, M., Poo, M. M., Tessier-Lavigne, M. and Stein, E.** (1999). A ligand-gated association between cytoplasmic domains of UNC5 and DCC family receptors converts netrin-induced growth cone attraction to repulsion. *Cell* **97**, 927-41.
- Honigberg, L. and Kenyon, C.** (2000). Establishment of left/right asymmetry in neuroblast migration by UNC-40/DCC, UNC-73/Trio and DPY-19 proteins in *C. elegans*. *Development* **127**, 4655-68.
- Howell, B. W., Hawkes, R., Soriano, P. and Cooper, J. A.** (1997). Neuronal position in the developing brain is regulated by mouse *disabled-1*. *Nature* **389**, 733-737.
- Hu, H., Marton, T. F. and Goodman, C. S.** (2001). Plexin B Mediates Axon Guidance in *Drosophila* by Simultaneously Inhibiting Active Rac and Enhancing RhoA Signaling. *Neuron* **32**, 39-51.
- Ishii, N., Wadsworth, W. G., Stern, B. D., Culotti, J. G. and Hedgecock, E. M.** (1992). UNC-6, a laminin-related protein, guides cell and pioneer axon migrations in *C. elegans*. *Neuron* **9**, 873-81.

Keino-Masu, K., Masu, M., Hinck, L., Leonardo, E. D., Chan, S. S., Culotti, J. G. and Tessier-Lavigne, M. (1996). Deleted in Colorectal Cancer (DCC) encodes a netrin receptor. *Cell* **87**, 175-85.

Keleman, K. and Dickson, B. J. (2001). Short- and Long-Range Repulsion by the *Drosophila* Unc5 Netrin Receptor. *Neuron* **32**, 605-617.

Kennedy, T. E., Serafini, T., de la Torre, J. R. and Tessier-Lavigne, M. (1994). Netrins are diffusible chemotropic factors for commissural axons in the embryonic spinal cord. *Cell* **78**, 425-35.

Lee, T., Feig, L. and Montell, D. J. (1996). Two distinct roles for Ras in a developmentally regulated cell migration. *Development* **122**, 409-418.

Leung-Hagesteijn, C., Spence, A. M., Stern, B. D., Zhou, Y., Su, M. W., Hedgecock, E. M. and Culotti, J. G. (1992). UNC-5, a transmembrane protein with immunoglobulin and thrombospondin type 1 domains, guides cell and pioneer axon migrations in *C. elegans*. *Cell* **71**, 289-99.

Liebl, E. C., Forsthoefel, D. J., Franco, L. S., Sample, S. H., Hess, J. E., Cowger, J. A., Chandler, M. P., Shupert, A. M. and A., S. M. (2000). Dosage-Sensitive, Reciprocal Genetic Interactions between the *Abl* Tyrosine Kinase and the Putative GEF *trio*'s Role in Axon Pathfinding. *Neuron* **26**, 107-118.

Liu, Y. and Montell, D. J. (2001). *jing*: a downstream target of *slbo* required for developmental control of border cell migration. *Development* **128**, 321-330.

Lundquist, E. A., Reddien, P. W., Hartweg, E., Horvitz, H. R. and Bargmann, C. I. (2001). Three *C. elegans* Rac proteins and several alternative Rac regulators control axon guidance, cell migration and apoptotic cell phagocytosis. *Development* **128**, 4475-4488.

- Luo, L., Jan, L. Y. and Jan, Y.-N.** (1997). Rho family small GTP-binding proteins in growth cone signaling. *Current Opinion in Neurobiology* 7, 81-86.
- Machesky, L. M., Mullins, R. D., Higgs, H. N., Kaiser, D. A., Blanchoin, L., May, R. C., Hall, M. E. and Pollard, T. D.** (1999). Scar, a WASp-related protein, activates nucleation of actin filaments by the Arp2/3 complex. *Proc Natl Acad Sci U S A* 96, 3739-3744.
- Merz, D. C., Zheng, H., Killeen, M. T., Krizus, A. and Culotti, J. G.** (2001). Multiple Signaling Mechanisms of the UNC-6/netrin Receptors UNC-5 and UNC-40/DCC *in vivo*. *Genetics* 158, 1071-1080.
- Ming, G. L., Song, H. J., Berninger, B., Holt, C. E., Tessier-Lavigne, M. and Poo, M. M.** (1997). cAMP-dependent growth cone guidance by netrin-1. *Neuron* 19, 1225-35.
- Montell, D. J.** (1999). The genetics of cell migration in *Drosophila melanogaster* and *Caenorhabditis elegans* development. *Development* 126, 3035-3046.
- Newsome, T. P., Schmidt, S., Dietzl, G., Keleman, K., Asling, B., Debant, A. and Dickson, B. J.** (2000). Trio Combines with Dock to Regulate Pak Activity during Photoreceptor Axon Pathfinding in *Drosophila*. *Cell* 101, 283-294.
- Ng, J., Nardine, T., Harms, M., Tzu, J., Goldstein, A., Sun, Y., Dietzl, G., Dickson, B. J. and Luo, L.** (2002). Rac GTPases control axon growth, guidance and branching. *Nature* 416, 442-447.
- Nobes, C. D. and Hall, A.** (1995). Rho, Rac and Cdc42 GTPases Regulate the Assembly of Multimolecular Focal Complexes Associated with Actin Stress Fibers, Lamellipodia, and Filopodia. *Cell* 81, 53-62.
- Nobes, C. D. and Hall, A.** (1999). Rho GTPases Control Polarity, Protrusion, and Adhesion during Cell Movement. *The Journal of Cell Biology* 144, 1235-1244.

- Park, H. T., Wu, J. and Rao, Y. (2002).** Molecular control of neuronal migration. *BioEssays* **24**, 821-827.
- Prehoda, K. E., Scott, J. A., Mullins, R. D. and Lim, W. (2000).** Integration of Multiple Signals Through Cooperative Regulation of the N-WASP-Arp2/3 Complex. *science* **290**, 801-806.
- Rao, Y., Wong, K., Ward, M., Jurgensen, C. and Wu, J. Y. (2002).** Neuronal migration and molecular conservation with leukocyte chemotaxis. *Genes and Development* **16**, 2973-2984.
- Ridley, A. J. and Hall, A. (1992).** The Small GTP-Binding Protein rho Regulates the Assembly of Focal Adhesions and Actin Stress Fibers in Response to Growth Factors. *Cell* **70**, 389-399.
- Ridley, A. J., Paterson, H. F., Johnston, C. L., Diekmann, D. and Hall, A. (1992).** The Small GTP-Binding Protein rac Regulates Growth Factor-Induced Membrane Ruffling. *Cell* **70**, 401-410.
- Rohatgi, R., Ho, H.-y. H. and Kirschner, M. W. (2000).** Mechanism of N-WASP Activation by CDC42 and Phosphatidylinositol 4,5-biphosphate. *The Journal of Cell Biology* **150**, 1299-1309.
- Serafini, T., Colamarino, S. A., Leonardo, E. D., Wang, H., Beddington, R., Skarnes, W. C. and Tessier-Lavigne, M. (1996).** Netrin-1 is required for commissural axon guidance in the developing vertebrate nervous system. *Cell* **87**, 1001-14.
- Sheldon, M., Rice, D. S., D'Arcangelo, G., Yoneshima, H., Nakajima, K., Howell, B. W., Cooper, J. A., Goldowitz, D. and Curran, T. (1997).** *Scrambler* and *yotari* disrupt the *disabled* gene and produce a *reeler*-like phenotype in mice. *Nature* **389**, 730-733.

Silver, D. L. and Montell, D. J. (2001). Paracrine Signaling through the JAK/STAT Pathway Activates Invasive Behavior of Ovarian Epithelia Cells in *Drosophila*. *Cell* **107**, 831-841.

Stern, M. J. and Horvitz, H. R. (1991). A normally attractive cell interaction is repulsive in two *C. elegans* mesodermal cell migration mutants. *Development* **113**, 797-803.

Steven, R., Kubiseski, T. J., Zheng, H., Kulkarni, S., Mancillas, J., Ruiz Morales, A., Hogue, C. W., Pawson, T. and Culotti, J. (1998). UNC-73 activates the Rac GTPase and is required for cell and growth cone migrations in *C. elegans*. *Cell* **92**, 785-95.

Sulston, J. E. and Horvitz, H. R. (1977). Post-embryonic cell lineages of the nematode, *Caenorhabditis elegans*. *Dev Biol* **56**, 110-56.

Sundaram, M., Yochem, J. and Han, M. (1996). A Ras-mediated signal transduction pathway is involved in the control of sex myoblast migration in *Caenorhabditis elegans*. *Development* **122**, 2823-2833.

Sym, M., Robinson, N. and Kenyon, C. (1999). MIG-13 positions migrating cells along the anteroposterior body axis of *C. elegans*. *Cell* **98**, 25-36.

Tessier-Lavigne, M. and Goodman, C. S. (1996). The molecular biology of axon guidance. *science* **274**, 1123-33.

Vikis, H. G., Li, W., He, Z. and Guan, K.-L. (2000). The semaphorin receptor plexin-B1 specifically interacts with active Rac in a ligand-dependent manner. *Proc Natl Acad Sci U S A* **97**, 12457-12462.

Wadsworth, W. G., Bhatt, H. and Hedgecock, E. M. (1996). Neuroglia and pioneer neurons express UNC-6 to provide global and local netrin cues for guiding migrations in *C. elegans*. *Neuron* **16**, 35-46.

Ware, M. L., Fox, J. W., Gonzalez, J. L., Davis, N. M., Lambert de Rouvroit, C., Russo, C. J., Chua, S. C., Jr, Goffinet, A. M. and Walsh, C. A. (1997). Aberrant Splicing of a Mouse *disabled* Homolog, *mdab1*, in the *scrambler* Mouse. *Neuron* **19**, 239-249.

Weaver, A. M., Young, M. E., Lee, W.-L. and Cooper, J. A. (2003). Integration of signals to the Arp2/3 complex. *Current Opinion in Cell Biology* **15**, 23-30.

Whangbo, J. and Kenyon, C. (1999). A Wnt signaling system that specifies two patterns of cell migration in *C. elegans*. *Mol Cell* **4**, 851-8.

Yu, T. and Bargmann, C. I. (2001). Dynamic regulation of axon guidance. *Nature Neuroscience* **4**, 1169-1176.

Zipkin, I. D., Kindt, R. M. and Kenyon, C. J. (1997). Role of a new Rho family member in cell migration and axon guidance in *C. elegans*. *Cell* **90**, 883-94.

Chapter Two: Identification Of Genes That Regulate A Left-Right Asymmetric Neuronal Migration In *Caenorhabditis elegans*

ABSTRACT

In *C. elegans*, cells of the QL and QR neuroblast lineages migrate with left-right asymmetry; QL and its descendants migrate posteriorly whereas QR and its descendants migrate anteriorly. One key step in generating this asymmetry is the expression of the Hox gene *mab-5* in the QL descendants but not in the QR descendants. The observed asymmetry appears to be coupled to the asymmetric polarizations and movements of QL and QR as they migrate, and relies on an asymmetric response to an EGL-20/Wnt signal. To identify genes involved in these complex layers of regulation and to isolate targets of *mab-5* that direct posterior migrations, a visual screen for mutants with cell migration defects in the QL and QR lineages was performed. A set of new mutants is described (*qid-5*, *qid-6*, *qid-7*, *qid-8* and *qid-9*) that primarily disrupt the migrations of the QL descendants. Most of these mutants were defective in *mab-5* expression in the QL lineage, and might identify genes that interact directly or indirectly with the EGL-20/Wnt signaling pathway. In one of these mutants, the migrations in the QL lineage were defective even though *mab-5* was still expressed in these cells; this mutation could identify a candidate *mab-5* target.

INTRODUCTION

How migratory cells select one of many possible migratory programs to adopt a specific trajectory is a central question in developmental biology. In *Caenorhabditis elegans*, the QL and QR neuroblasts are left-right homologs that divide identically to give rise to the same neuron types, but that migrate in opposite directions (Sulston and Horvitz, 1977) (Figure 2-1). On the left, QL and its descendants migrate posteriorly, whereas on the right, QR and its descendants migrate anteriorly. A key determinant of patterning this left-right asymmetric migration is the expression of the Hox gene *mab-5* in the QL descendants, but not in the QR descendants. Thus, Q neuroblast migration in *C. elegans* is a convenient system in which to study how left-right asymmetry and Hox gene regulation intersect and affect cell migration.

The first step in these migrations involves the polarizations of the QL and QR neuroblasts and their subsequent movements over a short distance: QL moves dorsally and to the posterior, whereas QR moves dorsally and to the anterior. These migrations are the first visible manifestations of left-right asymmetry between these cell lineages. UNC-40 (the *C. elegans* netrin receptor) (Chan et al., 1996) and DPY-19 (a novel multipass transmembrane protein) are required to ensure that the QL and QR neuroblasts polarize in the correct direction during these migrations (Honigberg and Kenyon, 2000).

The QL-specific expression of *mab-5* begins during QL migration. Correct *mab-5* expression may be dependent on the proper polarizations and movements of the Q neuroblasts: in *unc-40* and *dpy-19* mutants, QL and QR not only polarize randomly but also express *mab-5* randomly (Honigberg and Kenyon, 2000). After their migrations, QL and QR divide. *mab-5* is expressed at high levels in the QL

descendants and is not expressed in the QR descendants (Figure 2-1B). *mab-5* specifies a posterior program of cell migration; in *mab-5(-)* mutants, the descendants of QL migrate anteriorly like the descendants of QR (Harris et al., 1996; Kenyon, 1986; Salser and Kenyon, 1992). In contrast, in wild-type animals, the descendants of QR do not turn on *mab-5* and therefore migrate anteriorly (Salser and Kenyon, 1992). If *mab-5* is inappropriately expressed in the QR descendants they migrate posteriorly (Salser and Kenyon, 1992), reinforcing the idea that the expression of *mab-5* acts as a critical switch between anterior and posterior migration.

Left-right asymmetry in *mab-5* expression is due to a left-right asymmetric response to a *C. elegans* Wnt signal encoded by the *egl-20* gene (Whangbo and Kenyon, 1999). The QL descendants are more sensitive to the EGL-20/Wnt signal than the QR descendants, and respond to this signal by turning on *mab-5* expression through the activity of a conserved, canonical Wnt signal transduction pathway (Eisenmann et al., 1998; Harris et al., 1996; Herman, 2001; Korswagen et al., 2002; Maloof et al., 1999; Sawa et al., 1996). In contrast, the QR descendants respond by migrating anteriorly (Whangbo and Kenyon, 1999). The alternate signaling pathway that mediates this second EGL-20/Wnt response is not well understood. Dose-response experiments indicate that high levels of EGL-20/Wnt activate the canonical Wnt pathway, while low levels signal through the alternate Wnt pathway (Whangbo and Kenyon, 1999). By utilizing different EGL-20/Wnt-dependent pathways that specify different migratory responses in the QL and QR lineages, the initial left-right asymmetry between these cells is maintained.

There are many molecular details that need to be elucidated in order to fully understand the complex but precise migrations of the cells in the QL and QR lineages. How the migrations of the QL and QR descendants are specified is unknown, as is the reason for cells of the QL lineage being more sensitive to given levels of EGL-20/Wnt than cells of the QR lineage. How *mab-5* expression might be coupled to the left-right asymmetric polarizations of the QL and QR cells is also a mystery. Whether *mab-5* expression is targeted to the QL lineage by dedicated pathway(s) or is regulated as part of a process that specifies the entire region-specific pattern of *mab-5* expression in the posterior is also not yet clear. Also, the genes that act downstream of *mab-5* to cause the descendants of QL to migrate posteriorly remain unidentified.

To resolve these uncertainties, a genetic screen to identify new genes required for these cell migrations was designed. The set of mutants, *qid-5*, *qid-6*, *qid-7*, *qid-8* and *qid-9* (for Q is defective), that primarily disrupt the migrations of cells of the QL lineage is described here. Characterization of these *qid* mutants indicated that the identified genes affect the expression, and possibly the function, of *mab-5* in the QL lineage.

RESULTS

Screening for mutations that disrupt cell migrations in the Q lineages

Previous genetic screens for mutants defective in the migrations of cells within the QL and QR lineages relied on screening at high magnification to locate the positions of the neurons generated by QL and QR (Du and Chalfie, 2001; Harris et al., 1996; Sym et al., 1999; Wang et al., 1993). These screens were laborious

because they required either mounting animals on slides for viewing at high magnification, or β -galactosidase staining.

To screen for mutants that disrupt the migrations of QL, QR and/or their descendants rapidly, animals bearing a chromosomally integrated *mec-7::GFP* fusion that expressed GFP at high levels were used. This GFP fusion is expressed specifically in six mechanosensory neurons (Chalfie et al., 1994), including one QL descendant (PVM) and one QR descendant (AVM) (Figure 2-2). These GFP-expressing neurons were visible under a dissecting microscope with epifluorescence capability, which permitted rapid and direct identification on a culture plate of mutants with misplaced QL and/or QR descendants.

Two chromosomal insertions were generated, *muIs32* (on LG II) and *muIs35* (on LG V), that contain the *mec-7::GFP* marker. These insertions did not affect the migrations of the QL or QR lineages (Figure 2-3; data not shown) and were used as starting strains for screens for mutants with misplaced QL and QR descendants. The mutants isolated were classified according to their most prominent phenotype. In the first class, the primary defect was misplaced QL descendants (some of these mutants also show subtle defects in the positioning of the QR descendants; see below). In the second class, the primary defect was misplaced QR descendants. The third class exhibited defects in both QL and QR descendants. In this study, the focus was on the first class of mutants whose most prominent phenotype is a cell migration defect in the QL lineage.

Identification of new genes that disrupt cell migrations in the QL lineage

From about 100,000 F₂ animals screened, a total of 37 mutants with misplaced PVM cells were isolated, indicative of a migration defect in the QL

lineage. A number of genes required for the migration of cells in the QL lineage have already been described (Baum and Garriga, 1997; Harris et al., 1996; Hedgecock et al., 1987; Honigberg and Kenyon, 2000; Kenyon, 1986; Maloof et al., 1999; Whangbo and Kenyon, 1999; Zipkin et al., 1997). Thus, this work sought to determine which mutations identified in this screen were lesions in these known cell migration genes and which mutations corresponded to new loci. These mutations were assigned to individual chromosomes by mapping them against a panel of Tc1 transposon insertions with known chromosomal locations (see Materials and Methods). For mutations that mapped to the same chromosome as known QL migration genes, complementation tests were performed to determine if these mutations were alleles of known genes.

This process revealed 31 mutations that represented new alleles of previously identified genes. Using this process of elimination, it was found that 6 mutations corresponded to new genes involved in the migrations of cells in the QL lineage (see Materials and Methods). Each of these mutations was found to be recessive, and therefore mostly likely represent reduction- or loss-of-function mutations. Further complementation tests among mutations that map to the same chromosome, as well as additional mapping that refined the position of these mutations (Table 2-2, Materials and Methods) indicated that these 6 mutations likely corresponded to lesions in 5 genes which have been named *qid-5* to *qid-9*, as listed in Table 2-2. For technical reasons (see Materials and Methods), complementation tests between *qid-8(mu327)* and *qid-9(mu342)* were not performed. Since these mutations map to a similar region on the X chromosome and share similar phenotypes (see below), it is still possible that they represent lesions in the same gene.

Further characterization of the new mutants with abnormal cell migrations in the QL lineage

What are the function(s) of these new genes in cell migration and other processes? This question was addressed by determining how these mutations affect the migrations of the cells in the QL lineage, as well as other related developmental events. This section lists the characterizations performed; summaries of these conclusions are detailed in the next section.

The final positions of both the QL and QR descendant cells (AVM, PVM, SDQR, and SDQL - collectively known as the Q.pax cells) were determined at high magnification and their distributions were compared with those of wild-type or *mul32[mec-7::GFP]* controls (Figure 2-3). This confirmed the cell migration phenotypes in the QL lineage and provided additional information about the penetrance and expressivity of these phenotypes. This analysis also revealed additional positioning defects for the QR descendants that were not readily visualized with the *mec-7::GFP* marker (see below).

These mutants were examined for other selected developmental phenotypes (listed below). The spectrum of observed phenotypes in a mutant, along with the specificity or pleiotropy of the defects, could suggest a potential developmental function for the corresponding gene. In addition, comparisons could be made between the set of phenotypes observed in the new mutants, and existing mutations in known genes to determine if the new genes are likely to function in a common pathway.

Other neuronal migrations: The final positions of other migratory neurons in these mutants were examined to determine if the migration defect was specific to

the QL and QR lineages, or if there were more general migration defects (Figure 2-4). These neurons included the hermaphrodite-specific neurons (HSNs), the canal-associated neurons (CANs), the anterior lateral microtubule neurons (ALMs) and the BDU neurons (Sulston et al., 1983). All of these neuronal migrations occur during late embryogenesis in the directions indicated in Figure 2-4. Each of these neurons is all bilateral and shows no apparent left/right asymmetry in its migration.

Axon guidance and outgrowth: The mutants were examined for defects in axon guidance and outgrowth to determine if the migration defects were specific to cell migrations, or if they also affected axonal outgrowth (Table 2-3, Fig 5), as some existing mutations are known to affect both axonal and cell migrations. The *mec-7::GFP* fusion was used to visualize the axons of the touch neurons in these mutant backgrounds as it permitted the examination of axons that are guided in different directions and along different axes: the axons of AVM and PVM grow ventrally and then anteriorly, while those of the ALMs and PLMs grow anteriorly.

Male tail development: Many existing mutants with misplaced QL descendants, such as *mab-5* and *egl-20*, show defects in anteroposterior patterning or cell fate determination that result in defective male tails. The Hox genes *mab-5* and *egl-5* that control the migrations of the cells in the QL lineage are also responsible for specifying the fates of many cells in the male tail. Thus the presence of certain characteristic male tail phenotypes could suggest defects in these Hox pathways (Chisholm, 1991; Kenyon, 1986; Salser and Kenyon, 1992). The new mutants were assessed for similar defects that could reveal a function in the same developmental processes (Table 2-4).

The development of the male tail relies upon a number of processes and events, including cell migration, cell-fate determination, neurogenesis, anteroposterior patterning and morphogenesis. By examining this one structure it was possible to survey a diverse set of developmental events (Sulston et al., 1980). Moreover, defects in specific structures in the male tail could be traced to particular cell lineages, aiding diagnosis of the phenotype (detailed in Sulston et al., 1980). This work focused on the following structures: (1) the nine rays on each lateral side, which are neuronal structures derived from a set of lateral epidermal cells located on the corresponding side near the tail of male *C. elegans*; (2) the hook and its associated cells derived from posterior ventral epidermal cells; (3) the mating spicules generated by a male-specific blast cell (the normal straight spicule morphology also requires the function of posterior sex muscles that are derived from migratory myoblasts).

Expression of *mab-5* in QL: *mab-5* expression in the QL but not QR lineage is a critical step during the left-right asymmetric migrations within these lineages as *mab-5* expression in these cells is necessary and sufficient to direct a program of posterior migration (Harris et al., 1996; Salser and Kenyon, 1992). Since *mab-5* is normally expressed only in the QL descendants, it also serves as a molecular marker for the left-right asymmetry between QL and QR. By examining the expression of a *mab-5::lacZ* reporter in the Q descendants of these mutants (Table 2-5), it could be inferred whether the cell migration defect is caused by defective or inappropriate *mab-5* expression or due to an inability of the migrating cells to respond properly to *mab-5*.

Phenotypes of the mutants with cell migration defects in the QL lineage

qid-5(mu245)II: In about 50% of the animals examined, the QL.pax cells were found in the anterior (Figure 2-3), consistent with a defect in *mab-5* expression in the QL daughters (Table 2-5). In this mutant, the ALM cell bodies also stopped prematurely (about 40% penetrant) and were positioned further to the anterior than normal (Figure 2-4). Other cell migrations appeared normal in *qid-5(mu245)* animals.

qid-6(mu252)III: This mutant developed fluid-filled blisters along its body. It was unlikely to be a lesion in *bli-5* (Hodgkin, 1997), a known mutation located on the same chromosome with a blistering phenotype (Bli), because *qid-6(mu252)* complemented *bli-5(e518)* and the QL descendants were not misplaced in *bli-5(e518)* animals (data not shown). In addition to the Bli phenotype, *qid-6(mu252)* animals were also somewhat sluggish (uncoordinated, Unc) and slightly short and fat (dumpy, Dpy). In this mutant, the QL.pax cells were found in the anterior about 40% of the time, most likely due to a defect in *mab-5* activation (Figure 2-3, Table 2-5); other neuronal migrations appeared normal. In the male tail, cell-fate and morphogenesis defects were observed, with animals showing missing rays or inappropriate ray fusion (Table 2-4). The positions of the rays also appeared slightly disorganized.

qid-7(mu255, mu326)II: Interestingly, in *qid-7(mu255)* mutants, about 80% of the QL descendants migrated abnormally to the anterior (Figure 2-3) even though *mab-5::lacZ* appeared to be expressed at almost wild-type frequency in the QL daughters (Table 2-5). This indicated that the defect was likely to be downstream or in parallel to *mab-5*. In addition, shortened migrations were seen in the QR.pax cells (~40% penetrant, Figure 2-3) and the HSN neurons (~20%

penetrant, Figure 2-4), with these cells stopping in more posterior positions than wild type. These studies were all performed on *qid-7(mu255)* because *qid-7(mu326)* appeared to be a weak mutation with very low penetrance cell migration phenotypes in the QL lineage.

qid-8(mu327)X: This mutant had pleiotropic phenotypes. In a population of *qid-8(mu327)* animals, the QL.pax cells were variably displaced along the body axis (Figure 2-3). This was consistent with the incompletely penetrant absence of *mab-5::lacZ* expression in the QL descendants (Table 2-5); even when *mab-5::lacZ* was expressed, the levels of staining were also often reduced in comparison to the wild-type controls. On the right side, the distribution of the QR.pax cells was consistently shifted posteriorly (Figure 2-3), a phenotype reminiscent of *egl-20/Wnt* mutants (Harris et al., 1996). *qid-8(mu327)* animals were very sick and exhibited low brood sizes. They were sluggish (Unc), slightly dumpy (Dpy), and egg-laying defective (Egl), often bloated with unlaidd eggs. This Egl phenotype may be partially accounted for by potential defects in vulval development suggested by the protruding vulva (Pvl) phenotype (Eisenmann and Kim, 2000; Eisenmann et al., 1998), and the strong HSN cell migration phenotype (Desai et al., 1988); more than 50% of the HSNs were either located further to the posterior than wild type or were not found in the body at all (Figure 2-4). In the axons of the touch neurons, a variety of defects was observed, including ectopic branching as well as aberrant trajectories (Figure 2-5B-D). Male tail development was severely disrupted (Table 2-4); rays were missing or disorganized. Crumpled spicules and missing or displaced hooks were also observed. Together, these defects in the male tail indicated developmental defects in the posterior-lateral/ventral epidermis and the sex muscles.

qid-9(mu342)X: This was also a very pleiotropic mutant with sluggish (Unc), Egl, Pvl, very weak Dpy phenotypes as well as very small brood sizes. In *qid-9(mu342)*, the final positions of the QL.pax cells were distributed along the body (Figure 2-3). This could be explained by the fact that *mab-5* expression is variably reduced in the QL daughters (Table 2-5). An *egl-20*/Wnt-like posterior shift was also seen in the distribution of the QR.pax cells (Figure 2-3). Among other migratory neurons, HSN showed a strong phenotype (Figure 2-4). The very small population of CAN and ALM neurons that were located further to the anterior than normal (Figure 2-4) raise the possibility that there might be very subtle migration phenotypes in these neurons. Inappropriate axon branching and guidance defects were seen in the touch neurons (Figure 2-5E and F). The male tail was also severely compromised with ray and hook defects that are likely due to lineage or cell-fate defects in the posterior-lateral and ventral epidermis (Table 2-4). Also, the presence of crumpled spicules indicated defects in the sex muscles (Table 2-4).

***lin-17*/Frizzled is required for normal PLM axonal outgrowth**

In this screen, *mu243*, an allele of *lin-17*/Frizzled (Sawa et al., 1996) that exhibited axon outgrowth defects in the PLM touch neurons, was isolated. In wild-type animals, the PLM neurons normally send out axons that extend slightly past the mid-body along the ventrolateral surface of the worm. These PLM axons were often truncated in *lin-17(mu243)* mutants (Table 2-3; Figure 2-5H). This phenotype was also detected in *lin-17(n671)* (Table 2-3; Figure 2-5G), a strong loss-of-function allele (Sawa et al., 1996). Mutations that disrupt other

components of the conserved Wnt pathway in *C. elegans*, such as *egl-20*, *mig-14* or *bar-1*, appeared wild type for PLM axon outgrowth (data not shown).

lin-17 has been implicated in cell-fate and cell-lineage decisions in *C. elegans* (Sawa et al., 1996; Sternberg and Horvitz, 1988). However, in *lin-17(mu243)* and *lin-17(n671)*, the PLM touch neurons still expressed *mec-7::GFP* (Figure 2-5G and H), a very specific differentiation marker, suggesting that the neurons were still adopting the correct touch-cell fate. Moreover, among the touch neurons scored, this defect was specific to PLM. Thus, it is possible that mutations in *lin-17* disrupt axonal outgrowth in the PLM neurons in a step distinct from the adoption of a touch-neuron fate.

DISCUSSION

The left-specific expression of the Hox gene *mab-5* in the QL lineage is controlled by at least three different sets of genes. The first set governs the polarization of the QL neuroblast properly toward the posterior. The second set allows the QL neuroblast and/or its progeny to receive the EGL-20/Wnt signal, and specifies the left-right asymmetric responses to this EGL-20/Wnt signal so that this signal is interpreted correctly. The third set of genes is turned on by *mab-5* and acts more directly to guide cells to the posterior. In this work, new mutants have been described that disrupt the migrations of the cells in the QL lineage, either by affecting the activation of *mab-5* in these cells or by impairing their ability to respond to *mab-5*. The corresponding genes are likely to function in these respective steps during the migration of the cells in the QL lineage.

The cell migration defects in these mutants allowed their placement in different steps of a large pathway that controls and coordinates these complex

left-right asymmetric cell migrations. This is summarized in Figure 2-6 and detailed below. With the caveat that most of these genes are represented by only one allele, the overall spectrum of phenotypes in these mutants allows well-grounded speculation about their broader roles in development and how these developmental processes might intersect with the migrations of the cells in the QL and QR lineages.

Genes isolated in this screen for cell migration mutants

In this large-scale screen, several new mutations that disrupt the cell migrations within the QL lineage were isolated. This was done rapidly by labeling these cells with a GFP reporter that could be seen under a dissecting microscope equipped with epifluorescent capabilities. However, this screen was not saturating, as many of the new genes presented here were represented by only single alleles. Hence the interpretation given here of their role in cell migrations (below) remains tentative until additional alleles are isolated.

In this screen, about 45% of the candidate mutants isolated were sterile or not viable. In the future, F₂ clonal screens that rely on examining a population of siblings for misplaced QL descendants might be more useful in isolating cell migration mutants of this class. Such a screen could also identify mutants with weak phenotypes that might be more obvious when observed in a population.

Possible role(s) of these genes in regulating *mab-5* expression

After the initial migrations, an EGL-20/Wnt signal triggers *mab-5* expression in the QL descendants through a conserved Wnt signaling pathway; this causes the cells to migrate posteriorly (Eisenmann et al., 1998; Harris et al.,

1996; Herman, 2001; Maloof et al., 1999; Salser and Kenyon, 1992; Sawa et al., 1996). Most of the mutants described here act at this step: the mutations in *qid-5*, *qid-6*, *qid-8* and *qid-9* all compromised *mab-5* expression in the QL descendants. This likely explains the anterior migrations of the QL descendants in these mutants. This phenotype indicated that these new genes intersect with the *egl-20/Wnt* pathway directly or indirectly during the activation of *mab-5* expression in the QL lineage.

egl-20/Wnt has a second role in the cell migrations of the QR descendants: it signals these cells to migrate anteriorly to their fullest extent and this appears to be mediated by unknown genes distinct from those required for the QL migrations (Eisenmann et al., 1998; Harris et al., 1996; Maloof et al., 1999; Whangbo and Kenyon, 1999). In *egl-20* mutants, the QR descendants migrate in the anterior direction but often stop short of the wild-type position. Among this set of mutants with *mab-5* expression defects, only *qid-8* and *qid-9* exhibited a posterior shift in the final positions of the QR descendants similar to that observed in *egl-20* (Harris et al., 1996). Also, there was considerable overlap between the other phenotypes of *egl-20* and these mutants, such as the HSN migration defect and the presence of crumpled spicules in males (Desai et al., 1988). This raised the possibility that these genes might function in a more integral part of the *egl-20/Wnt* pathway. However, *qid-8* and *qid-9* also exhibited many other phenotypes not seen in *egl-20* mutants, such as the axon outgrowth defects, and thus may act in additional pathways. Also, *egl-20* mutants have a defect in the asymmetric V5 cell division, a phenotype not detected in any of the new mutants in this screen, including *qid-8* and *qid-9* (data not shown).

The different roles of *egl-20*/Wnt in QL and QR migration highlight the complexities involved in interpreting this signal. Not only is it likely that different downstream signaling components are used in QL and QR, but there must also be factors that generate these distinct responses of QL and QR to a given level of EGL-20/Wnt (Whangbo and Kenyon, 1999). Mutations in *qid-5* and *qid-6* impaired one *egl-20*-dependent process (*mab-5* activation in QL descendants), but not the other (anterior migration of QR descendants). With the caveat that most of these genes are each defined by only one recessive mutation that might not be null, this suggests that these genes do not function in all aspects of EGL-20/Wnt signaling. This specificity is intriguing. It is speculated that these genes could act in any of three ways. First, they could represent links that couple the initial migrations of the QL neuroblast to the QL-specific activation of *mab-5*. Second, they could contribute to the left-right asymmetric response to *egl-20*/Wnt by acting to transduce the EGL-20 signal exclusively in the *mab-5* activation pathway. Third, these genes could function by predisposing the QL descendants to respond to an EGL-20 signal with *mab-5* activation instead of anterior migration.

qid-6(mu252) animals exhibited a blistered cuticle phenotype, suggesting a defect in cuticle formation. Genes encoding extracellular matrix molecules such as *bli-1* and *bli-2*, as well as proteases postulated to process these collagens (Peters et al., 1991; Thacker et al., 1995), can mutate to cause a similar blistered cuticle phenotype (Johnstone, 2000). A Bli phenotype was not sufficient to confer a cell migration defect in QL or its descendants, as *bli-5* animals exhibited normal placement of the QL descendants (data not shown). Perhaps *qid-6* affects cuticle synthesis or disrupts the extracellular matrix in a different way to, or at a

different time than, *bli-5*. It is possible that the *mab-5* activation defect could be due to related defects in extracellular matrix molecules that are required for the distribution or presentation of signals like EGL-20/Wnt, as analogous examples have been described in *Drosophila* and zebrafish (Hacker et al., 1997; Walsh and Stainier, 2001).

qid-6, *qid-8* and *qid-9* also affected male tail development, with phenotypes that resembled *mab-5* mutants, such as crumpled spicules, missing rays and missing hooks (Kenyon, 1986). This suggests that these genes might also function as regulators of *mab-5* during male tail development, raising the possibility that they represent more general regulators of *mab-5* activation or function in *C. elegans*.

Role of *qid-7* in potentiating or executing *mab-5* function

The mechanism by which *mab-5* directs posterior migration once it is expressed in the QL descendants is still poorly understood. In this light, *qid-7* was a particularly attractive gene because it appeared to be dispensable for *mab-5* expression in the QL lineage, even though the QL descendants migrated to the anterior in *qid-7(mu255)* mutants. Thus, *qid-7* is likely to function downstream of, or in parallel with, the Hox gene *mab-5*, possibly as an effector or a factor that permits or potentiates the response of the Q descendants to *mab-5*. *qid-7(mu255)* also shortened the migrations of the QR descendants and the HSNs, phenotypes reminiscent of *lin-39* and *egl-5* mutants - both of which also encode Hox genes (Chisholm, 1991; Clark et al., 1993; Wang et al., 1993). However, *qid-7(mu255)* did not affect other Hox-dependent developmental processes, such as male tail patterning or vulval formation (Chisholm, 1991; Clark et al., 1993; Eisenmann et

al., 1998; Kenyon, 1986). Thus, it is possible that *qid-7* functions as a common effector or co-factor for these three Hox genes specifically during cell migrations.

Conclusion

In summary, the collection of mutants identified here provides additional entry points into the study of the migrations of QL and its descendants, as well as of other cell migrations in *C. elegans*. Many of the known mutants that disrupt cell migrations in the QL lineage also affect other developmental processes in a manner similar to those affected by some of these new mutants. However, the additional phenotypes are not identical. Apart from the cell phenotypes in the QL lineage, some of the new mutants showed only a subset of the phenotypes displayed by known mutants that affect cell migrations in the QL lineage. This suggests that these new genes might act at specific times and places, rather than being obligate factors in previously characterized pathways. Other mutants such as *qid-6* exhibit phenotypes not seen in known cell migration mutants that affect the QL lineage; these new mutants might therefore act in new pathways that intersect with some of the known pathways during the migrations of QL and/or its descendants. Discerning their molecular identities and their relationships with the known pathways that control the migration in the QL lineage will be important in understanding the complex developmental processes that oversee the precise control of these intriguing cell migrations.

EXPERIMENTAL PROCEDURES

General methods and strains

Strains were cultured using standard methods (Brenner, 1974; Lewis and Fleming, 1995; Wood, 1988). All strains were maintained at 20°C, except where indicated. To generate males, the *him-5(e1490)* mutation was used; this mutation does not affect larval development.

In addition to the mutants isolated in the screen listed in Table 2-1, the following alleles/strains were used in this study according to linkage group (LG); all alleles are described in Hodgkin (1997) except where otherwise referenced:

LG I: *mig-1(e1787)*, *lin-17(n671)*

LG II: *mig-14(mu71)*

LG III: *mab-5(e2088)*

LG IV: *egl-20(n585)*

LG V: *him-5(e1490)*

LG X: *mig-13(mu31)*; *bar-1(ga80)* (Eisenmann et al., 1998)

RW7000 is a mapping strain containing Tc1 transposon insertions at defined positions throughout its genome (Williams, 1995; Williams et al., 1992).

The following transgenic strains were used in this study:

muIs3[mab-5::lacZ,rol-6(d)] on LG V (Cowing and Kenyon, 1992).

muIs4[mab-5::lacZ,rol-6(d)] on LG I (Cowing and Kenyon, 1992).

muIs32[mec-7::GFP,lin-15(+)] on LG II

muIs35[mec-7::GFP,lin-15(+)] on LG V.

The chromosomal insertions, *muIs32* and *muIs35*, were generated by γ -irradiating *lin-15(n765ts)* animals bearing an extrachromosomal array containing

mec-7::GFP and *lin-15(+)* (a kind gift from Lindsay Hinck and the laboratories of Cori Bargmann and Marc Tessier-Lavigne) as late L4 or young adults. At 25°C, *lin-15(n765ts)* animals have a multivulva (Muv) phenotype that is rescued by a genomic clone of the *lin-15* locus in this extrachromosomal array. The F₂ generation of these irradiated animals was screened for lines that did not give any Muv progeny at 25°C, indicating that the extrachromosomal array was stably inherited. These lines bearing putative chromosomal insertions of the extrachromosomal array were outcrossed three times to the wild-type N2 strain to remove *lin-15(n765ts)* and other possible mutations generated during the irradiation process. With the exception of a slightly longer generation time, animals bearing *mulS32* or *mulS35* did not exhibit any obvious developmental defects and had normal neuronal cell migrations (Figures 2-2 and 2-3; data not shown).

Mutagenesis and screening

Mutagenesis was performed as described previously (Anderson, 1995). Briefly, 15 separate pools of late L4 or young adult P₀ animals bearing either *mulS32* or *mulS35* were mutagenized with 25mM ethyl methanesulfonate (EMS) for 4 hours at 20°C. These animals were then washed several times in M9 to remove the EMS. Their F₁ progeny were collected at hatching and stored at 8°C in M9 to arrest their development. Batches of these developmentally arrested F₁s were plated out over several days and cultured at 20°C where they resumed development. These F₁s were allowed to self-fertilize to generate F₂ progeny. These F₂ progeny were collected and aged until many had reached the L4 larvae or young adult stage; at this point they were screened for misplaced QL and/or

QR descendants (see Figure 2-2C); approximately 100,000 F₂ animals were screened. These positive F₂s were placed individually on culture dishes and their F₃ progeny retested; viable lines that still exhibited migration defects in the QR and/or QR lineage were kept.

During the screening process, other *mec-7::GFP* positive cells were used as landmarks for determining the A/P orientation of the animal (Figure 2-2B-C) (Chalfie et al., 1994). These include the two PLM neurons in the tail and the two ALM neurons near the head. By locating the GFP-expressing PVM and/or AVM in relation to these GFP-expressing landmark cells, the rapid determination of whether PVM and/or AVM were misplaced was possible (up to 1,000-1,200 animals could be examined within 1 hour). Since *mec-7* encodes a mechanosensory neuron-specific β -tubulin, its expression also served as a marker for mechanosensory fate (Savage et al., 1989). This allowed the elimination of mutations that disrupt cell fate determination or differentiation in the QL and QR lineages.

Populations of young adults were screened long after the cell migrations are completed, after the end of the first larval stage. This permitted growth in the intervening larval stages to amplify the distance between wild-type and mutant positions by almost tenfold. Selecting mutants as adults also improved the recovery rate of candidate mutations.

Genetic mapping

Mapping against a standard panel of Tc1 markers in the RW7000 strain [*hP4* (I), *maP1* (II), *mgP21* (III), *sP4* (IV), *bP1* (V)] was performed as described (Williams, 1995; Williams et al., 1992). *muIs32* was mapped against *stP100*,

stP196, stP101, stP50, stP36, stP98 and *maP1* to about 2cM to the right of *maP1* on LG II, placing it at a map position of approximately +6.3. *mul35* was mapped against *stP3, stP192, stP23, bP1, stP6, stP18, stP108, stP105* and *stP128* to less than 1cM from *stP6* on LG V at the map position +5.9.

The mutations isolated in the screen were mapped in a similar fashion. Mutant hermaphrodites were crossed to wild-type males and the hermaphrodite progeny (F₁s) were examined for phenotypes to determine if the mutation was dominant. All the mutations examined were recessive for the cell migration phenotype in the QL lineage. Examining the F₁ male progeny enabled the determination of whether the mutation was X-linked. If the mutation was autosomal, these heterozygous F₁ males were mated to the RW7000 mapping strain. The F₂ progeny from this cross were picked onto individual plates, from which their homozygous mutant F₃ progeny were isolated. DNA was isolated from these mutants or from their entire set of progeny.

Further mapping was conducted using Tc1 markers linked to the respective mutation (listed from left to right on their respective linkage groups). *qid-5(mu245)* was mapped with *stP100, stP196, stP101, stP50, stP36, stP98* and *maP1* on LG II. *qid-6(mu252)* was mapped with *stP19, stP120, mgP21, stP127* and *stP17* on LG III. *qid-7(mu255), qid-8(mu327)* and *qid-9(mu342)* were mapped with *stP41, stP40, stP156, stP33, stP103, stP129, stP61, stP72* and *stP2* on LG X. All recombinants obtained are listed below along with their frequency of occurrence and are designated by the Tc1 markers present in the recombinant chromosome that also carries the *qid* mutation.

qid-5(mu245): These recombinants placed *mu245* to the right of *maP1*: *stP100, stP196, stP101, stP50, stP36, stP98, maP1* (1/17): *stP100, stP196, stP101, stP50,*

(1/17); *stP100*, *stP196* (4/17); *stP100* (6/17). 5/17 of the *qid-5* animals obtained were non-recombinants.

qid-6(mu252): These recombinants placed *mu252* to the left of *stP17*: *stP17* (4/18). This double recombinant placed it between *stP19* and *stP17*: *stP19* and *stP17* (1/18). 13/18 of the *qid-6* animals were non-recombinants. No recombination (0/18) was observed between *qid-6* and the markers in the cluster (*stP120*, *mgP21*, *stP127*).

qid-7(mu255): These recombinants placed *mu255* to the right of *stP72*: *stP41*, *stP40*, *stP156*, *stP33*, *stP103*, *stP129*, *stP61*, *stP72* (3/27); *stP41*, *stP40*, *stP156*, *stP33*, *stP103*, *stP129*, *stP61* (1/27); *stP41*, *stP40*, *stP156*, *stP33*, *stP103* (3/27); *stP41*, *stP40*, *stP156* (1/27); *stP41*, *stP40* (2/27); *stP41* (4/27). These recombinants placed it to the left of *stP2*: *stP2* (4/27). One double recombinant was obtained: *stP41*, *stP40*, *stP156*, *stP33*, *stP103*, *stP129*, *stP61*, *stP72*, *stP2* (1/27). 8/27 of the *qid-7* animals were non-recombinants.

qid-8(mu327): These recombinants placed *mu327* to the right of *stP103*: *stP41*, *stP40*, *stP156*, *stP33*, *stP103* (2/27); *stP41*, *stP40*, *stP156*, *stP33* (3/27); *stP41*, *stP40*, *stP156* (2/27); *stP41*, *stP40* (3/27); *stP41* (1/27). These recombinants placed it to the left of *stP61*: *stP2* (3/27); *stP61*, *stP72*, *stP2* (3/27). These double recombinants were obtained: *stP41*, *stP40* and *stP2* (3/27); *stP41* and *stP2* (1/27). 6/27 of the *qid-8* animals obtained were non-recombinants.

qid-9(mu342): These recombinants placed *mu342* to the right of *stP129*: *stP41*, *stP40*, *stP156*, *stP33*, *stP103*, *stP129* (2/23); *stP41*, *stP40*, *stP156* (1/23); *stP41*, *stP40* (2/23); *stP41* (3/23). These recombinants placed it to the left of *stP61*: *stP2* (7/23); *stP61*, *stP7*, *stP2* (1/23). One double recombinant was obtained: *stP41*,

stP40 and *stP61*, *stP7*, *stP2* (1/23). 6/23 of the *qid-9* animals obtained were non-recombinants.

During the mapping process, the *mec-7::GFP* marker (*mulS32* or *mulS35*) was retained to permit detection of cell migration defects in the QL lineage. Hence the mapping process would indicate linkage to these chromosomal insertions as well as to the mutation. Since the chromosomal location of the *mec-7::GFP* marker was known, the location of the mutation could be inferred. A small number of the mutations showed linkage to the *mec-7::GFP* marker; in these cases the mapping process showed only linkage to the one chromosome bearing both the mutation and the *mec-7::GFP* marker.

Complementation tests

Complementation tests were performed when two or more mutants with similar cell migration phenotypes mapped to the same linkage group. These tests were conducted as follows. For autosomal mutations in which the males were capable of mating, spontaneous males bearing the mutation of interest and the *mec-7::GFP* marker were crossed into hermaphrodites bearing a known mutation but no *mec-7::GFP* marker. Cross progeny were identified by the presence of the *mec-7::GFP* marker and the positions of the QL descendants were scored using this marker.

For autosomal mutations where the males were not capable of mating, heterozygous males were generated by crossing mutant hermaphrodites also carrying the *mec-7::GFP* marker with wild-type or *him-5(e1490)* males. The heterozygous male progeny from this cross were mated with hermaphrodites bearing a known mutation but no *mec-7::GFP* marker. Cross progeny were

identified by the presence of the *mec-7::GFP* marker and their QL descendant positions were scored as above, with the expectation that 50% of the progeny would be heterozygous for the cell migration mutation.

Complementation tests between *qid-8(mu327)* and *qid-9(mu342)* were unable to be performed, because these mutations were X-linked and the males were not capable of mating. Using a *tra-1* mutation to generate heterozygous XX males for mating also failed: the low mating efficiency of *tra-1* XX males was exacerbated by the low brood size and the low hermaphrodite mating efficiency of these two mutants. Since *qid-8(mu327)* and *qid-9(mu342)* map to the same general region on LG X and share many phenotypes, it is quite possible that they are allelic. Different names have been assigned to these two mutants as they have not been shown to correspond to lesions in the same gene.

Whenever a mutation mapped to a particular chromosome, complementation tests were performed against all the known genes that affected the migrations of QL and/or its descendants on the same chromosome, as listed in Table 2-1. Although these tests were extensive for published mutations that affect these cell migrations, the possibility cannot be ruled out that these mutations correspond to lesions in known genes whose QL migration phenotype has not been described. These tests were performed as described above, except for those against *egl-20*. For complementation tests against *egl-20(n585)*, candidate *egl-20* alleles were first mated with *dpy-20(e1282); him-5(e1490)* males. The *dpy-20* mutation served as a linked marker for *egl-20*. The male progeny from this cross, which were heterozygous for the putative *egl-20* mutation, were then mated with *egl-20(n585) dpy-20(e1282)* hermaphrodites. To assay for

complementation, the final positions of the Q descendants were determined in the non-Dpy progeny of this cross.

Mutants that complemented all other mutations known to disrupt the migrations of QL and/or its descendants were considered to represent new genes affecting this cell migration. However, because these genes are mostly represented by one allele, it remains possible that they correspond to known genes whose existing alleles do not display cell migration phenotypes in the QL lineage.

Sequencing *egl-20* alleles

Two regions of the predicted *egl-20*/Wnt gene were PCR amplified from *egl-20(mu320)* and *egl-20(mu241)*. Exons 1-4 were amplified with JW1: 5'-CTTAACCAGGCAAATCGGAA-3' and JW5: 5'-CACACATAAGACAACACCTG-3'; exons 5-10 were amplified with JW3: 5'-CGTGTCGTTATGAAATACGC-3' and JW4: 5'-TCTTGTTTTGCTAGGTCCCG-3'. These amplified regions included the entire coding region and all intron/exon boundaries of the predicted *Wnt* gene. Fragments were cloned and sequenced, as described in Maloof et al. (1999), from two independent PCR reactions.

The *mu320* allele contains an opal mutation in the second exon of *egl-20*. The predicted *mu320* protein product has only 48 amino acids in addition to the presumptive signal sequence and thus may be a null allele. The *mu241* allele changes an invariant splice-donor GT sequence to AT in the second intron.

Outcrossing and strain construction

The mutations were initially isolated as strains bearing a *mec-7::GFP* marker (either *mul32* or *mul35*). These mutations were outcrossed three times prior to further characterization. Only *qid-5(mu245)* was retained in the *mec-7::GFP* background because it was tightly linked to the *mul32* insertion bearing the *mec-7::GFP* marker. After the outcrossing process, confirmation that these mutations affected the migrations of cells in the QL lineage was made by examining the final positions of the QL descendants, PVM and SDQL (Figure 2-3), and comparing these positions to wild-type or *mul32* controls.

For the first outcross, mutant hermaphrodites were mated with either *mul32; him-5(e1490)* or *mul35* males. The heterozygous cross progeny (F₁s) were cloned out onto individual plates and were confirmed as cross progeny by scoring the frequency of the mutant phenotype in the next generation (F₂s). F₃s bearing the mutation, a *mec-7::GFP* marker, and if possible, the *him-5(e1490)* mutation were re-isolated from these F₂s.

For the second outcross, hermaphrodites from lines re-isolated from the first outcross were mated with wild-type males. The heterozygous progeny from this cross were mated with *him-5(e1490)*, males for a third outcross. From these crosses, the mutation was re-isolated in the absence of the *mec-7::GFP* marker and *him-5(e1490)* as well as in double mutant combinations with the *mec-7::GFP* marker or *him-5(e1490)*. The *mec-7::GFP* and *him-5(e1490)* double mutants permitted scoring of axon phenotypes and male tail development respectively (see Results). The heterozygous males from this outcross were also mated into a *mab-5::lacZ* reporter strain (*mul3* or *mul4*) (Cowing and Kenyon, 1992) to generate double mutants bearing both the mutation and the *mab-5::lacZ* reporter.

In the case of *qid-5*, the mutation was tightly linked to the *mulS32* insertion on LG II and it was not separated from *mulS32* during these outcrosses. Thus, for this mutation, all controls were performed in a *mulS32* background.

β-galactosidase staining

β-galactosidase staining was performed as described (Salser and Kenyon, 1992). Staged populations of animals bearing *mulS3* or *mulS4* (Cowing and Kenyon, 1992) along with the mutations of interest were fixed and stained approximately 4 hours after hatching, at the time of the first division of QL where *mab-5::lacZ* is expressed (Salser and Kenyon, 1992). In an otherwise wild-type background, the *mab-5::lacZ* reporters *mulS3* and *mulS4* were expressed in the QL descendants but not the QR descendants (Table 2-5). The expression of these reporters in the QL descendants in the *egl-20(n585)* background was also examined. Consistent with prior observations (Harris et al., 1996), *egl-20(+)* is required for *mab-5* expression in these cells (Table 2-5). Unfortunately, it was not possible to use these *lacZ* fusions to examine *mab-5* expression in other tissues, as they do not recapitulate the complex expression of *mab-5* in these tissues (Salser and Kenyon, 1996).

Microscopy and scoring of phenotypes

During screening or strain construction, cell migration mutants that affect the QL lineage were identified by observing the positions of PVM in larvae. This was carried out using either a Leica stereo dissecting microscope equipped with a Kramer epifluorescence unit or a Zeiss M²Bio stereo dissecting microscope with a similar epifluorescence unit. For more detailed analyses of cell positions and

cell fates, animals were mounted on agarose pads and examined using Nomarski/DIC optics on a Zeiss Axiophot microscope with a 100X objective. The positions of the Q descendants, AVM, PVM, SDQR, and SDQL were scored as described (Harris et al., 1996). Briefly, the positions of the Q descendants in relation to the stationary V cells were noted in larvae near the end of the L1 larval stage; animals were deemed to be at the correct point in development when all the P nuclei had descended into the ventral cord, as the Q migrations in wild-type animals were complete by this point. The positions of other migratory neurons, HSN, CAN, ALM, and BDU, were also scored at this point. Expression of *mab-5::lacZ* in stained animals was scored using Nomarski/DIC optics with a 100x objective.

During the examination of the male tail, animals were immobilized with 1mM levamisole. Cells and other anatomical features were identified as described in Sulston and Horvitz (1977). Wild-type or *him-5(e1490)* animals exhibited a low frequency of ray defects in which one ray derived from either V5 or V6 (V rays) is missing as previously reported (Sulston et al., 1980). Only mutants with defects significantly more penetrant than this background were considered to have a male tail phenotype.

Axon morphology was visualized using the *mec-7::GFP* fusions *muIs32* and *muIs35* under the 20x objective of the Zeiss M²Bio stereo dissecting microscope. To facilitate scoring of the axons, the animals were partially immobilized by chilling at 2-4°C in a cold room for 5-15 minutes. This process did not affect axon morphology; worms treated this way did not differ significantly in their axon morphology from control worms (data not shown). A small number of animals bearing the *muIs32* and *muIs35* insertions display defects in

their axon morphology. Only mutants with significantly more penetrant defects were considered as having a *bona fide* axon outgrowth phenotype.

ACKNOWLEDGMENTS

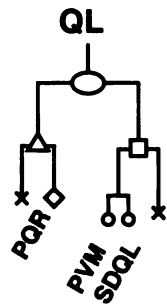
We wish to thank past and present members of the Kenyon Lab for discussions and advice. We are indebted to Cori Bargmann, Lucie Yang, Scott Alper, John Williams, Phil Anderson and anonymous reviewers for critical and helpful comments on the manuscript. We are also grateful to Lucie Yang for her assistance in mapping the *mec-7::GFP* insertions, Lindsay Hinck, Marc Tessier-Lavigne, Cori Bargmann and the *Caenorhabditis elegans* Genetics Center for strains and to Tom Kornberg and Cori Bargmann for use of equipment. Q. C. was a Howard Hughes Medical Institute Predoctoral Fellow, L. W. and J. S. W. were National Science Foundation Predoctoral Fellows, M. S. was a Postdoctoral Fellow of the Jane Coffin Childs Memorial Fund for Medical Research, Y. S. L. is a Postdoctoral Fellow of the Cancer Research Fund of the Damon Runyon-Walter Winchell Foundation (DRG 1669), C. K. is the Herbert Boyer Professor of Biochemistry and Biophysics. This research was supported by the National Institutes of Health (Grant GM37053).

Figure 2-1. The left-right asymmetric migrations of the QL and QR lineages.

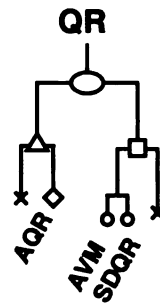
(A) The cell division pattern of QL and QR. These neuroblasts divide in identical patterns. The anterior daughters of QL and QR (QL.a and QR.a respectively) are represented by triangles, while the posterior daughters of QL and QR (QL.p and QR.p) are represented by squares. Additional cell divisions result in the generation of three neurons (diamonds and circles; names of three neurons are shown), as well as cells that undergo programmed cell death (Xs).

(B) The different steps of the left-right asymmetric cell migrations. The migrations of QL, QR and their respective descendants occur in several steps as shown. (See introduction for details). *mab-5* is only expressed in the QL lineage (indicated by dark gray shading); the QR lineage does not express *mab-5* (no shading). The final positions of the QL and QR descendants are indicated in the final set of animals at the bottom.

(a) Left - QL Lineage



Right - QR Lineage



(b) QL and its descendants migrate posteriorly.

QR and its descendants migrate anteriorly.

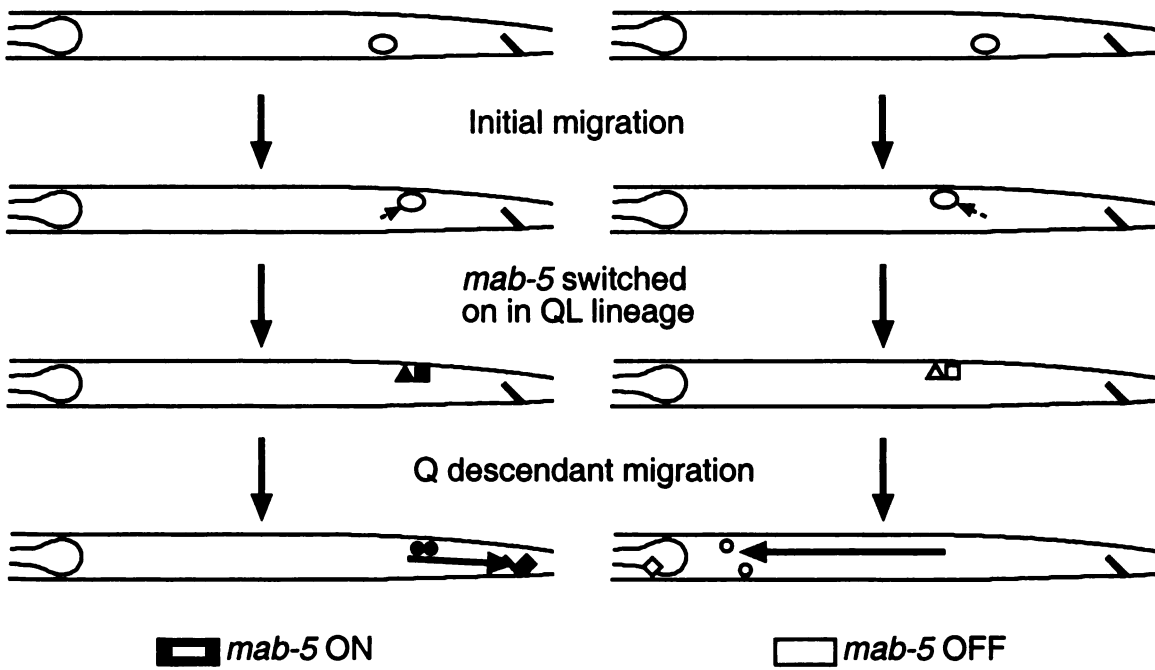
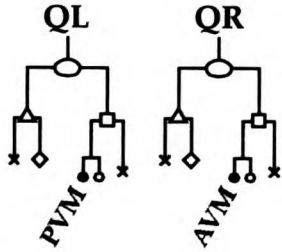


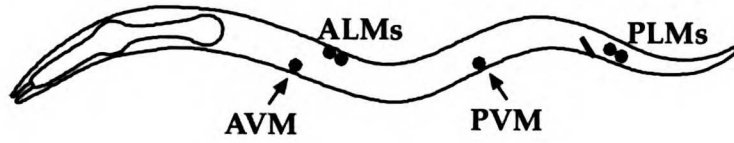
Figure 2-2. The screen for cell migration mutants.

(A) *mec-7::GFP* labels one cell in each Q lineage: PVM from QL and AVM from QR. The *mec-7::GFP* expressing cells are labeled and shaded. (B) The expression pattern of *mec-7::GFP*. *mec-7::GFP* is expressed at high levels in these touch neurons: two bilateral ALMs, two bilateral PLMs, AVM and PVM. (C) Isolation of mutants with misplaced Q descendants. Arrowheads indicate the positions of the respective QL and QR descendants, PVM and AVM. Candidate mutants were identified by misplaced *mec-7::GFP* expressing cells near the ventral side of the animal which correspond to PVM and AVM respectively. Below each picture is a schematic of the inferred migrations, based on the final positions of the GFP-labeled Q descendants; gray arrows indicate mutant migrations.

(a)



(b)



(c)

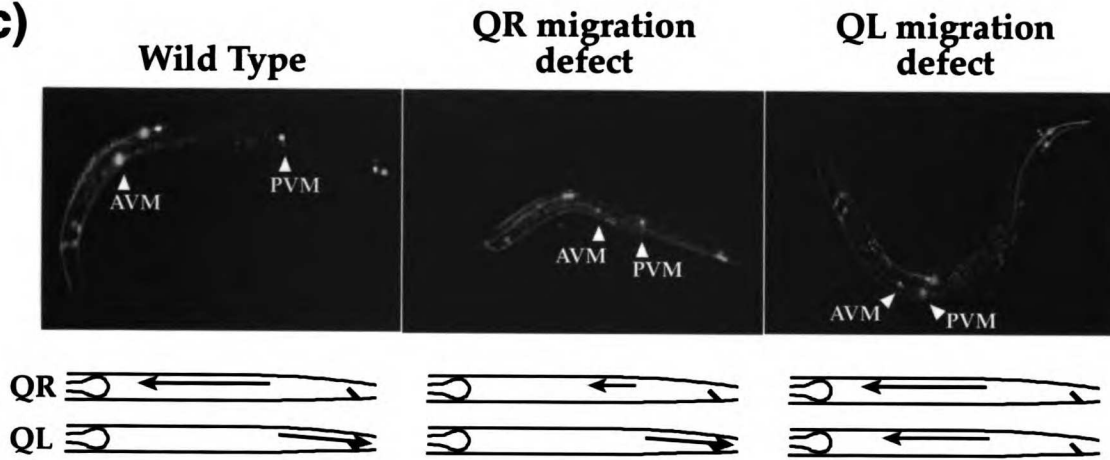


Figure 2-3. The distribution of the final positions of the QL and QR descendants in the cell migration mutants.

The positions of the QL descendants SDQL and PVM (collectively known as the QL.pax cells) are shown on the left. The positions of the QR descendants SDQR and AVM (collectively known as the QR.pax cells) are shown on the right. The positions of these cells are scored relative to the stationary Vn.a and Vn.p cells indicated on the x-axis. At least 28 sides were scored for each chart. Arrows indicate the extent and direction of cell migration, (*) indicates the starting positions of QL and QR on their respective sides, and the dotted lines indicate the position beyond which the migrations are considered wild type.

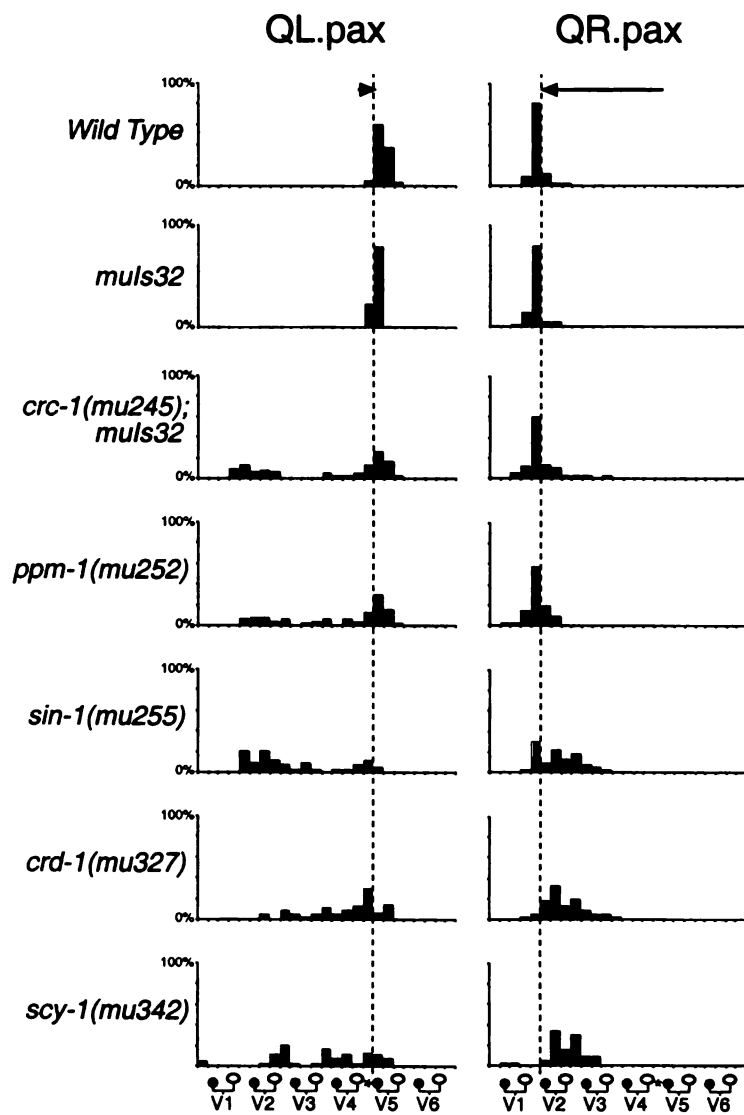


Figure 2-4. The distribution of the final positions of the migratory neurons BDU, ALM, CAN, and HSN in the cell migration mutants.

The positions of these cells are scored relative to the stationary Vn.a and Vn.p cells indicated on the x-axis. At least 28 sides were scored for each chart. Arrows indicate the extent and direction of cell migration, (*) indicates the starting positions of these cells and the dotted lines indicates the positions beyond which the migrations were considered wild-type position. In some animals, the migratory HSN cell was not found within the body; these are indicated separately by clear bars with dotted lines. This could be due the inability of HSN to migrate out of the posterior ganglion with high numbers of neurons, or to the absence of HSN.

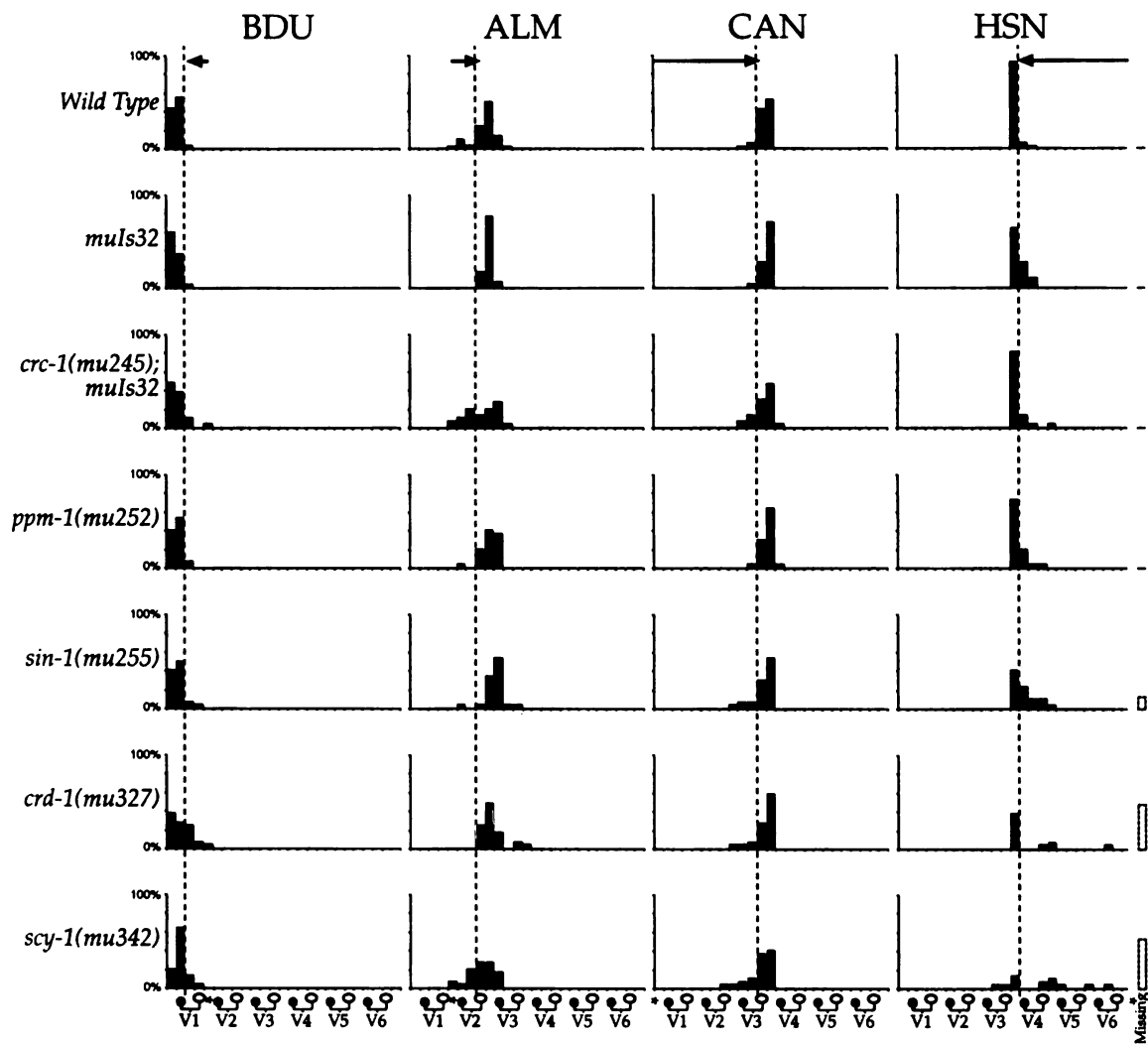


Figure 2-5. Cell migration mutants with axon outgrowth defects.

All panels show the posterior half of L1-L2 larvae. Anterior is to the left in all cases. (A) In wild-type animals, the PLM cell body is located in the posterior and sends an axon anteriorly to the mid-body. (B, C and D) In *qid-8(mu327)* animals, the PLM axons can exhibit defects and dorso-ventral guidance (B), premature shortening (C) and ectopic branch formation (D). (E and F) In *qid-9(mu342)* mutants, the PLM axon exhibits ectopic branch formation and dorso-ventral guidance defects. (G and H) In *lin-17(n671)* (G) and *lin-17(mu243)* (H) animals, the PLM axon stops prematurely. * indicates the position of the PLM cell body. Arrows indicate points of ectopic branch formation. Arrowheads indicate the position of premature axon truncation.

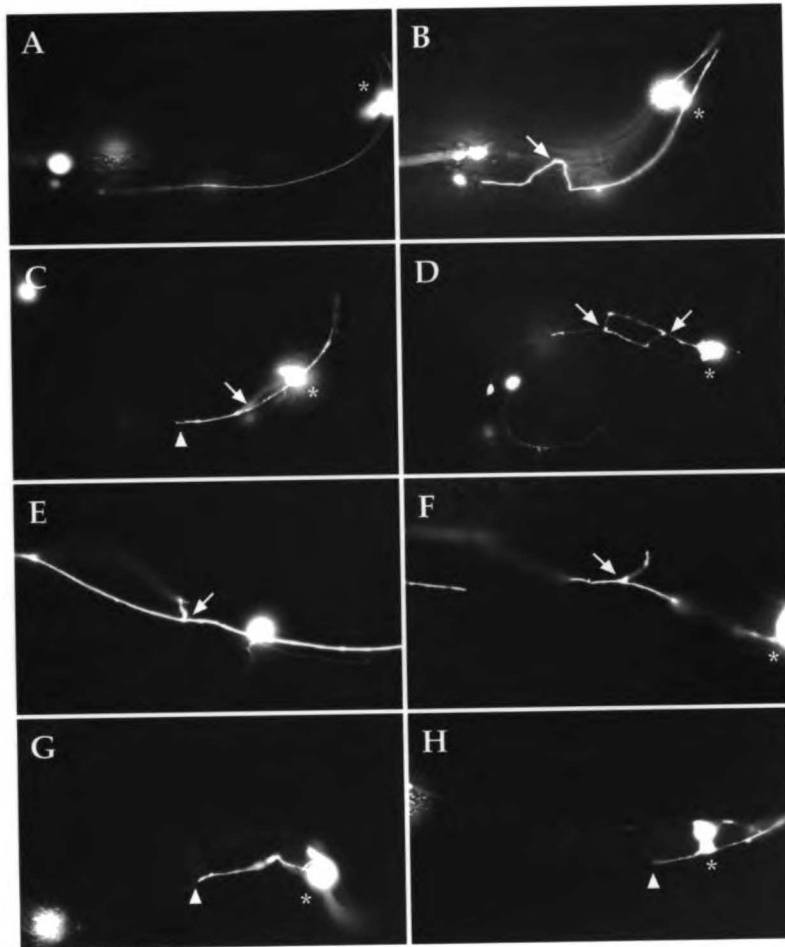


Figure 2-6. A genetic pathway for cell migrations in the QL and QR lineages.

The new genes described in this study are indicated in bold.

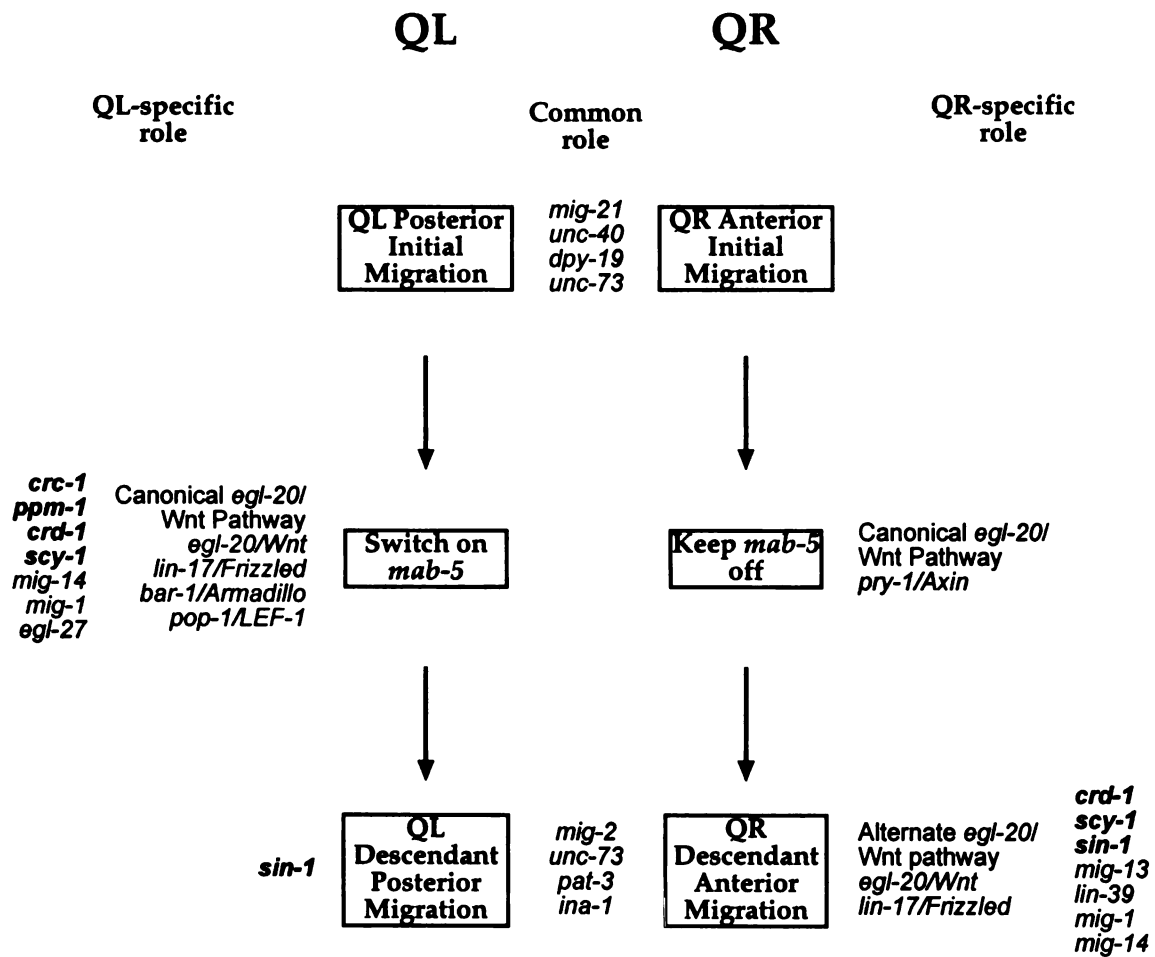


Table 2-1. New Mutations in known QL and QR cell migration genes

Gene	LG	No. of new alleles	New alleles
<i>mig-1</i>	I	4	<i>mu237, mu251, mu312, mu340</i>
<i>lin-17</i>	I	1	<i>mu243</i>
<i>mig-14</i>	II	3	<i>mu246, mu316, mu317</i>
<i>mab-5</i>	III	5	<i>mu247, mu250, mu308, mu318, mu319</i>
<i>egl-20</i>	IV	13	<i>mu234, mu241, mu253, mu254, mu259, mu309, mu310, mu320, mu323, mu332, mu333, mu341, mu344</i>
<i>bar-1</i>	X	5	<i>mu235, mu236, mu313, mu324, mu347</i>

LG – linkage group.

Table 2-2. New genes involved in the migrations of cells in the QL lineage

Gene	LG	Approximate Map Position (Fraction of Recombinants)	No. of Alleles	Alleles	Other Visible Phenotypes
<i>qid-5</i>	II	right of <i>maP1</i> [4.2] (1/17)	1	<i>mu245</i>	
<i>qid-6</i>	III	between <i>stP19</i> [-4.42] (1/18) and <i>stP17</i> [20.22] (5/18)	1	<i>mu252</i>	Bli, weak Dpy, Unc
<i>qid-7</i>	X	between <i>stP72</i> [6.5] (4/27) and <i>stP2</i> [24.0] (5/27)	2	<i>mu255</i> , <i>mu326</i>	
<i>qid-8</i>	X	between <i>stP103</i> [-1.3] (2/27) and <i>stP61</i> [5.0] (3/27)	1	<i>mu327</i>	Egl, Unc, Pvl, weak Dpy
<i>qid-9</i>	X	between <i>stP129</i> [2.2] (2/23) and <i>stP61</i> [5.0] (2/23)	1	<i>mu342</i>	Egl, Unc, Pvl, weak Dpy

LG refers to linkage group. Numbers in square brackets [] indicate the map position of the nearest marker(s) the mutation was mapped to; fractions in parentheses () indicate the frequency of recombinants between mutation and listed marker(s) derived in multi-point genetic mapping experiments (see Materials and Methods for a detailed list of recombinants scored). Phenotypes: Bli (blistered cuticle), Dpy (dumpy; short and fat), Unc (uncoordinated; movement defects), Egl (egg laying defective), Pvl (protruding vulva).

Table 2-3. Axon outgrowth phenotypes

Strain	mutant (%)	N	Phenotype
wild type	2	43	
(<i>muIs32</i>)			
wild type	3	63	
(<i>muIs35</i>)			
<i>qid-5(mu245)</i>	8	59	
<i>qid-6(mu252)</i>	7	91	
<i>qid-7(mu255)</i>	2	60	
<i>lin-17(mu243)</i>	62	50	PLM stops short
<i>lin-17(n671)</i>	61	49	PLM stops short
<i>qid-8(mu327)</i>	24	42	Extra branches in PLM axons, dorsal/ventral guidance defects in PLM, PVM and AVM
<i>qid-9(mu342)</i>	35	83	Extra branches in PLM and ALM axons, dorsal/ventral guidance defects in PLM and AVM

All strains contain *mec-7::GFP* (either *muIs32* or *muIs35*) for visualizing the axons of all the touch neurons. See Figure 2-5 for examples of abnormal axon outgrowth. *N* refers to number of sides scored.

Table 2-4. Male tail phenotypes

Strain	mutant (%)				Other Male Tail Phenotypes
	Hook	Spicules	Rays	<i>N</i>	
wild type	0	0	2 (1)	55	
<i>muIs32</i>	0	0	11 (1)	44	
<i>qid-5(mu245); muIs32</i>	0	2	7 (1)	42	
<i>qid-7(mu255)</i>	2	0	17 (1)	41	
<i>qid-6(mu252)</i>	7	0	47 (1-2)	30	Rays disorganized, ray fusion
<i>qid-8(mu327)</i>	82	7	100 (1-6)	28	Rays disorganized
<i>qid-9(mu342)</i>	95	64	100 (1-6)	22	Rays disorganized

All strains contain the *him-5(e1490)* mutation to spontaneously generate males.

Hook – frequency of missing or displaced hooks. Spicules – frequency of crumpled spicules. Rays – frequency of missing rays; the number in parenthesis indicates the number of missing rays seen in mutant cases. *N* refers to the number of sides scored.

Table 2-5. Expression of *mab-5::lacZ* in QL.d

Strain	<i>mab-5::lacZ</i> ON in QL.d (%)	<i>mab-5::lacZ</i> ON in QR.d (%)	N
wild type (<i>mulS3</i>)	100	0	40
wild type (<i>mulS4</i>)	95	1	107
<i>egl-20(n585); mulS3</i>	2	0	54
<i>egl-20(n585); mulS4</i>	3	0	35
<i>mulS32; mulS3</i>	94	0	35
<i>qid-5(mu245) mulS32</i>	38	0	42
<i>qid-6(mu252)</i>	61	0	51
<i>qid-7(mu255)</i>	87	0	55
<i>qid-8(mu327)</i>	72	0	61
<i>qid-9(mu342)</i>	47	0	60

All strains contain a *mab-5::lacZ* reporter (either *mulS3* or *mulS4*). N refers to the number of animals scored.

Table 2-6. Summary of mutant phenotypes

Strain	Cell Migrations						Axons	Male Tail
	QL	QR	BDU	ALM	CAN	HSN		
<i>qid-5(mu245)</i>	*			*				
<i>qid-6(mu252)</i>	*							*
<i>qid-7(mu255)</i>	*	^				*		
<i>qid-8(mu327)</i>	*	^				*	*	**
<i>qid-9(mu342)</i>	*	^				*	*	**

* indicates incompletely penetrant phenotype. ** indicates fully penetrant phenotype. ^ refers to a slight but reproducible posterior shift in the final position of the QR.pax cells.

This page has been left intentionally blank.

REFERENCES

- Anderson, P.** (1995). Mutagenesis. In *Caenorhabditis elegans: Modern Biological Analysis of an Organism*, vol. 48 (ed. D. C. Shakes), pp. 31-58. San Diego: Academic Press.
- Baum, P. D. and Garriga, G.** (1997). Neuronal Migrations and Axon Fasciculation Are Disrupted in *ina-1* Integrin Mutants. *Neuron* **19**, 51-62.
- Brenner, S.** (1974). The genetics of *C. elegans*. *Genetics* **77**, 71-94.
- Chalfie, M., Tu, Y., Euskirchen, G., Ward, W. W. and Prasher, D. C.** (1994). Green fluorescent protein as a marker for gene expression. *Science* **263**, 802-5.
- Chan, S. S., Zheng, H., Su, M. W., Wilk, R., Killeen, M. T., Hedgecock, E. M. and Culotti, J. G.** (1996). UNC-40, a *C. elegans* homolog of DCC (Deleted in Colorectal Cancer), is required in motile cells responding to UNC-6 netrin cues. *Cell* **87**, 187-95.
- Chisholm, A.** (1991). Control of cell fate in the tail region of *C. elegans* by the gene *egl-5*. *Development* **111**, 921-32.
- Clark, S. G., Chisholm, A. D. and Horvitz, H. R.** (1993). Control of cell fates in the central body region of *C. elegans* by the homeobox gene *lin-39*. *Cell* **74**, 43-55.
- Cowing, D. W. and Kenyon, C.** (1992). Expression of the homeotic gene *mab-5* during *Caenorhabditis elegans* embryogenesis. *Development* **116**, 481-90.
- Desai, C., Garriga, G., McIntire, S. L. and Horvitz, H. R.** (1988). A genetic pathway for the development of the *Caenorhabditis elegans* HSN motor neurons. *Nature* **336**, 638-46.
- Du, H. and Chalfie, M.** (2001). Genes regulating touch cell development in *Caenorhabditis elegans*. *Genetics* **158**, 197-207.

Eisenmann, D. M. and Kim, S. K. (2000). Protruding vulva mutants identify novel loci and Wnt signaling factors that function during *Caenorhabditis elegans* vulva development. *Genetics* **156**, 1097-116.

Eisenmann, D. M., Maloof, J. N., Simske, J. S., Kenyon, C. and Kim, S. K. (1998). The beta-catenin homolog BAR-1 and LET-60 Ras coordinately regulate the Hox gene *lin-39* during *Caenorhabditis elegans* vulval development. *Development* **125**, 3667-80.

Hacker, U., Lin, X. and Perrimon, N. (1997). The *Drosophila* *sugarless* gene modulates Wingless signaling and encodes an enzyme involved in polysaccharide biosynthesis. *Development* **124**, 3565-73.

Harris, J., Honigberg, L., Robinson, N. and Kenyon, C. (1996). Neuronal cell migration in *C. elegans*: regulation of Hox gene expression and cell position. *Development* **122**, 3117-31.

Hedgecock, E. M., Culotti, J. G., Hall, D. H. and Stern, B. D. (1987). Genetics of cell and axon migrations in *Caenorhabditis elegans*. *Development* **100**, 365-82.

Herman, M. (2001). *C. elegans* POP-1/TCF functions in a canonical Wnt pathway that controls cell migration and in a noncanonical Wnt pathway that controls cell polarity. *Development* **128**, 581-90.

Hodgkin, J. (1997). Appendix 1 - Genetics. In *C. elegans II*, (ed. J. R. Priess), pp. 882-1047. Cold Spring Harbor: Cold Spring Harbor Laboratory Press.

Honigberg, L. and Kenyon, C. (2000). Establishment of left/right asymmetry in neuroblast migration by UNC-40/DCC, UNC-73/Trio and DPY-19 proteins in *C. elegans*. *Development* **127**, 4655-68.

Johnstone, I. L. (2000). Cuticle collagen genes. Expression in *Caenorhabditis elegans*. *Trends Genet* **16**, 21-7.

- Kenyon, C.** (1986). A gene involved in the development of the posterior body region of *C. elegans*. *Cell* **46**, 477-87.
- Korswagen, H. C., Coudreuse, D. Y., Betist, M. C., van de Water, S., Zivkovic, D. and Clevers, H. C.** (2002). The Axin-like protein PRY-1 is a negative regulator of a canonical Wnt pathway in *C. elegans*. *Genes Dev* **16**, 1291-302.
- Lewis, J. A. and Fleming, J. T.** (1995). Basic Culture Methods. In *Caenorhabditis elegans: Modern Biological Analysis of an Organism*, vol. 48 (ed. D. C. Shakes), pp. 3-29. San Diego: Academic Press.
- Maloof, J. N., Whangbo, J., Harris, J. M., Jongeward, G. D. and Kenyon, C.** (1999). A Wnt signaling pathway controls *Hox* gene expression and neuroblast migration in *C. elegans*. *Development* **126**, 37-49.
- Peters, K., McDowall, J. and Rose, A. M.** (1991). Mutations in the *bli-4* (I) locus of *Caenorhabditis elegans* disrupt both adult cuticle and early larval development. *Genetics* **129**, 95-102.
- Salser, S. J. and Kenyon, C.** (1992). Activation of a *C. elegans Antennapedia* homologue in migrating cells controls their direction of migration. *Nature* **355**, 255-8.
- Salser, S. J. and Kenyon, C.** (1996). A *C. elegans Hox* gene switches on, off, on and off again to regulate proliferation, differentiation and morphogenesis. *Development* **122**, 1651-61.
- Savage, C., Hamelin, M., Culotti, J. G., Coulson, A., Albertson, D. G. and Chalfie, M.** (1989). *mec-7* is a beta-tubulin gene required for the production of 15-protofilament microtubules in *Caenorhabditis elegans*. *Genes Dev* **3**, 870-81.
- Sawa, H., Lobel, L. and Horvitz, H. R.** (1996). The *Caenorhabditis elegans* gene *lin-17*, which is required for certain asymmetric cell divisions, encodes a putative

seven-transmembrane protein similar to the *Drosophila* frizzled protein. *Genes Dev* **10**, 2189-97.

Sternberg, P. W. and Horvitz, H. R. (1988). *lin-17* mutations of *Caenorhabditis elegans* disrupt certain asymmetric cell divisions. *Dev Biol* **130**, 67-73.

Sulston, J. E., Albertson, D. G. and Thomson, J. N. (1980). The *Caenorhabditis elegans* male: postembryonic development of nongonadal structures. *Dev Biol* **78**, 542-76.

Sulston, J. E. and Horvitz, H. R. (1977). Post-embryonic cell lineages of the nematode, *Caenorhabditis elegans*. *Dev Biol* **56**, 110-56.

Sulston, J. E., Schierenberg, E., White, J. G. and Thomson, J. N. (1983). The embryonic cell lineage of the nematode *Caenorhabditis elegans*. *Dev Biol* **100**, 64-119.

Sym, M., Robinson, N. and Kenyon, C. (1999). MIG-13 positions migrating cells along the anteroposterior body axis of *C. elegans*. *Cell* **98**, 25-36.

Thacker, C., Peters, K., Srayko, M. and Rose, A. M. (1995). The *bli-4* locus of *Caenorhabditis elegans* encodes structurally distinct *kex2*/subtilisin-like endoproteases essential for early development and adult morphology. *Genes Dev* **9**, 956-71.

Walsh, E. C. and Stainier, D. Y. (2001). UDP-glucose dehydrogenase required for cardiac valve formation in zebrafish. *Science* **293**, 1670-3.

Wang, B. B., Muller, I. M., Austin, J., Robinson, N. T., Chisholm, A. and Kenyon, C. (1993). A homeotic gene cluster patterns the anteroposterior body axis of *C. elegans*. *Cell* **74**, 29-42.

Whangbo, J. and Kenyon, C. (1999). A Wnt signaling system that specifies two patterns of cell migration in *C. elegans*. *Mol Cell* **4**, 851-8.

Williams, B. D. (1995). Genetic Mapping with Polymorphic Sequence-Tagged Sites. In *Caenorhabditis elegans: Modern Biological Analysis of an Organism*, vol. 48 (ed. D. C. Shakes), pp. 81-97. San Diego: Academic Press.

Williams, B. D., Schrank, B., Huynh, C., Shownkeen, R. and Waterston, R. H. (1992). A genetic mapping system in *Caenorhabditis elegans* based on polymorphic sequence-tagged sites. *Genetics* **131**, 609-24.

Wood, W. B. (1988). *The Nematode Caenorhabditis elegans*. New York: Cold Spring Harbor Laboratory.

Zipkin, I. D., Kindt, R. M. and Kenyon, C. J. (1997). Role of a new Rho family member in cell migration and axon guidance in *C. elegans*. *Cell* **90**, 883-94.

**Chapter 3: The Roles Of The Genes *mig-21*, *ptp-3*, and *mig-15*
In Establishing the Left-Right Asymmetry of Q Neuroblast
Migration In *C. elegans***

ABSTRACT

The QL and QR neuroblasts are bilaterally symmetric homologs that polarize and migrate in opposite directions along the anterior-posterior body axis. QL and its descendants migrate towards the posterior, whereas QR and its descendants migrate towards the anterior. The netrin receptor UNC-40 and the novel transmembrane protein DPY-19 are required for the early asymmetry of the Q cells. The Hox gene *mab-5* is expressed in QL, but not QR, and is necessary and sufficient for the posterior migrations of cells in the QL lineage.

mig-21 and the LAR-like phosphatase *ptp-3* were characterized and were found to be required for the asymmetric polarizations and migrations of the Q cells. *mig-21* was cloned and found to encode a novel transmembrane protein that is specifically expressed in the Q cells during their migrations. Thus, MIG-21 may act as a receptor within the Q cells to guide their migrations. *mig-15*, a STE20/NIK ortholog, was characterized and found to be required for the migrations, but not the polarizations, of the Q cells. *mig-15* also appears to be required for *mab-5* expression specifically in the QL lineage.

INTRODUCTION

The development of a multicellular organism requires numerous cell rearrangements, cell shape changes, and the migrations of cells and growth cones along well-defined and often complex trajectories. These cell migrations invariably must be carried out with exquisite precision. Studies in a number of model systems have elucidated various mechanisms underlying cellular responses to migratory stimuli. For example, neutrophils respond to chemoattractive stimuli by polarizing and then migrating towards the attractant. This process involves the activation of a PI3K feedback loop localized at the leading edge of the migrating cell (Rickert et al., 2000; Wang et al., 2002; Weiner et al., 2002). In the nematode *C. elegans*, commissural axons travel along circumferential migratory paths guided by the signaling molecule netrin/UNC-6, and its receptors UNC-40 and UNC-5 (Chan et al., 1996; Hamelin et al., 1993; Hedgecock et al., 1990; Ishii et al., 1992; Wadsworth et al., 1996; Wadsworth and Hedgecock, 1996). The nematode *C. elegans* is an ideal model organism in which to study cell migration, for a number of reasons. Firstly, the animal is transparent, allowing the visualization of individual cells as they undertake their migrations *in vivo*. In addition, the complete cell lineage is precisely known and is invariant between animals. Furthermore, the fully sequenced *C. elegans* genome allows for extensive genetic analysis. Various cell migrations take place during *C. elegans* embryonic and post-embryonic development: the left-right asymmetric migrations of the Q neuroblasts are of particular interest as they provide an entry point into several aspects of cell migration and asymmetry.

The QL and QR neuroblasts are left-right homologs that divide identically to give rise to identical neuron types, but which migrate in opposite directions

(Chalfie and Sulston, 1981; Sulston and Horvitz, 1977)(Figure 3-1). QL and QR are born in bilaterally symmetric positions along the anteroposterior axis of the worm, QL on the left and QR on the right. Shortly after hatching, the cells display a striking asymmetry: QL sends out a long cytoplasmic projection dorsally and to the posterior, whereas QR sends out a projection dorsally and to the anterior. The Q cell nuclei and cell bodies then migrate into these projections, QL to the posterior and QR to the anterior. This asymmetry is then further reinforced by the expression of the Hox gene *mab-5* in QL, but not QR. *mab-5* expression is both necessary and sufficient for posterior migration of the Q descendants (Harris et al., 1996; Salser and Kenyon, 1992). QL and QR undergo an identical series of cell divisions and programmed cell deaths to give rise to 3 neurons: AQR, AVM, and SDQR on the right, and PQR, PVM, and SDQL on the left. The Q cells thus provide an entry point into the investigation of many questions in cell polarization and migration: what is the signal that instructs the Q cells to polarize? how do the cells detect and respond to this signal? how is this information relayed to the actin cytoskeleton to generate movement? why do the left and right cells migrate in opposite directions?

Previous studies have identified several genes that are involved in establishing the early asymmetry of the Q cells. The transmembrane protein DPY-19 and the netrin receptor UNC-40 are required for the correct asymmetry of Q cell polarization (Honigberg and Kenyon, 2000). In *unc-40* or *dpy-19* mutants, the Q cells polarize randomly, and the cells fail to migrate. This randomization is also manifested in the stochastic expression of *mab-5* in these mutants: either QL or QR can express *mab-5*. Interestingly, neither the netrin UNC-6 nor the UNC 40 co-receptor UNC 5 appears to be required for this initial

asymmetry (Honigberg and Kenyon, 2000). The cell motility genes *unc-73* and *mig-2* are required for the early migrations, although the initial L/R asymmetry of the polarizations is preserved in these mutants. Thus *unc-40* and *dpy-19* are required for the establishment of asymmetry, and information from their gene products is relayed to *mig-2* and *unc-73* to generate cell movement. Clearly, the identification of additional genes in this pathway is necessary to further understand how Q cell asymmetry is established.

This work describes the phenotypic characterization of three genes required for the L/R asymmetry of the Q cells: *mig-21*, *ptp-3*, and *mig-15*. Mutations in *mig-21* and *ptp-3* disrupt the polarizations and migrations of the Q cells and their descendants, resulting in a left-right randomization. *mig-21* encodes a novel transmembrane protein expressed in the Q cells at the time of their migrations, suggesting that MIG-21 may act as a receptor or co-receptor for an as yet unidentified signal that instructs the Q cells to polarize asymmetrically. *ptp-3* encodes a LAR-like phosphatase whose role in epidermal morphogenesis in the worm has been described elsewhere (Harrington et al., 2002). LAR family phosphatases have also been shown to have roles in axon guidance and outgrowth, and actin filament reorganization during oogenesis (Baker and Macagno, 2000; Bateman et al., 2001; Desai et al., 1996; Desai et al., 1997; Frydman and Spradling, 2001; Garrity et al., 1999; Harrington et al., 2002; Krueger et al., 1996; Tian et al., 1991; Wills et al., 1999; Yang et al., 1991). The role of LAR in guiding axons during outgrowth and target recognition has been best described for *Drosophila* photoreceptor axon targeting and motor axon guidance. Motor axons in *Dlar* mutant embryos fail to synapse onto the ventral muscles, and instead bypass their normal target region (Desai et al., 1997; Krueger et al.,

1996). Dlar mutants also have marked defects in photoreceptor axon targeting: specifically, R1-R6 photoreceptor axons target to the lamina correctly, but fail to choose the correct pattern of target neurons (Clandinin et al., 2001). Dlar functions cell-autonomously for this process, and also appears to have both cell-autonomous and cell-nonautonomous roles in the projection of the photoreceptor R7 (Clandinin et al., 2001; Maurel-Zaffran et al., 2001).

Interestingly, Lar appears to have a role in the modulation of cell adhesion in axon targeting – photoreceptor axons in Dlar mutants initially project into the appropriate layer, but later retract (Clandinin et al., 2001; Maurel-Zaffran et al., 2001). This is supported by the observation that Dlar interacts with β -integrin to coordinate actin filaments at the basal surface of the follicular epithelium and to control the polarization of somatic follicle cells (Bateman et al., 2001; Frydman and Spradling, 2001). Other downstream effectors of Lar also point to a role in organizing the actin cytoskeleton. *Drosophila* Abl, an intracellular kinase, and its target Ena, a well-characterized regulator of actin cytoskeletal dynamics (Gertler et al., 1996; Renfranz and Beckerle, 2002), bind directly to the Dlar cytoplasmic domain. Abl also acts as a strong suppressor of the Dlar mutant phenotype. Furthermore, Abl and Ena can act as substrates for Dlar *in vitro* (Wills et al., 1999).

Mutations in *mig-15* do not affect the asymmetric polarizations of the Q cells, but shorten their migrations and disrupt *mab-5* expression. Thus, MIG-15 appears to have a general role in cell motility and a specific role in the control of *mab-5* expression in the QL lineage.

RESULTS

***mig-21* and *ptp-3* are required for asymmetric Q cell polarization and migration**

Candidate mutants from a large scale Q descendant (Q.pax) migration screen (Ch'ng et. al., submitted, see Chapter 2) were examined for defects in the early migrations of the Q cells at 3-4 hours after hatching. Mutations in *mig-21* and *ptp-3* were found to affect these migrations (Figure 3-3). This phenotype has been reported previously for *mig-21* (Du and Chalfie, 2001). *ptp-3*, a gene required for epidermal morphogenesis (Harrington et al., 2002), has not previously been reported to affect the migrations of the Q cells or their descendants. In these strains, the migrations of the Q nuclei were shortened or completely blocked in most animals. Additionally, both QL and QR could migrate in either direction, indicating that the L/R asymmetry of these migrations had been disrupted in these mutants. This suggested that mutations in *mig-21* and *ptp-3* may also affect asymmetric polarizations of the Q cells in addition to the cell migrations. To observe the polarizations of the Q cells prior to their migrations, *muIs57* (*scm::GFP::CAAX*, Figure 3-2), a membrane localized GFP construct, was introduced into *mig-21(mu238)* and *ptp-3(mu256)* mutant backgrounds. The shapes of the Q cells were then recorded approximately 2-3 hours after hatching, before they underwent their first cell division (Figure 3-4). The Q cells were found to be polarized randomly in both *mig-21(mu238)* and *ptp-3(mu256)* animals. Whereas QL always polarizes strongly to the posterior in wild type, QL could polarize, strongly or weakly, in either direction or remain unpolarized in *mig-21(mu238)* animals. A similar QL polarization phenotype, although less penetrant, was observed in *ptp-3(mu256)* animals. Similarly, QR,

which always polarizes strongly to the anterior in wild-type animals, could polarize in either direction or remain unpolarized in both *mig-21(mu238)* and *ptp-3(mu256)* animals.

Q cells can change direction of polarization in *mig-21* and *ptp-3* mutant animals

The randomized polarizations observed in *mig-21* and *ptp-3* mutants may be explained in two ways: either some cells always polarize to the anterior and some cells always to the posterior; or a Q cell may change direction of polarization over time in a single animal. To determine whether Q cells are able to change their direction of polarization, single animals were monitored over time and snapshots of the Q cells taken at 15-20 minute intervals, from hatching until the Q cells divided. Various phenotypes were observed for both *mig-21* and *ptp-3* mutants (Figure 3-5). For example, the Q cells could extend and retract a process in a single direction, either anterior or posterior (i.e. the extent, but not direction of polarization changed in a single animal). In addition, a cell could remain unpolarized until its division. Finally, a cell could reverse its direction of polarization over time, first polarizing to the anterior, then to the posterior, or *vice versa*.

***mig-15* is required for Q cell migration but is not required for polarization**

mig-15 has been reported previously as having Q.pax migration defects on both the left and right sides of the animal (Zhu, 1998). These later migration defects may result from defects in the initial migrations of the Q neuroblasts. To investigate this possibility, Q cells were scored at the point of their first cell

division as described above. The migrations of the Q cells were found to be shortened relative to those observed in wild type (Figure 3-3). Unlike *mig-21* and *ptp-3* mutants, however, the Q cells always migrate in the correct direction in *mig-15(rh80)* animals. Examination of the Q cells 3 hours after hatching showed that the Q cells still polarize fully in the correct direction in *mig-15(rh80)* animals (Figure 3-4). This indicates that *mig-15* is not required to establish the left-right asymmetry, but rather appears to be involved in cell motility.

The migrations of the Q.pax cells are defective in *mig-21*, *ptp-3*, and *mig-15* mutant animals

mig-21(mu238) and *ptp-3(mu256)* were isolated in a screen for mutants with misplaced Q.pax cells. The positions of these cells in N2, *mig-21(mu238)*, and *ptp-3(mu256)* are shown in Figure 3-6a. In wild-type animals, the QL.pax cells always remain in the posterior near the stationary seam cells V5.a and V5.p. In *mig-21(mu238)* or *ptp-3(mu256)* animals, however, these cells can be found in various positions along the anterior-posterior axis of the animal. Similarly, on the right, the QR.pax cells are spread throughout the body axis in *mig-21(mu238)* and *ptp-3(mu256)* mutants, instead of being located exclusively in the anterior, as they are in N2.

***mab-5* is required for the Q descendants to remain in the posterior in *mig-21*, *ptp-3*, and *mig-15* mutants**

In order to determine whether *mab-5* is required for the Q.pax cells to remain in the posterior in *mig-21*, *ptp-3* and *mig-15* mutants, double mutants were

constructed. In all double mutant strains examined, *ptp-3(mu256); mab-5(e2088)* *mig-21(mu238) mab-5(e2088)* and *mab-5(e2088); mig-15(rh80)* all of the Q descendants, on both the left and right sides, migrate to a position anterior to their birthplace (Figure 3-6c) . This suggests that in the single mutants, the cells that remain in the posterior, on both the left and the right sides, do so because they express *mab-5*.

Mutations in *mig-21* specifically disrupt Q cell migration, whereas mutations in *ptp-3* affect other neuronal migrations

The positions of other migratory neurons in *mig-21(mu238)* and *ptp-3(mu256)* animals were determined in order to examine whether the migration defect was specific to the Q lineage, or whether it represented a more general defect. These neurons include the hermaphrodite-specific neurons (HSNs) that migrate from the tail of the worm to the mid-body, the canal-associated neurons (CANs) and anterior lateral microtubule neurons (ALMs) that migrate from the head to the mid-body, and the BDU neurons that make a short anterior migration near the head (Sulston et al., 1983). Each of these migrations occurs during late embryogenesis. The neurons are all bilateral and show no apparent left/right asymmetry in their migrations. Cell body positions were examined in 50 animals. No defects were observed in *mig-21(mu238)* animals, indicating that *mig-21* is specifically required for migrations in the Q lineage (data not shown). The positions of the ALM neurons were anteriorly misplaced in a small number of *ptp-3(mu256)* animals, indicating that the ALM migrations are somewhat shortened in this strain. HSN and BDU cell body positions were normal in *ptp-3(mu256)* animals.

Mutations in *unc-40* and *ptp-3* enhance the Q descendant migration phenotype of *mig-21* mutants

unc-40(e1430) and *ptp-3(mu256)* have migration defects in the Q lineage very similar to those of *mig-21(mu238)*. This raises the strong possibility that all of these genes act in the same genetic pathway to control Q cell polarization and migration. To investigate this possibility, the *unc-40(e1430); mig-21(mu238)* and *ptp-3(mu256); mig-21(mu238)* double mutants were constructed, and the positions of the Q.pax cells were scored in these double mutant strains. The *unc-40(e1430); ptp-3(mu256)* double mutant appears to be inviable (see Discussion). It was found that mutations in *unc-40* or *ptp-3* have synergistic effects on the positions of the Q.pax cells in a *mig-21* mutant background.

In *unc-40(e1430); mig-21(mu238)* animals, the Q.pax cells are shifted to a more anterior position than is observed in either single mutant alone (Figure 3-6b). This effect is observed for both QL.pax and QR.pax, but is stronger for QL.pax. In *unc-40(e1430); mig-21(mu238)*, 7.1% of the QL.pax cells were posterior to V3.p, compared with 85.3% of cells in *unc-40(e1430)*, and 33.2% of cells in *mig-21(mu238)*. For the QR.pax cells, 3.6% of the cells remained in the posterior in *unc-40(e1430); mig-21(mu238)*, compared with 8% of cells in both *unc-40(e1430)* and *mig-21(mu238)*. This suggests that *mig-21* and *unc-40* may act in parallel genetic pathways to position the Q descendants.

In *ptp-3(mu256); mig-21(mu238)* animals, the QR.pax cells are shifted to a more posterior position than is observed in either single mutant alone (Figure 3-6b). In *ptp-3(mu256); mig-21(mu238)* animals, 42% of the QR.pax cells were posterior to V3.p, compared with 8% in *mig-21(mu238)*, and 2% in *ptp-3(mu256)*.

The phenotype of the *ptp-3(mu256); mig-21(mu238)* double mutant is strongly suggestive of a completely randomized phenotype, indicating that perhaps all elements of a signal transduction pathway have now been removed and the cells are truly behaving as though no external signal is being detected.

***mig-21* encodes a novel transmembrane protein with thrombospondin type I domains**

mig-21 was cloned using standard positional mapping and transformation rescue techniques (see Experimental Procedures). *mig-21* encodes a predicted single-pass transmembrane protein with two thrombospondin type I domains in the extracellular portion of the protein. The positions of 8 molecular lesions associated with *mig-21* mutations are shown in Figure 3-7c. The *mu238* mutation is an early stop in the intracellular portion of the protein. All other mutations shown had similar defects in the migrations of the Q descendants, suggesting that all alleles may represent loss-of-function alleles. Deficiency analysis was unable to confirm this, as the only deficiency that covers the *mig-21* locus was unstable.

The intracellular domain is quite small (38 amino acids) and contains no conserved domains or motifs. A partial cDNA containing most of the predicted gene and the 3'-UTR was isolated using RT-PCR (3'-RACE - see Experimental Procedures). This was found to differ from the AceDB predicted gene in the splicing pattern at the final exon. This difference in splicing also introduces a frameshift relative to the predicted gene, resulting in a different amino acid sequence at the C-terminus of the protein. Interestingly, no signal sequence was detected for the predicted *mig-21* gene product. A search for such a signal

sequence was conducted by manually translating the region immediately downstream of every start codon 4kb upstream of the predicted open reading frame. One such signal was identified and primers were designed to amplify DNA from this potential start site, but no PCR product was obtained. Thus, MIG-21 may lack a signal peptide. This has been observed previously – most notably, UNC-5, a single-pass type I transmembrane protein with Ig and TSP-1 domains, also seems to lack a signal peptide.

***mig-21* is expressed in the Q cells at the time of their migrations**

In order to determine where *mig-21* is expressed, transcriptional, N-terminal translational, and C-terminal translational *mig-21::GFP* transgenes were constructed. The C-terminal translational construct was found to have partial rescuing activity in 1/27 lines, however, many animals were observed in which the Q cells had failed to divide by the end of L1 (data not shown). This suggests that the presence of the GFP is disrupting the function of MIG-21 in these lines. The N-terminal translational construct was found to have partial rescuing activity in 1/5 lines (data not shown). In lines obtained with the translational construct, *mig-21::GFP* was expressed in both QL and QR at the time of their migration (2-4 hours after hatching). No other GFP expressing cells were observed in early L1 in the rescuing line, strongly suggesting that *mig-21* functions within the polarizing and migrating Q cell. Curiously, no expression in the Q cells was observed for the transcriptional fusion (data not shown), indicating that essential regulatory sequences are present in one or more of the introns. In the C-terminal translational construct, *mig-21* expression was also observed later in development - during the L2 larval stage in the posterior

daughters of the seam cell V5, and in the postdereid, a non-migratory neuronal structure descended from the V5.p cells. While expression in the postdereid was observed in the N-terminal translational construct, no expression in V5.p was noted, therefore its significance is unclear. It is worth noting that the level of expression observed for the N-terminal construct was much lower than was seen for the C-terminal construct.

DISCUSSION

***mig-21* and *ptp-3* are required for the early asymmetry of the Q cells**

This work found that mutations in *mig-21* and *ptp-3* disrupt the earliest asymmetry of the Q neuroblasts. Specifically, the polarizations of the Q cells appear to be randomized and compromised in these mutants, as though they have lost the ability to sense a directional cue. Instead of polarizing in the wild-type direction, each cell sends out only a short projection in a random direction, and the direction of this projection can change over time. This phenotype is identical to that observed in *unc-40* and *dpy-19* mutants, suggesting that *unc-40*, *dpy-19*, *mig-21*, and *ptp-3* may be part of a signaling pathway necessary to respond to a guidance signal that instructs the Q cells to polarize asymmetrically. Mutations in these genes also result in a randomization of the Q migrations: the cells typically migrate a significantly shorter distance than in wild type, and these shortened migrations can be in either direction, anterior or posterior.

mig-21 encodes a predicted single pass transmembrane protein with two TSP-1 domains in the extracellular portion of the protein. In addition, *mig-21* is expressed specifically in the polarizing and migrating Q cells – indeed, *mig-21::GFP* was not observed in any other cells or tissues early in L1. This suggests

that MIG-21 may act as a receptor for an as yet unidentified ligand that instructs the Q cells to polarize and migrate. The role of the netrin receptor UNC-40 in Q migrations has been described previously, and has also been proposed to function as a receptor in the Q cells to guide their migrations (Honigberg and Kenyon, 2000). Alternatively, UNC-40 may be acting outside the Q cells to guide their migrations. *unc-40::GFP* is expressed in the Q cells and in the commissural axons which run along the circumference of the worm. Although UNC-40 has been shown to function cell-autonomously in commissural axon guidance (Chan et al., 1996), it is possible that it may also have a cell-nonautonomous function in the Q cells. Mosaic analysis or cell-specific promoter fusions could be used to address this issue.

One possible explanation for the existence of two receptor-like proteins guiding the Q cells is that UNC-40 and MIG-21 are acting as co-receptors in the migrating cells. For example, UNC-40 is known to act as a co-receptor with UNC-5, a transmembrane protein containing two TSP-1 domains and two Ig domains, in the guidance of dorsally directed migrations away from a ventral source of the secreted UNC-6 signal (Hamelin et al., 1993; Hedgecock et al., 1990; Leung-Hagesteijn et al., 1992). Mutations in both *mig-21* and *unc-40* result in a Q descendant migration phenotype stronger than in either single mutant. Specifically, the QL.pax cells and the QR.pax cells are shifted anteriorly with respect to *unc-40* or *mig-21* single mutants. This suggests a partial redundancy in gene function between *unc-40* and *mig-21*, indicating that these genes may act in parallel or partially parallel pathways. This has also been observed with *unc-40* and *unc-5* in the guidance of distal tip cell migration – UNC-40 and UNC-5 can partially substitute for one another as receptors in the guidance of the DTCs

(Merz et al., 2001). The genetic interaction between *mig-21* and *unc-40* also suggests that their protein products may be acting as co-receptors, again, by analogy with the interactions between *unc-5* and *unc-40*.

Mutations in *ptp-3* result in a similar Q polarization and migration phenotype as is observed for *mig-21* and *unc-40* mutants. *ptp-3* encodes a LAR-like receptor protein tyrosine phosphatase (Harrington et al., 2002). LAR-like phosphatases have been implicated in numerous cell biological processes, including axon outgrowth, guidance and fasciculation (Baker and Macagno, 2000; Desai et al., 1996; Desai et al., 1997; Krueger et al., 1996; Sun et al., 2000; Wills et al., 1999), axon target recognition (Clandinin et al., 2001; Garrity et al., 1999; Maurel-Zaffran et al., 2001), planar polarity in the follicular epithelium in *Drosophila* (Bateman et al., 2001; Frydman and Spradling, 2001), and early embryonic morphogenesis in the worm (Harrington et al., 2002). Mutations in *ptp-3* result in defects in embryonic morphogenesis at low penetrance (Harrington et al., 2002). These defects are a result of neuroblast and epidermal cell movements during embryogenesis, and the phenotype is enhanced by mutations in the Eph receptor *vab-1* (Harrington et al., 2002).

What is the role of *ptp-3* in directing the polarizations and migrations of the Q cells? *ptp-3* is expressed in the Q cells during their migrations, as well as surrounding tissues (Harrington et al., 2002). Therefore, *ptp-3* could be acting either cell-autonomously or cell-non-autonomously to guide Q cell migration. The *Drosophila* homolog of *ptp-3*, *Dlar*, appears to have both cell-autonomous and cell-nonautonomous roles in the projection of the photoreceptor R7 (Clandinin et al., 2001; Maurel-Zaffran et al., 2001), thus there is precedent for either model. This issue could be clarified with tissue-specific promoter fusions.

ptp-3 shows a marked genetic interaction with *mig-21*: the double mutant has a QR descendant phenotype significantly stronger than that of either single mutant. Interestingly, the Q descendant phenotype of *ptp-3(mu256); mig-21(mu238)* strongly resembles a complete randomization of the direction of migration of QL and QR, with approximately half of the cells on either side remaining in the posterior, and half of the cells migrating into the anterior. There is also a slight enhancement of the Q migration phenotype: in the double mutant, more cells remain in their birth position and divide without migrating. This enhancement suggests that *mig-21* and *ptp-3* have partially redundant roles in guiding Q cell migration. One possibility is that *ptp-3* acts on *mig-21* and another substrate in the Q migration pathway. A good candidate for this other substrate may be *unc-40*. All attempts to isolate an *unc-40; ptp-3* double mutant in this work were unsuccessful, implying that the two genes have a strong genetic interaction. A strongly enhanced lethal phenotype in *unc-40; ptp-3* is probable: eggs isolated from a putative *unc-40; ptp-3 +/+ bli-1* heterozygous mutant animal failed to hatch at a far greater rate than was observed in either *unc-40; bli-1* or *ptp-3* mutants. That *unc-40* and *ptp-3* have a strong genetic interaction for viability suggests that they may also interact in Q cell migration.

Notably, none of these genes has provided any insight into the left-right asymmetry of the Q cells, although all of the genes affect the earliest visible asymmetry. Broadly, there are two models for the asymmetry of the Q cells in which the location of a single polarizing signal governs the left-right differences: the signal itself, still unidentified, may be left-right asymmetrically localized, and the Q cells respond in the same fashion to this signal; alternatively, the Q cells have different responses, one attractive and one repulsive, to a left-right

symmetric signal (Figure 3-9). In the latter model, one of the Q cells may contain a factor or factors that modulates the response to the polarizing signal, as in the modulation of UNC-40 by UNC-5 in the response to UNC-6. The latter model would also predict the existence of one or more genes which, when mutated, would affect only one of the Q cells. Alternatively, QL and QR may be responding to two different polarizing signals.

The role of *mig-15* in Q cell migration: cell motility and *mab-5* expression

In contrast to *mig-21* and *ptp-3* mutants, *mig-15* mutants are able to polarize appropriately. This indicates that *mig-15* acts downstream of the directional guidance pathway, and is required for the motility of the Q cells rather than for their guidance, since the migrations are shortened in *mig-15* mutants, but are always in the correct direction. *mig-15* encodes the sole *C. elegans* member of the STE20/NIK/GCK family of serine/threonine kinases (Zhu, 1998). *mig-15* mutants are highly pleiotropic, revealing a role for *mig-15* in a variety of processes. Mutations in *mig-15* result in defects in several cell migrations, outgrowth of the excretory canals, muscle positioning, and muscle arm targeting. *mig-15* mutants also have more general defects – mutants have a protruding vulva (Pvl) or occasionally have an ectopic lateral vulva or several pseudo-vulvae (Muv), are egg-laying defective (Egl), and display uncoordinated movement (Unc) (Zhu, 1998). This array of phenotypes underscores the importance of *mig-15* in several cellular events.

MIG-15 has a dual function in the regulation of cell dynamics and the control of gene transcription (review ref). The function of MIG-15 in cell motility is mediated through integrins, heterodimeric ($\alpha\beta$) transmembrane receptors for

ECM molecules (Poinat et al., 2002). Integrins have a critical role in the regulation of cellular adhesion to a substrate, and are also required for signaling from the environment. MIG-15 binds directly to the cytoplasmic portions of both INA-1, the single α -integrin present in the *C. elegans* genome, and PAT-3, a β -integrin (Poinat et al., 2002). The relevance of this physical interaction is supported by the observation that RNAi of *pat-3* or *ina-1* in a *mig-15* reduction of function background, or double mutant analysis using reduction of function alleles of *ina-1* and *mig-15*, results in an enhancement of commissural axon guidance defects observed in the single mutants. Neuronal-specific RNAi of *mig-15* or *pat-3* also produces these defects, indicating that *mig-15* and *pat-3* act cell-autonomously in axon guidance (Poinat et al., 2002). RNAi and double mutant analysis also suggests a genetic interaction between *mig-15* and the small GTPases *ced-10*, *rac-2* and *mig-2*, further supporting a role for *mig-15* function in the regulation of the actin cytoskeleton (Poinat et al., 2002).

The role of *ina-1* in Q cell migration has been described previously elsewhere (Baum and Garriga, 1997). Mutations in *ina-1* cause defects in many cell migrations, and all of these migrations occur more slowly than in wild type (Baum and Garriga, 1997). INA-1 acts cell-autonomously for Q cell migrations, and functions with PAT-3 as a heterodimer (Baum and Garriga, 1997), consistent with the results described above. Thus, MIG-15 appears to act in concert with INA-1 and PAT-3 to regulate cell adhesion and motility. This is supported by the finding that a *mig-15::GFP* expression construct is localized to adherens junctions in migrating cells (Zhu, 1998).

As well as regulating cell motility and adhesion, STE20/NIK kinases have been shown to activate the SAPK/JNK family of MAP kinases. The SAPK/JNK

pathway functions to inhibit cell growth and promotes cell death in the presence of an external stress stimulus such as heat shock, UV- or γ - radiation, or inflammatory cytokines. A MAP kinase pathway has been implicated in dorsal closure and planar polarity signaling in *Drosophila*. A similar role in *C. elegans* has yet to be demonstrated. Specifically, it is not known whether any MAP kinases are required for Q cell migration. Using a candidate gene approach, several *C. elegans* MAPK genes were scored for a Q migration phenotype, but no defects were found (data not shown). Thus, it is presently unclear whether the role of MIG-15 in Q neuroblast migration is solely to function in motility, or whether there is also a separate role for MIG-15 in signaling and the control of gene expression.

Another aspect of the role of MIG-15 in Q migration is the control of *mab-5* expression in QL. Previous work has shown that the expression and localization of MIG-15 is unchanged in a *mig-5/dsh* mutant background. *mig-5* is an ortholog of *Drosophila* Dishevelled and is required for the activation of *mab-5* in QL as part of the EGL-20/Wnt signaling pathway (Zhu, 1998). However, *mab-5* is not expressed in QL in some *mig-15* mutant animals. Also, *mab-5* is required for the QL descendants to remain in the posterior in *mig-15* mutants, since all the cells in the *mab-5; mig-15* double mutant migrate anteriorly, although many of these migrations are shortened with respect to *mab-5* single mutants. That *mig-15* acts upstream of *mab-5* activation is also demonstrated by the fact that all the Q descendants remain in the posterior body region in *mab-5(gf); mig-15* double mutants (Zhu, 1998). How does *mig-15* control *mab-5* expression? Is this function coupled to and downstream of the pathway controlling migration, or is it a separate pathway independent of Q migration? These questions are presently

unanswered, although it is clear that the early polarizations of the Q cells can be uncoupled from *mab-5* activation, since *mig-15* mutants have defects in *mab-5* expression but not Q cell polarization.

A model for Q cell polarization and migration

The identification of a number of genes required for Q neuroblast migration makes it possible to speculate about a signaling pathway controlling the Q cells (Figure 3-10). In one such model, MIG-21 and UNC-40 act together as receptors receiving an unknown polarizing signal. *unc-40* and *mig-21* are both expressed symmetrically in both QL and QR, thus are not responsible for the establishment of symmetry. The polarizing signal may be left-right asymmetrically localized, or the Q cells may respond differently to the polarizing signal. The activity of one or both of these receptors may be modified by the phosphatase PTP-3, as a rescuing *ptp-3::GFP* construct is expressed in both QL and QR (data not shown). PTP-3 may also be responsible for relaying signaling information downstream to the motility genes MIG-15, MIG-2, UNC-73, INA-1, and PAT-3 to reorganize the cytoskeleton and effect cell movement. The control of *mab-5* expression may be directly linked to the polarization and migration to the posterior of QL, or it may be under separate genetic control. Since all known mutations that result in defective Q polarizations also result in defects in *mab-5* expression, it seems likely that the two steps are linked. Polarization and *mab-5* expression can be separated genetically, as demonstrated by the phenotype of *mig-15* mutants, in which the Q polarizations are normal but the Q migrations and *mab-5* expression are defective. It is still possible, however, that they are linked in a single pathway, and that *mig-15* simply acts downstream of the

polarization step in the control of *mab-5* expression. Presently, no mutation has been isolated that affects Q cell polarization but not *mab-5* expression.

In conclusion, a signaling pathway guiding the left-right asymmetric polarizations and migrations of the Q neuroblasts is beginning to emerge. Further experiments, as outlined in Chapter 4, should further expand the knowledge of this pathway.

EXPERIMENTAL PROCEDURES

Strains and genetics

C. elegans (Bristol N2 wild type) were grown on NG plates under standard conditions (Brenner). All alleles of *mig-21* and *ptp-3(mu256)* were isolated from *mul32* or *mul35* animals treated with EMS (Ch'ng et al, submitted). Other strains used in this work include:

LGI: *unc-40(e1430)*

LGII: *ptp-3(op147)*, *ptp-3(mu256)*, *mul32*, *bli-1(e769)*

LGIII: *mab-5(e2088)*, *dpy-17(e164)*, *unc-32(e189)*

LGV: *him-5(e1490)*, *mul35*

LGX: *mig-15(rh80)*

Microscopy

Migrations of the Q nuclei were scored early in L1 (3-4 hours after hatching) using Nomarski/DIC optics with a 100x objective. Animals were mounted on 2% agarose pads, covered with a glass coverslip, and the positions of the Q cells relative to the stationary V and P cells were noted at the time of their first division.

Polarizations of the Q cells were scored in animals bearing the integrated array *muIs57*, in which the lateral seam cells, including the Q cells in the first larval stage, express GFP. The shapes of the Q cells were noted 2.5-3 hours after hatching, a time when all of the Q cells are polarizing strongly in *muIs57* animals. For timecourses in which single Q cells were followed over time, newly hatched larvae were mounted on 2% agarose pads (one animal per pad) and the Q cells located by Nomarski optics. Every 15-30 minutes, a 50-100ms fluorescent snapshot was taken using a Zeiss fluorescein filter set and a Uniblitz shutter (Vincent Associates) connected to a Pentium Pro PC. Images were collected using the Metamorph 4.6 software to control the shutter speed and to control the image accumulation on a Photometrics Imagepoint CCD camera.

The positions of the Q descendants, AVM, PVM, SDQR, and SDQL were scored as described previously (Sulston et al., 1983). Briefly, their positions in relation to the stationary V cells were noted in larvae near the end of the L1 larval stage; animals were deemed to be at the correct point in development when all the P nuclei had descended into the ventral cord, as the Q migrations are complete at this point in wild-type animals. The positions of other migratory neurons, HSN, CAN, ALM, and BDU, were also scored at this point.

Construction of double mutants

ptp-3(mu256); mab-5(e2088)

e2088/+ males were mated into *mu256; dpy-17(e164) unc-32(e189)* hermaphrodites and the hermaphrodite progeny were allowed to self-fertilize. *mu256* candidate F2s were picked on the basis of the Mig phenotype, and F3 progeny of these animals which gave Dpy Unc F4 progeny were selected. The

nDpy nUnc siblings were then selected, and those which gave no Dpy Unc progeny were candidate double mutants. The presence of the *e2088* deletion mutation was confirmed by PCR, and the *mu256* mutation was confirmed by complementation.

ptp-3(mu256); mig-21(mu238)

mu256/+; + mu238 +/dpy-17(e164) + unc-32(e189) animals were allowed to self-fertilize, and Mig F2 animals selected. Those animals which gave Dpy Unc progeny were inferred to contain the *mu256* mutation, and the nDpy nUnc F3 animals were then picked. Animals which gave no Dpy Unc progeny were candidate double mutants. Both mutations were checked by complementation.

unc-40(e1430); mig-21(mu238)

e1430/+; + mu238 +/dpy-17(e164) + unc-32(e189) F1 animals were allowed to self-fertilize and the Unc F2 progeny were picked. nDpy nUnc F3s from F2s which gave both Dpy Unc and nDpy nUnc progeny were selected, and animals which gave no Dpy Uncs were selected as the candidate double mutant. The presence of the *mu238* mutation was confirmed by complementation.

mig-21(mu238) mab-5(e2088)

mul32; mu238 +/+ e2088; e1490 F1 hermaphrodites (approximately 300) were picked onto individual plates and were allowed to self-fertilize. Approximately 600 Mig F2 animals from these hermaphrodites were picked onto individual plates. The Mig F2 animals were then allowed to self-fertilize, and plates containing both Mab and nMab male progeny were kept, since this indicated that recombination between *mig-21* and *mab-5* had occurred. Furthermore, since the original Mig F2 animal gave Mab and nMab progeny, these F2s must contain the *mu238* mutation, rather than the *e2088* mutation.

Individual hermaphrodites were picked from these plates, and those giving all Mab male progeny were kept. The *muIs32* and *e1490* markers were removed from *muIs32; mig-21(mu238) mab-5(e2088); e1490* by backcrossing to N2 males. The presence of the *e2088* deletion mutation was confirmed by PCR, and the presence of the *mu238* mutation was confirmed by complementation.

Mapping

mig-21 was mapped to LGIII between the Tc1 markers stP19 and stP120 using a PCR-based transposon mapping method (Williams et al., 1992). Deficiency analysis placed *mu238* between the deficiencies sDf121 and sDf125. The genetic endpoints of these deficiencies placed *mu238* between the genes *daf-4* (-1.53) and *let-774* (-1.42). This position was confirmed with a 3-factor cross between *mig-21(mu238)* and *dpy-17(e164) unc-32(e189)*. 19/49 Dpy nUnc recombinants segregated Mig progeny, and 41/63 Unc nDpy recombinants segregated Mig progeny. These data placed *mig-21(mu238)* at approximately -1.34 and -1.43 respectively.

Cloning

Cosmids were provided by A. Coulson of the Wellcome Trust Sanger Institute (Cambridge, UK) and J. Sulston of the Medical Research Council (Cambridge, UK). The region between *daf-4* and *let-774* was covered by 18 cosmids. Cosmid pools spanning this interval were injected into *mig-21(mu238)* animals using pTG96 (*sur-5::GFP*) (Gu et al., 1998) as a co-injection marker, and F2 and F3 progeny of F1 transformants were assayed for rescue of the QL.pax phenotype. Partial rescue was obtained from injection of the cosmid F01F1, and

this rescuing activity was narrowed to a 7.5kb PCR product that contains the predicted genes F01F1.2 and F01F1.13. Sequencing of DNA from several *mig-21* mutants revealed mutations in F01F1.13. Each lesion was identified in more than one independent PCR product. The 3' end of the *mig-21* cDNA, including the 3'-UTR, was identified by RT-PCR using RACE (Frohman, 1993). RT was from RNA isolated from L1 larvae (a gift from C. Murphy) using the Q_T primer (5'-ccagtgagcagagtgacgaggactcgagctcaagctttttttttttttt-3'). PCR primers were designed to span predicted exon-exon boundaries, to ensure specificity to the cDNA and to prevent amplification of unprocessed RNA or possible contaminant genomic DNA. The 3'- end of the cDNA, including the 3'-UTR, was isolated using the Q_o primer (ccagtgagcagagtgacg) at the 3'-end of the coding region, and primer QD17 (cacttattcaatttgaattgcatccgtcc) which spans the exon1-exon2 boundary. Various primers to the predicted 5'-end of the ORF failed to amplify the 5' *mig-21* cDNA (see results), as did the GeneRacer kit (Invitrogen), which removes the cap structure from full-length mRNA and ligates an oligo to the 5'-end of this uncapped mRNA. PCR from this oligo failed to yield the 5' end of the *mig-21* coding region.

Expression constructs

The GFP expression constructs were built using a PCR-fusion method (see Experimental Procedures and (Hobert et al., 1999). Transcriptional (P_{*mig-21*}::GFP), N-terminal translational, and C-terminal translational (*mig-21*::GFP) expression constructs were built using a fusion PCR method (Hobert et al., 1999). Briefly, for the transcriptional fusion, PCR primers were designed to amplify a 4.5kb product immediately upstream of the *mig-21* coding region that has an overhang

to pPD95.75 (a gift from A. Fire), which contains the GFP coding sequence. Additional primers were designed to amplify the GFP coding region of pPD95.75 such that it contained an overhang to the 3' end of the *mig-21* promoter region. These two overhangs were complementary, and an additional round of PCR using nested primers resulted in a fusion product that consisted of 4.5kb of the *mig-21* promoter fused to GFP. The C-terminal translational construct contained the GFP at the very C-terminus of the protein. Construction of the *mig-21::GFP* N-terminal translational fusion required 3 rounds of PCR: the first round generated 3 products: 1) the promoter and 138bp of the 5'-end of the *mig-21* gene, 2) the GFP coding region, and 3) the 3-end of the *mig-21* gene and 2kb of downstream genomic sequence. The GFP coding region is 36nt upstream of the first TSP-1 domain. Amplification of the *mig-21* sequence was performed from genomic DNA isolated from N2 animals, and amplification of the GFP coding region was from pPD95.85 (a gift from A. Fire). The second round of PCR fused products 1 and 2, and the third round of PCR fused this product to 3. The transcriptional and translational constructs were injected into wild type, and *mig-21(mu238)* animals, respectively.

Figure 3-1. The left-right asymmetric migrations of the QL and QR lineages.

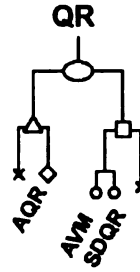
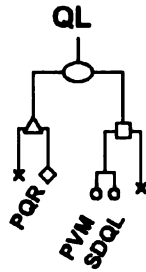
(a) The QL and QR lineages. The neuroblasts undergo an identical set of cell divisions and cell deaths. The anterior daughters of QL and QR (QL.a and QR.a respectively) are represented by triangles, while the posterior daughters of QL and QR (QL.p and QR.p) are represented by squares. Additional cell divisions result in the generation of three neurons (diamonds and circles; the names of the neurons are shown) as well as cells that undergo programmed cell death (Xs).

(b) The different steps of the left-right asymmetric cell migrations. The migrations of QL, QR and their respective descendants occur in several steps as shown. (See Introduction for details). QL and QR are born between the lateral seam cells, V4 and V5. At 1-2 hours after hatching, the neuroblasts begin to polarize in opposite directions: QL to the posterior and QR to the anterior. The cells then migrate over the respective seam cell, and divide after these short initial migrations. *mab-5* is expressed only in the QL lineage (indicated by dark gray shading); the QR lineage does not express *mab-5* (no shading). The migrations of the Q descendants are indicated in the final set of worms in the figure.

(a)

Left - QL Lineage

Right - QR Lineage



(b)

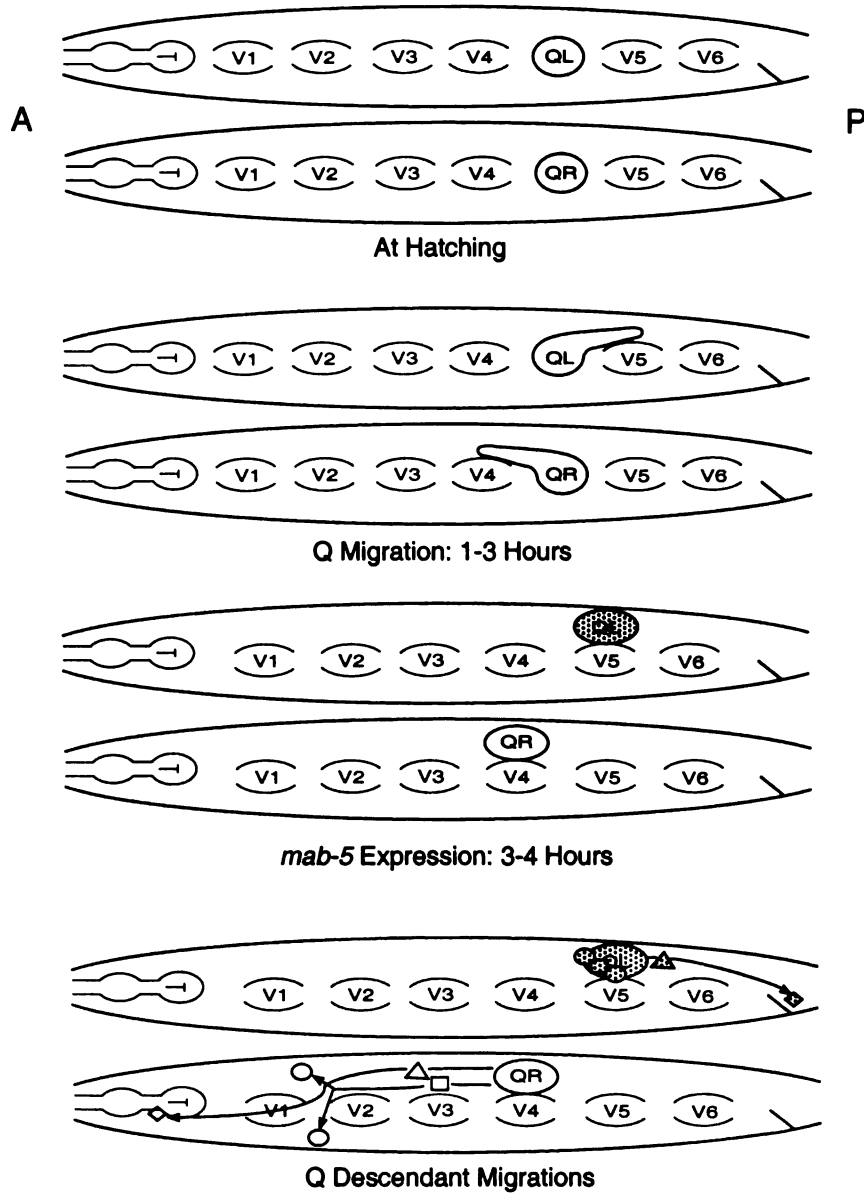


Figure 3-2. Polarization and migration of a QL neuroblast in a *muIs57*

(*scm::GFP::CAAX*) Animal.

In *muIs57* animals the lateral seam cells and Q cells express *scm::GFP::CAAX*, a membrane localized GFP construct. This allows the visualization of the shapes of the Q cells as they undergo their polarizations and migrations. Anterior is to the left in all panels, and time after hatching is noted for all frames. QL has divided in the last panel, as indicated by the lineage bars.

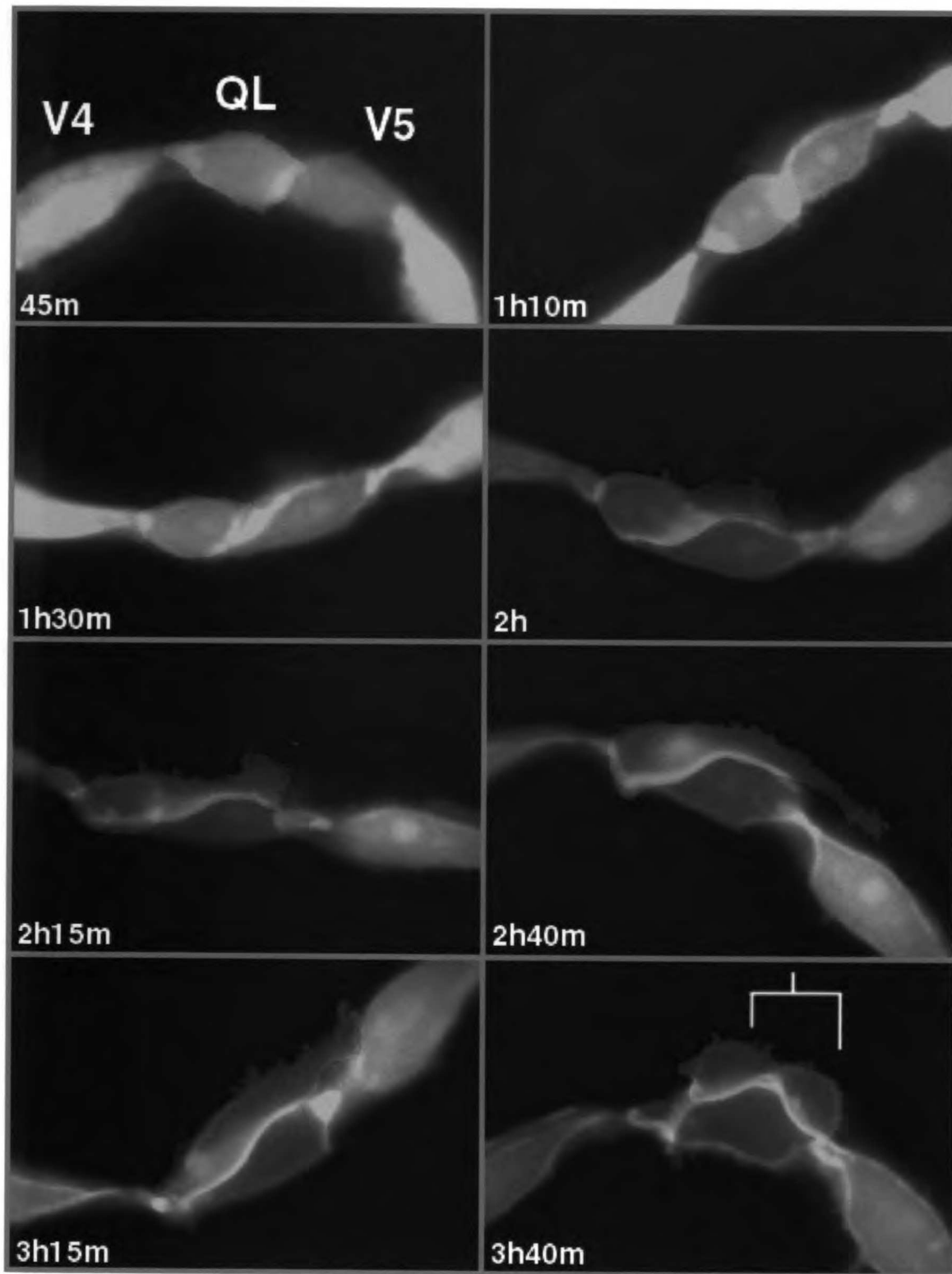


Figure 3-3. Migrations of the Q nuclei in N2, *mig-21(mu238)*, *ptp-3(mu256)* and *mig-15(rh80)* animals.

The cells are scored at the time of their division early in L1 (3-4 hours after hatching). Q Cell positions are scored relative to the stationary V and P cells. Anterior is to the left in all charts. (a) In N2 (black bars), QL undergoes a short migration dorsally and towards the posterior, whereas QR migrates dorsally and to the anterior. The positions in which the Q neuroblasts are born are indicated by red arrows at the bottom of the figure. In *mig-21(mu238)* mutant animals (green bars), the Q cells mostly fail to migrate, and divide in their birthplace. Some of the QL cells migrate a shortened distance to the anterior, and some of the QR cells migrate a shortened distance to either the anterior or the posterior. (b) In *ptp-3(mu256)* mutant animals (pink bars), QL mostly fails to migrate, but sometimes migrates a short distance to the anterior. QR is not as strongly affected by the *mu256* mutation, as many of the cells do migrate to the anterior, albeit a shorter distance than in N2. (c) Migrations of the Q nuclei in *mig-15(rh80)* animals (red bars) are shortened compared with N2, but always in the same direction as wild type.

ptp-3(mu256)
 hours after
 and P cells
 undergoes a shift
 dorsally
 are indicated
 at animals
 birthplace
 and some of
 the posterior
 migrate, but
 strongly
 to the anterior
 in *mig-15^{rh80}*
 in the same

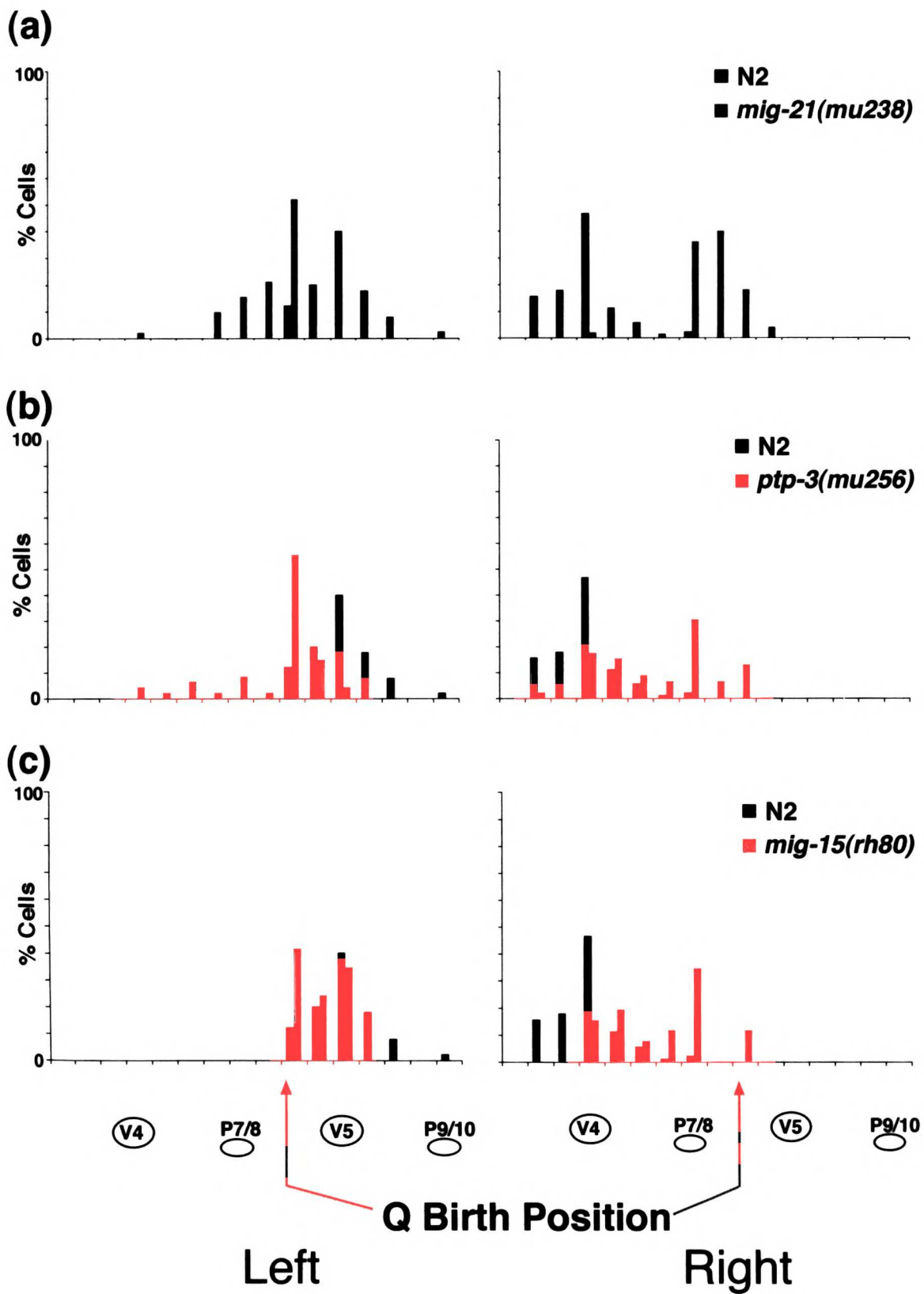


Figure 3-4. Polarizations of the Q cells in N2, *mig-21(mu238)*, *ptp-3(mu256)*, and *mig-15(rh80)* animals.

The strength of the Q cell polarization was scored as strong (<<</>>>) if the process extended beyond the midpoint of the adjacent V cell, moderate (<</>>) if it extended approximately to the midpoint of the adjacent V cell, or weak (</>) if the process was clearly polarized but not to the midpoint of the adjacent V cell. The cell was considered unpolarized (--) if there was no clear direction of polarization. Polarization strengths were scored at approximately 3 hours after hatching, shortly before the Q cells divide. Anterior is to the left in all charts. In N2 animals (black bars in all charts), QL always polarized to the posterior, either strongly or moderately, before dividing. By contrast, QR always polarized (moderately to strongly) to the anterior. (a) In *mig-21(mu238)* animals (green bars), many (~50%) of the cells, QL and QR, were unpolarized at 3 hours after hatching. Many of the cells, both QL and QR, polarize weakly or moderately to the anterior, and a small percentage (3% of cells in *mig-21(mu238)*, and 2% of cells in *ptp-3(mu256)*) polarized strongly to either the anterior or the posterior. (b) In *ptp-3(mu256)* animals (pink bars), QR usually polarized in the correct direction, with 90% of the cells polarizing weakly to strongly to the anterior, and only 10% remaining unpolarized or polarizing to the posterior. By contrast, the polarization of QL appears to be randomized, with approximately equal numbers of cells remaining unpolarized or polarizing to the anterior or posterior. (c) In *mig-15(rh80)* animals (red bars), the Q cells polarize normally.

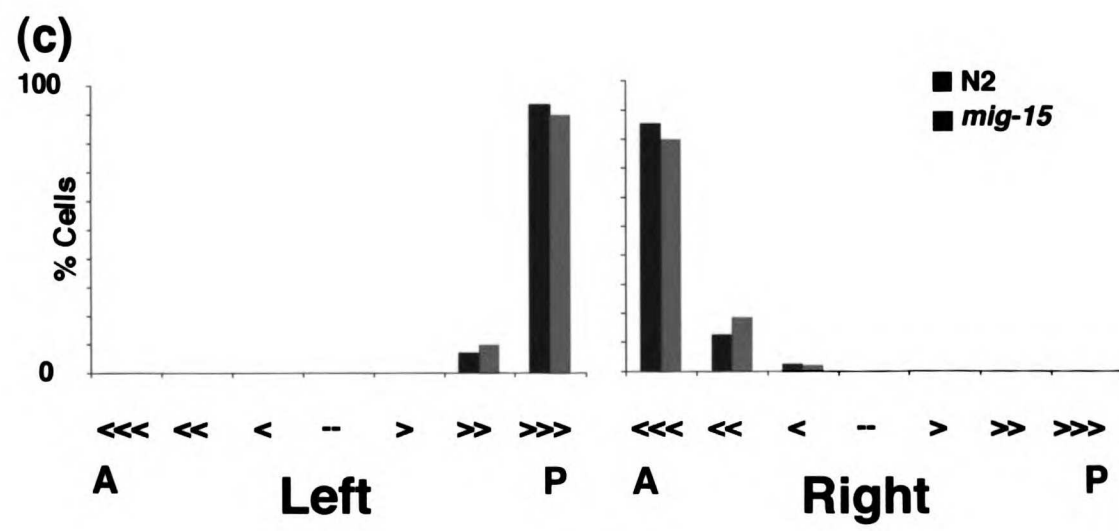
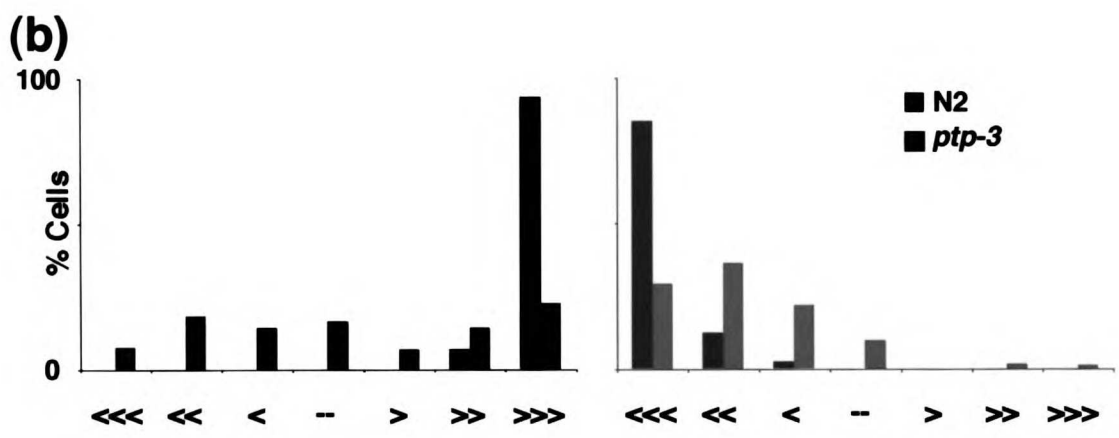
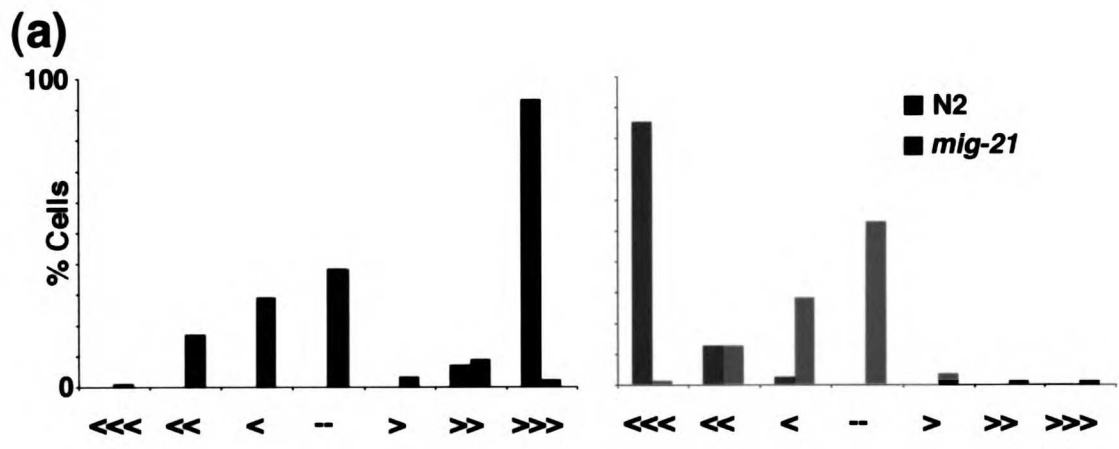
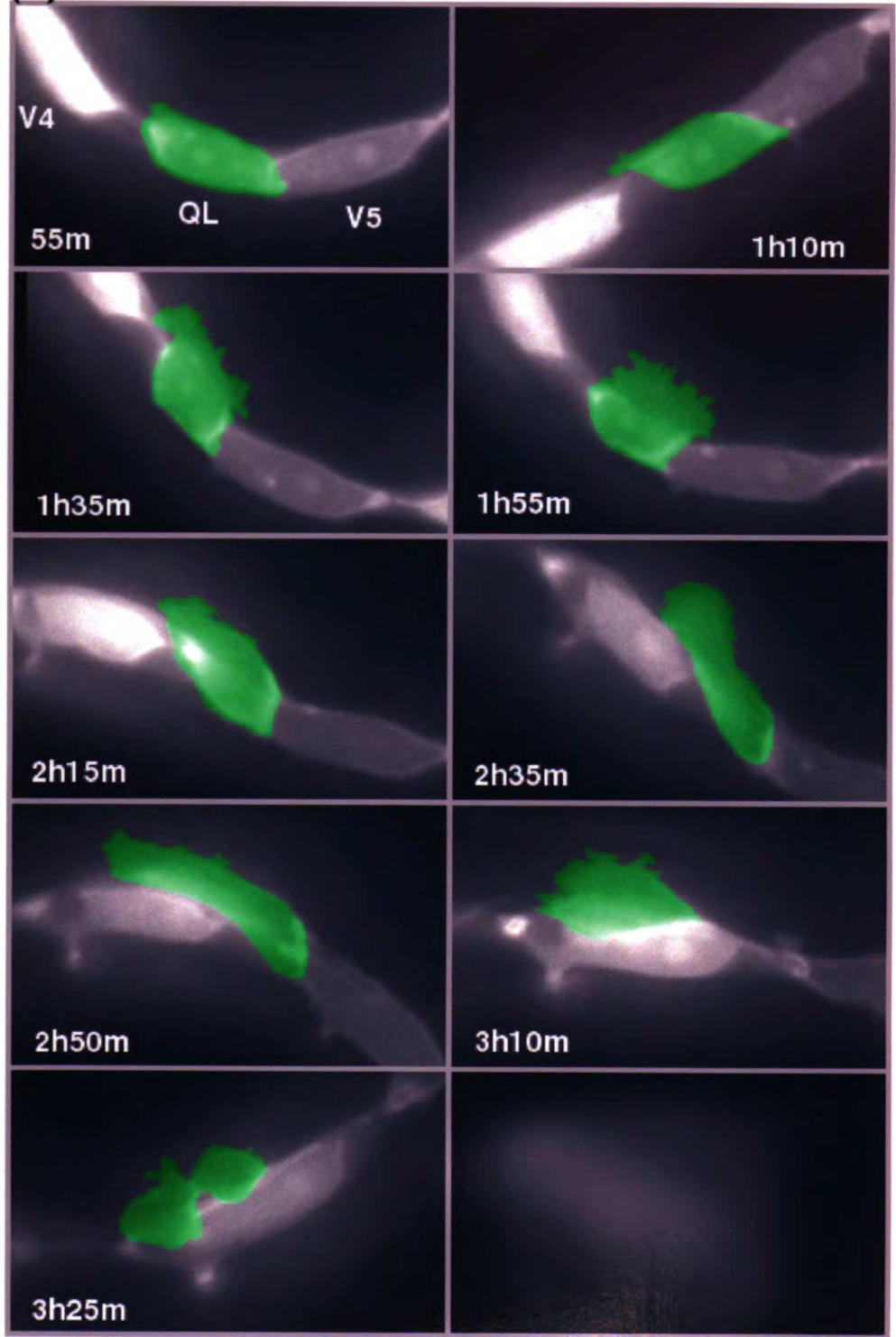


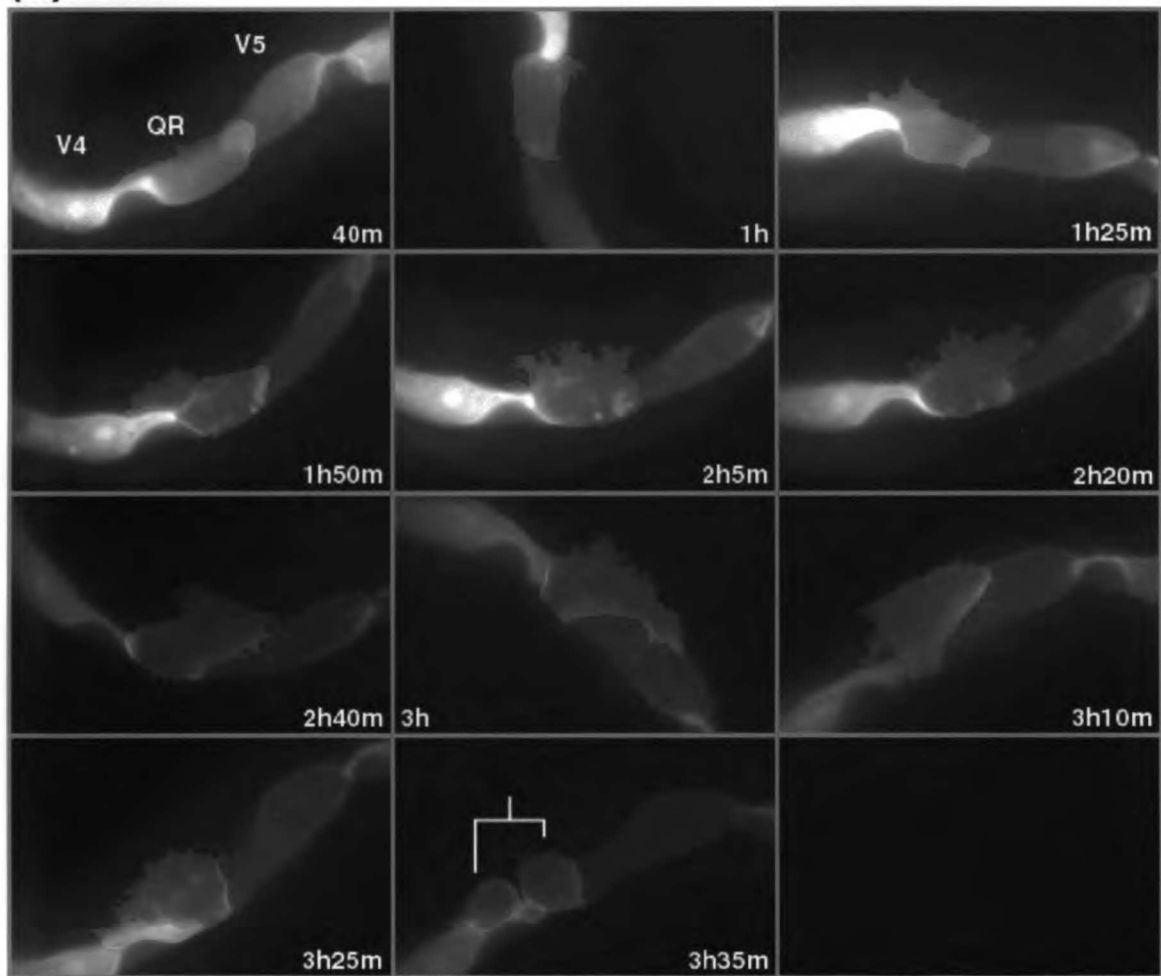
Figure 3-5. Polarization of a single Q cell can change over time in *mig-21* and *ptp-3* animals.

The direction and extent of polarization of Q cells in single animals were followed over time. Snapshots were taken every 15-20 minutes, from approximately 30 minutes after hatching until the Q cells had divided. Anterior is to the left in all panels, and time after hatching is noted for each frame. The Q cell has divided in the last panel for each timecourse, indicated by the lineage bars. For ease of viewing, the Q cells have been enhanced with green color using Adobe Photoshop. **(a)** QL can polarize and migrate inappropriately to the anterior in *mig-21(mu238)* animals. **(b)** The direction of polarization can change over time in *mig-21(mu238)* and *ptp-3(mu256)* animals. Panels outlined in red indicate the change in polarization: at 1h25m, QR is polarizing to the anterior; at 2h5m, QR is unpolarized; at 3h QR is polarizing to the posterior. **(c)** A Q cell can migrate in a direction opposite to its direction of polarization in *ptp-3(mu256)* animals. In this animal, QL initially polarizes to the anterior, but migrates towards the posterior. **(d)** Summary of polarization phenotypes observed in *mig-21(mu238)* and *ptp-3(mu256)* mutants. Cells can extend and retract a process in one direction before polarizing, either strongly or weakly (rows 1 and 2 for anterior polarization, rows 4 and 5 for posterior polarization); remain unpolarized (row 3); or change direction of polarization (row 7). The number of cells observed for each phenotype versus the total number of cells scored for both QL and QR is shown.

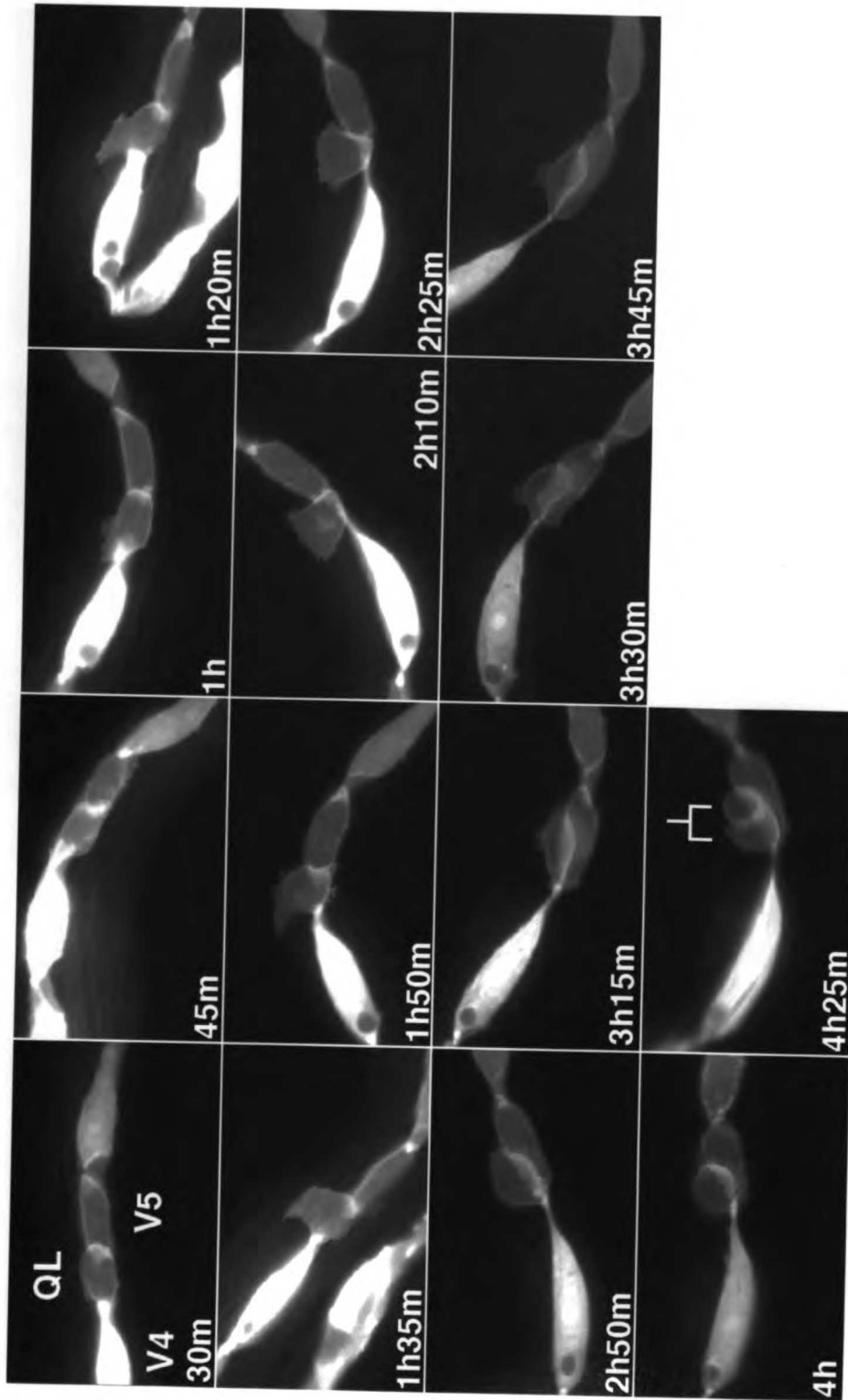
(a)



(b)



(c)














A	↔	P	<i>mig-21(mu238)</i>		<i>ptp-3(mu256)</i>	
			QL	QR	QL	QR
			5/9	1/9	3/11	4/12
			2/9	4/9	0/11	6/12
			0/9	1/9	0/11	0/12
			0/9	0/9	2/11	2/12
			0/9	0/9	4/11	0/12
			2/9	3/9	2/11	0/12

Figure 3-6. Mutations in *unc-40* or *ptp-3* synergize with *mig-21* in Q descendant migration, and *mab-5* is required for the Q descendants to remain in the posterior in *mig-21* and *ptp-3* mutants.

Positions of the QL descendants SDQL and PVM (QL.pax) are shown on the left, and the QR descendants SDQR and AVM (QR.pax) are shown on the right. The positions of these cells are scored at the end of L1 larvae, relative to the stationary Vn.a and Vn.p cells indicated on the horizontal axis. % of cells in each position is indicated on the vertical axis. At least 100 animals were scored for each chart. **(a)** Positions of QL.pax and QR.pax in N2, *mig-21(mu238)*, *ptp-3(mu256)*, *mig-15(rh80)*. **(b)** *unc-40(e1430)* and *ptp-3(mu256)* synergize with *mig-21(mu238)* in the migrations of the Q descendants. Left panel: QL.pax and QR.pax distributions in *mig-21(mu238)*, *ptp-3(mu256)* and *ptp-3(mu256); mig-21(mu238)*. Right panel: QL.pax and QR.pax distributions in *mig-21(mu238)*, *unc-40(e1430)*, and *unc-40(e1430); mig-21(mu238)*. The vertical red lines indicate the peak position in the distribution of Q.pax cells in N2. **(c)** *mab-5* is required for the Q.pax cells to remain in the posterior in *mig-21(mu238)*, *ptp-3(mu256)* and *mig-15(rh80)* animals. Left panel: QL.pax and QR.pax distributions in *mig-21(mu238)*, *mab-5(e2088)*, and *mig-21(mu238) mab-5(e2088)* animals. Center panel: QL.pax and QR.pax distributions in *ptp-3(mu256)*, *mab-5(e2088)*, and *ptp-3(mu256); mab-5(e2088)* animals. Right panel: QL.pax and QR.pax distributions in *mig-15(rh80)*, *mab-5(e2088)*, and *mab-5(e2088); mig-15(rh80)* animals.

-21 in Q
 ndants to reax
 shown on the z
 on the right: s
 re to the
 % of cells
 ere scored for
 238), ptp-
 gize with m
 pax and
 w256); mig-
 21(mu238) as
 s indicate th
 required for
 56) and mig-
 mig-21(mu238)
 el: QL-pax
 56); mab-
 mig-15(mu

(a)

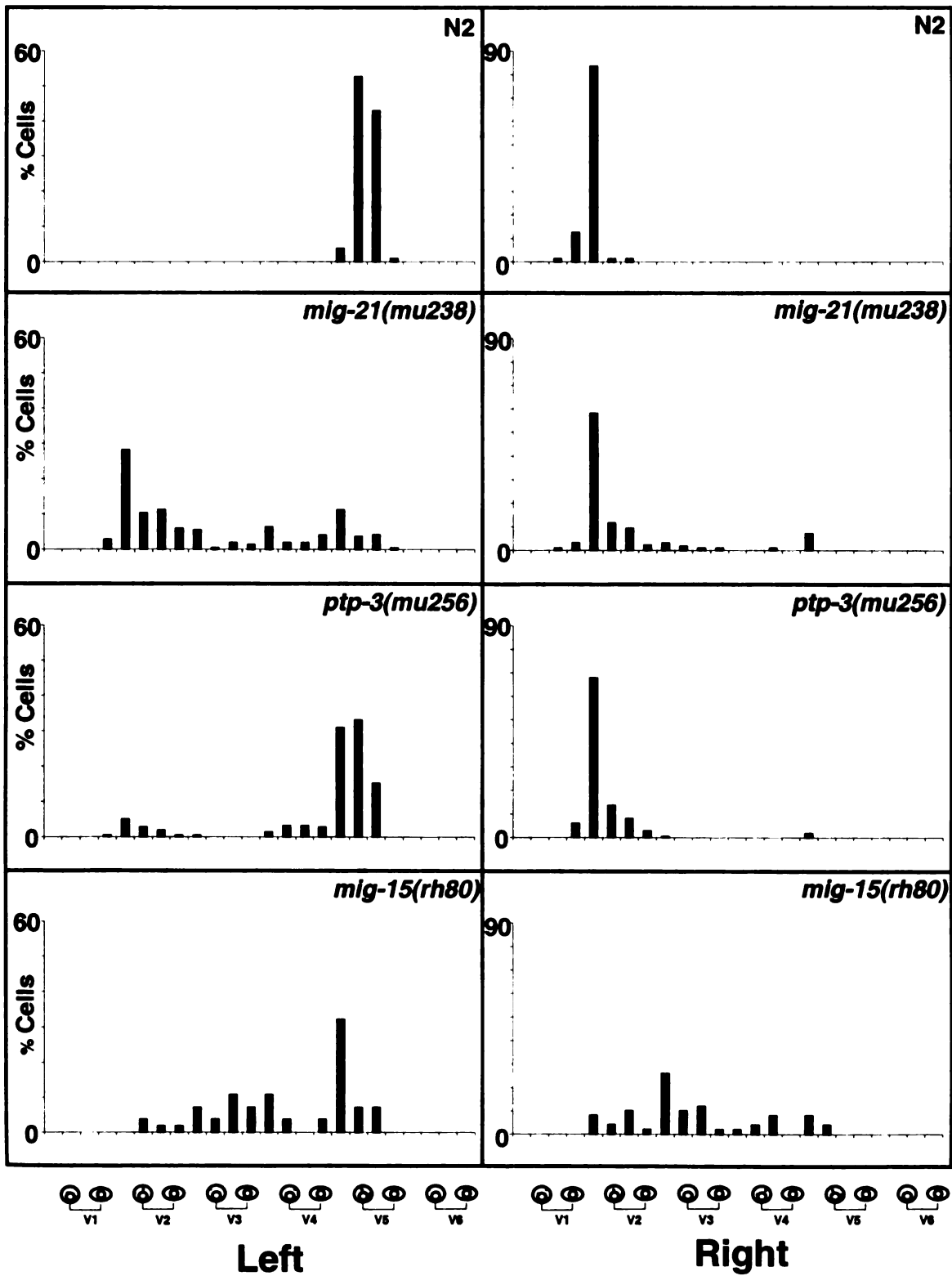
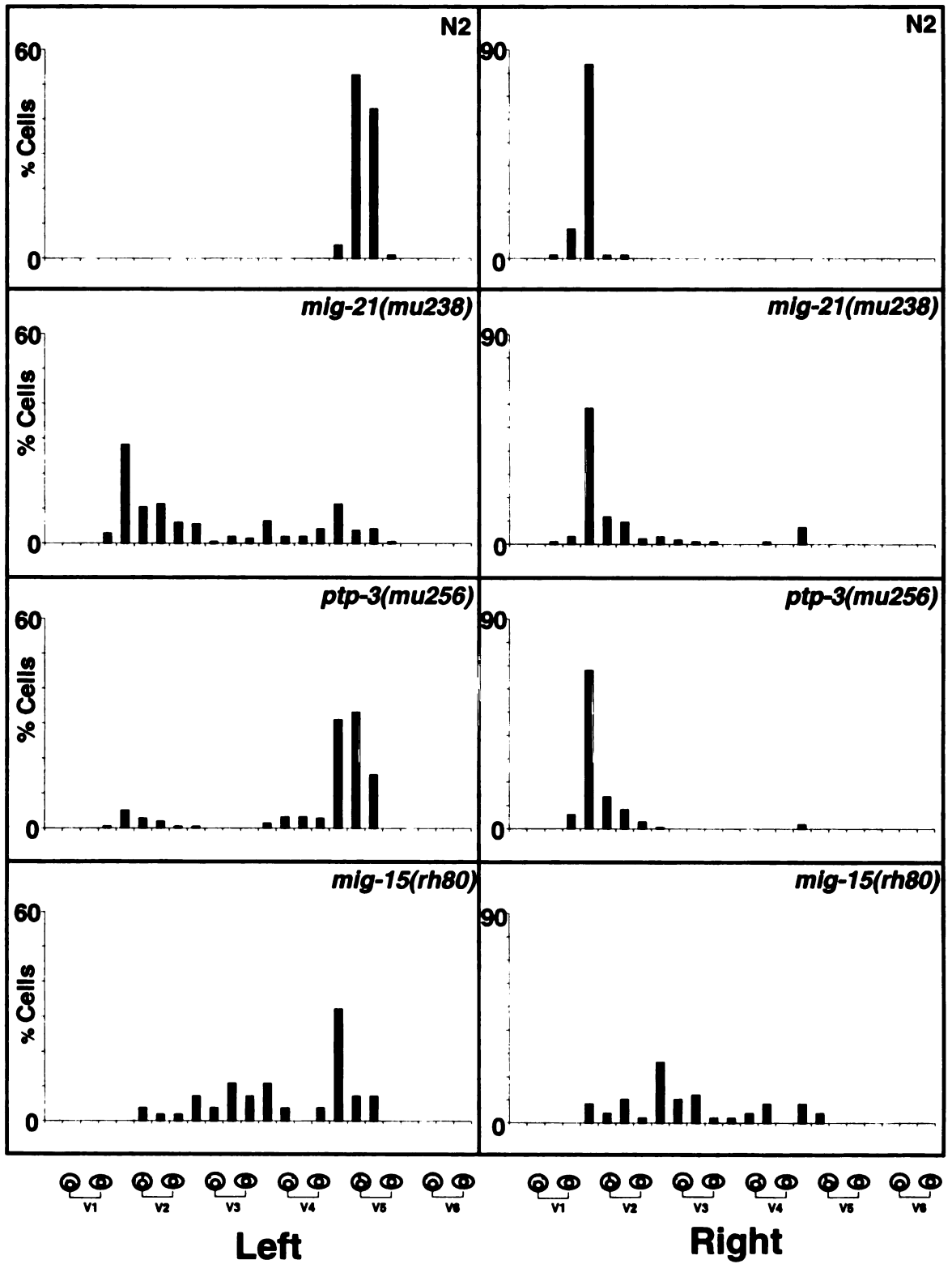


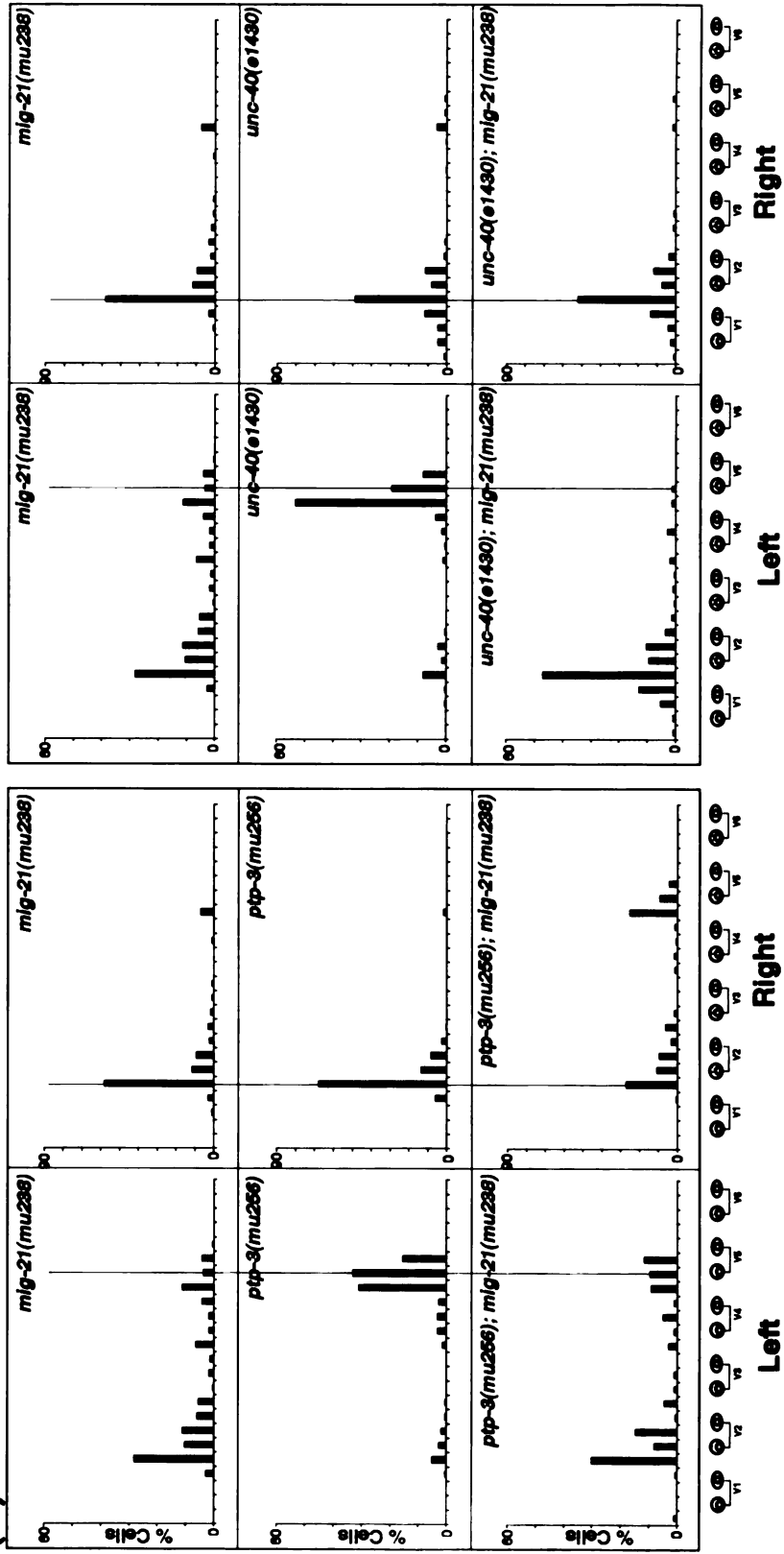
Figure 3-6. Mutations in *unc-40* or *ptp-3* synergize with *mig-21* in Q descendant migration, and *mab-5* is required for the Q descendants to remain in the posterior in *mig-21* and *ptp-3* mutants.

Positions of the QL descendants SDQL and PVM (QL.pax) are shown on the left, and the QR descendants SDQR and AVM (QR.pax) are shown on the right. The positions of these cells are scored at the end of L1 larvae, relative to the stationary Vn.a and Vn.p cells indicated on the horizontal axis. % of cells in each position is indicated on the vertical axis. At least 100 animals were scored for each chart. (a) Positions of QL.pax and QR.pax in N2, *mig-21(mu238)*, *ptp-3(mu256)*, *mig-15(rh80)*. (b) *unc-40(e1430)* and *ptp-3(mu256)* synergize with *mig-21(mu238)* in the migrations of the Q descendants. Left panel: QL.pax and QR.pax distributions in *mig-21(mu238)*, *ptp-3(mu256)* and *ptp-3(mu256); mig-21(mu238)*. Right panel: QL.pax and QR.pax distributions in *mig-21(mu238)*, *unc-40(e1430)*, and *unc-40(e1430); mig-21(mu238)*. The vertical red lines indicate the peak position in the distribution of Q.pax cells in N2. (c) *mab-5* is required for the Q.pax cells to remain in the posterior in *mig-21(mu238)*, *ptp-3(mu256)* and *mig-15(rh80)* animals. Left panel: QL.pax and QR.pax distributions in *mig-21(mu238)*, *mab-5(e2088)*, and *mig-21(mu238) mab-5(e2088)* animals. Center panel: QL.pax and QR.pax distributions in *ptp-3(mu256)*, *mab-5(e2088)*, and *ptp-3(mu256); mab-5(e2088)* animals. Right panel: QL.pax and QR.pax distributions in *mig-15(rh80)*, *mab-5(e2088)*, and *mab-5(e2088); mig-15(rh80)* animals.

(a)



(b)



(c)

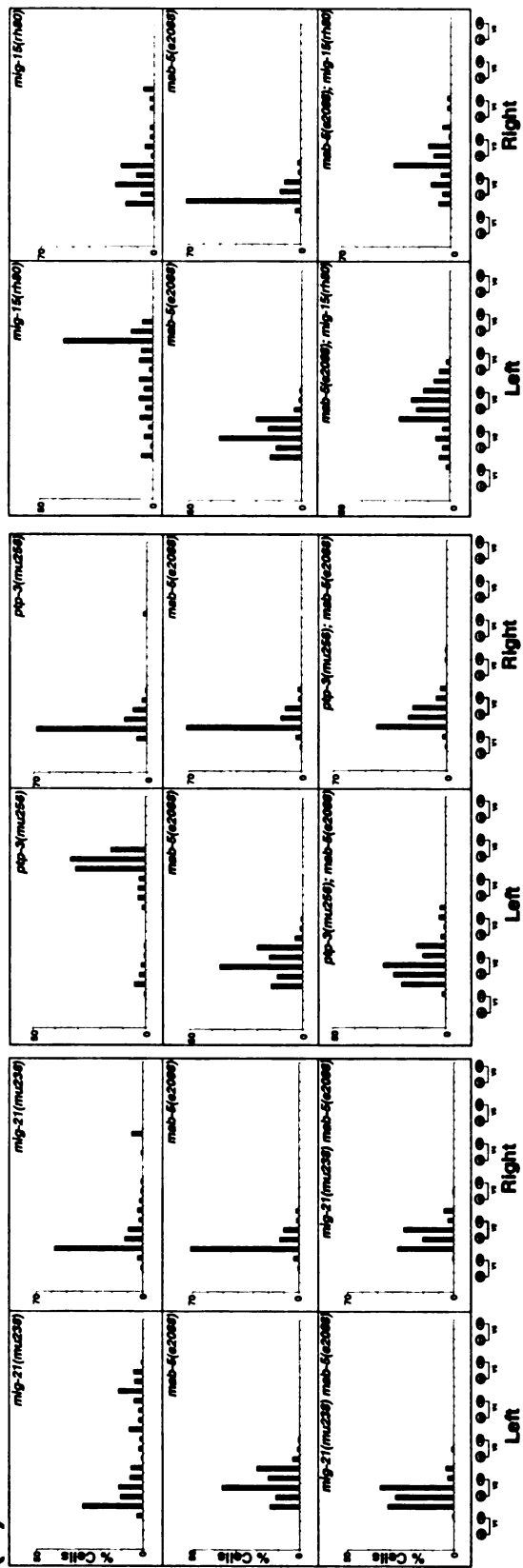
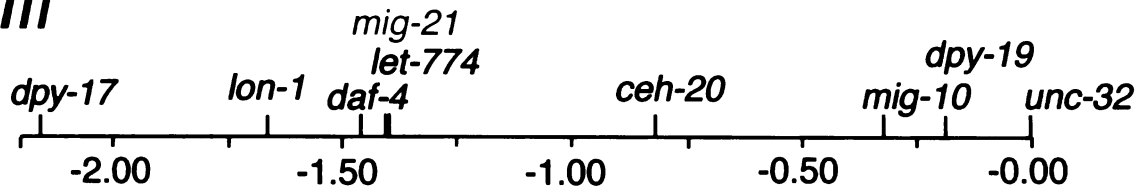


Figure 3-7. *mig-21* encodes a novel single-pass transmembrane protein with two thrombospondin type I domains.

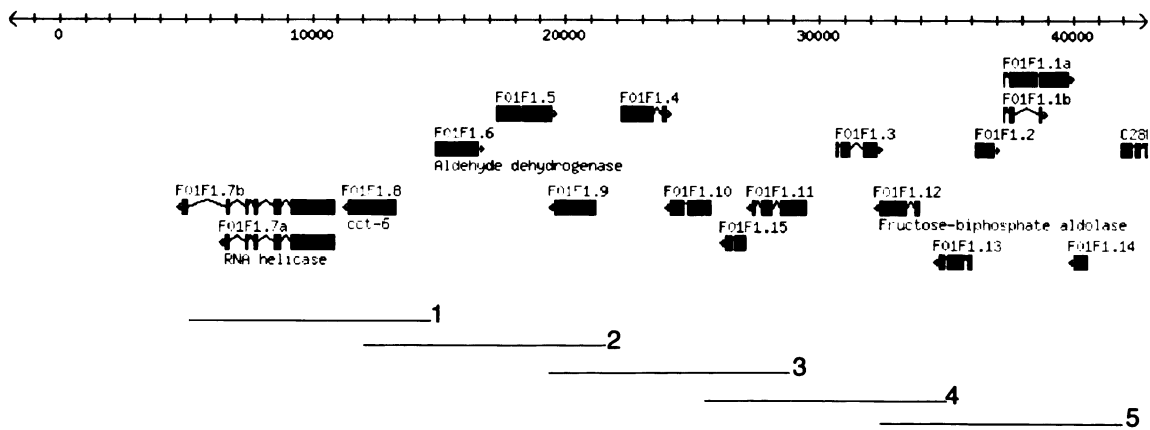
(a) Partial genetic map of the *mig-21* region. *mig-21* was mapped to a small interval on chromosome III by Tc1 mapping, Df mapping, and 3-factor mapping. Deficiency analysis placed *mig-21* between *daf-4* and *let-774*. **(b)** Physical map of the *mig-21* region. Overlapping cosmids from this region were injected into *mig-21(mu238)* animals and a single cosmid, F10F4 (canonical for F01F1) was found to rescue the QL.pax migration phenotype. This cosmid contains 15 predicted open reading frames. Injection of overlapping PCR products narrowed the rescuing activity to a 7.5 kb fragment, shown in green. Non-rescuing PCR fragments are shown in red. Sequencing of mutant DNA revealed that *mig-21* corresponds to F01F1.13. **(c)** Genomic structure of the *mig-21* locus and locations of 8 of the mutations identified. Genomic DNA corresponding to this fragment was sequenced in the mutant strains, and mutations were found in one candidate ORF, F01F1.13. A partial cDNA for this ORF was isolated by RT-PCR from RNA isolated from L1 larvae using primers predicted to be specific to the cDNA (see Experimental Procedures). **(d)** Protein sequence of MIG-21, with thrombospondin domains shown in blue and transmembrane domain shown in green. **(e)** Genomic sequence of the *mig-21* locus. Coding sequence is bold. *mig-21* contains a 90nt 3'-UTR, shown in blue.

(a)

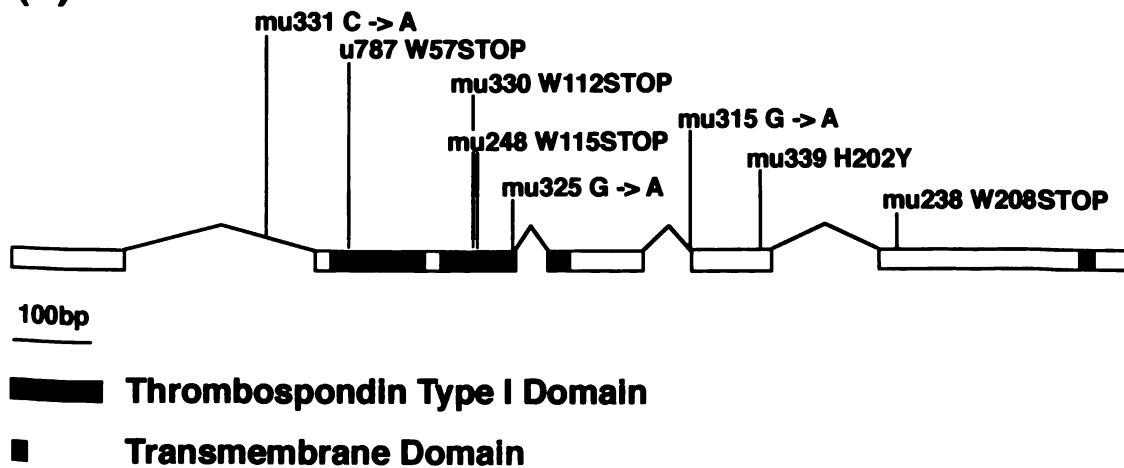
///

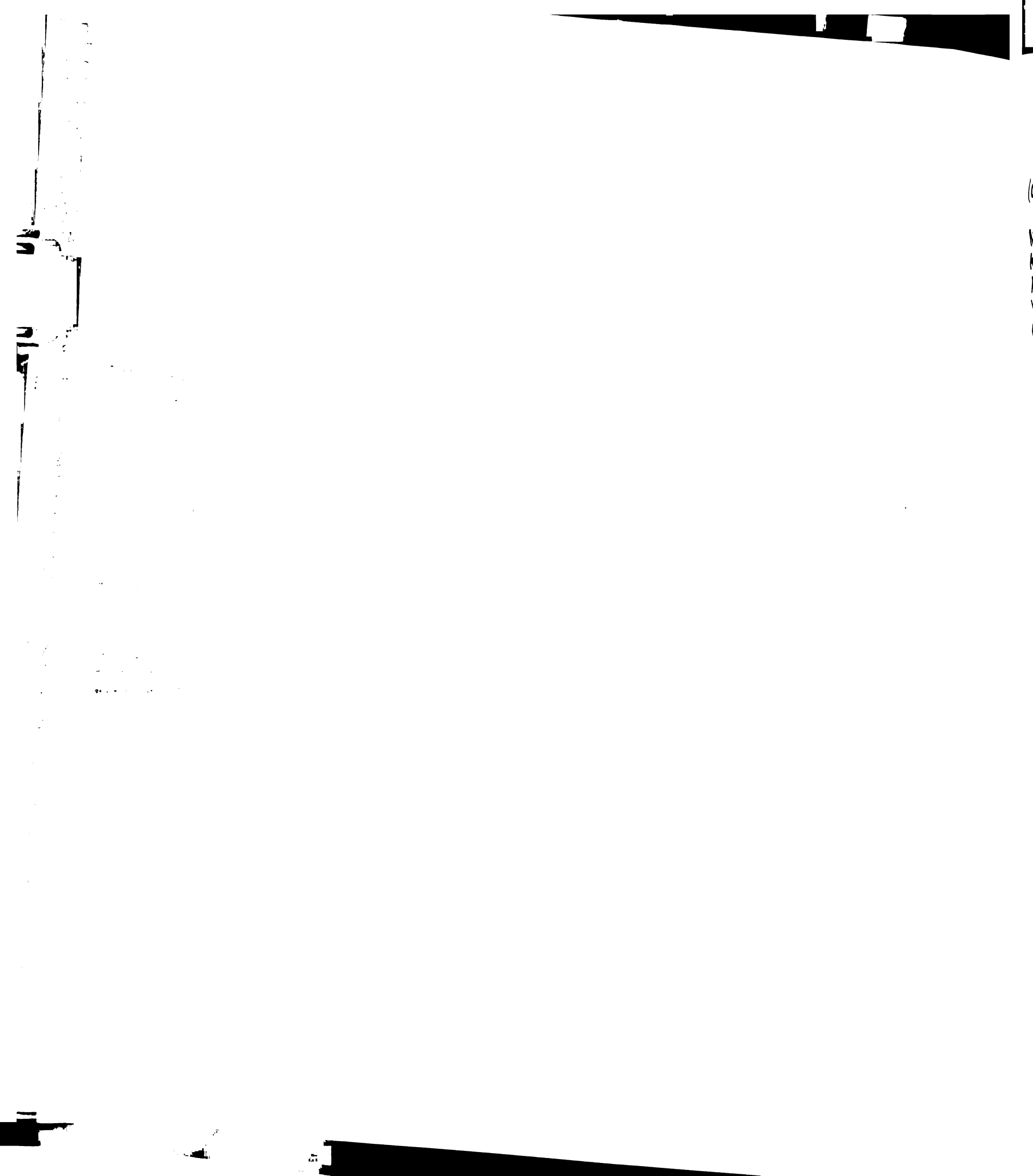


(b)



(c)





(d)

**MERDSNTAKSEIFYSNPAIWRHLKDGKGEGMSKSEKRN
KKHGCRNFTYSIWNCIRPGGWSTWSKWSKCREGIRKRR
RTCNNPLPIGTTCSGQKVEKQSCAISSNVPEYLFGSWTS
WNPWSRCDCLRSLRIRTRHCKGNSCEGCDKDYEDCRP
DECPISKKWSEWTDWVNYGIEQVRFSAWCSSSNVANTE
VGIRKETQDSMKHANWSEWHMHPGVAYRYRLLHNSISI
EHLLSRFTSSCLPLHFAIPIFCFCILTGSFFKILFIGWNR
KRRFIRLNYSYDSNPRDYP SHLIRSPGPKDESF**

(e)

**atggagcgcgactctaacactgcaaaaagtgaattttctacagtaaccctgccatctggcgac
atctgaaagatggaaaaggagaaggaatgtcgaaatctgaaaagagaaacaaacatgggtgt
agaaattcacttattcagtaagaactgagttcatagaaaatgattgcatggtttgtaatatcttcgttt
cgtcaatttcatattcgttggttaattaaatgattctagcattttatattctcaagttgctctaataagtgtc
atctaataatggtatattctggaatgttcgaaacaaggcggagaaattaaggttctacattcaaaaagat
aaaaccaattcaataaaaatttgatgcagatttggaaatgcatccgtccaggaggttggtcaacgtg
gtcaaaaatggtcgaaatgtagagaaggatccgaaaaagaagacgaacgtgtaataatcctta
ccaattggtaccactgttctggccagaaagttgagaagcaatctgtgcaatttctcaaatgtac
cggagtatcttttggatcctggacatcctggaatccatggtctcgatgcgattgtgatcgtagcct
gaggatacggtaggtcaacaattgggaaatgtacagtaaccaagttcagaactcggcactgca
aaggtaatcctcgcgagggatgtgacaaggatcgaagattgccgccagatgagtgccaatt
agtaaaaaatggtccgaatggacagattgggtgaattatggtatgggtctcattacgctgaaatata
caacaaattgtaatgattaattcaggaattgagcaagtacggtttcagcctggtgttcgcatcaa
acgtggcgaatactgaagtgggaatacgggaaggagactcaagactcaatgaagcatggtatta
atlttagtaaaaaattcgaagaaccataactgaagactaaattgaaagttcaaagtacaatgtccac
ttactgtctaaattttgtgttagtaacaacatgataaaaaattaatgagaataattccagccaactggtc
tgaatggcatatgcatccaggagttgcataccgttatcgtcttctcacaacttctatttccatcga
acaccatcttattcaagattcacgtcatcatgtcttcccttgcaatttgaattccaatattttgtttg
tattctcacgggttcttctcaaaaatattattattgtgtggaatcgtttaaaaggagattcataa
gattgaattattcgtatgattcaatccacgtgactatccttctcattgattcgttctccgggtcccc
gaaagatgaaagttttggtgaattcggatgcttcgagaacagtcctgtctgcccatttctcacg
ccacgataataaaagtattcattgatcaaaaaaaaaaaaaaaaa**

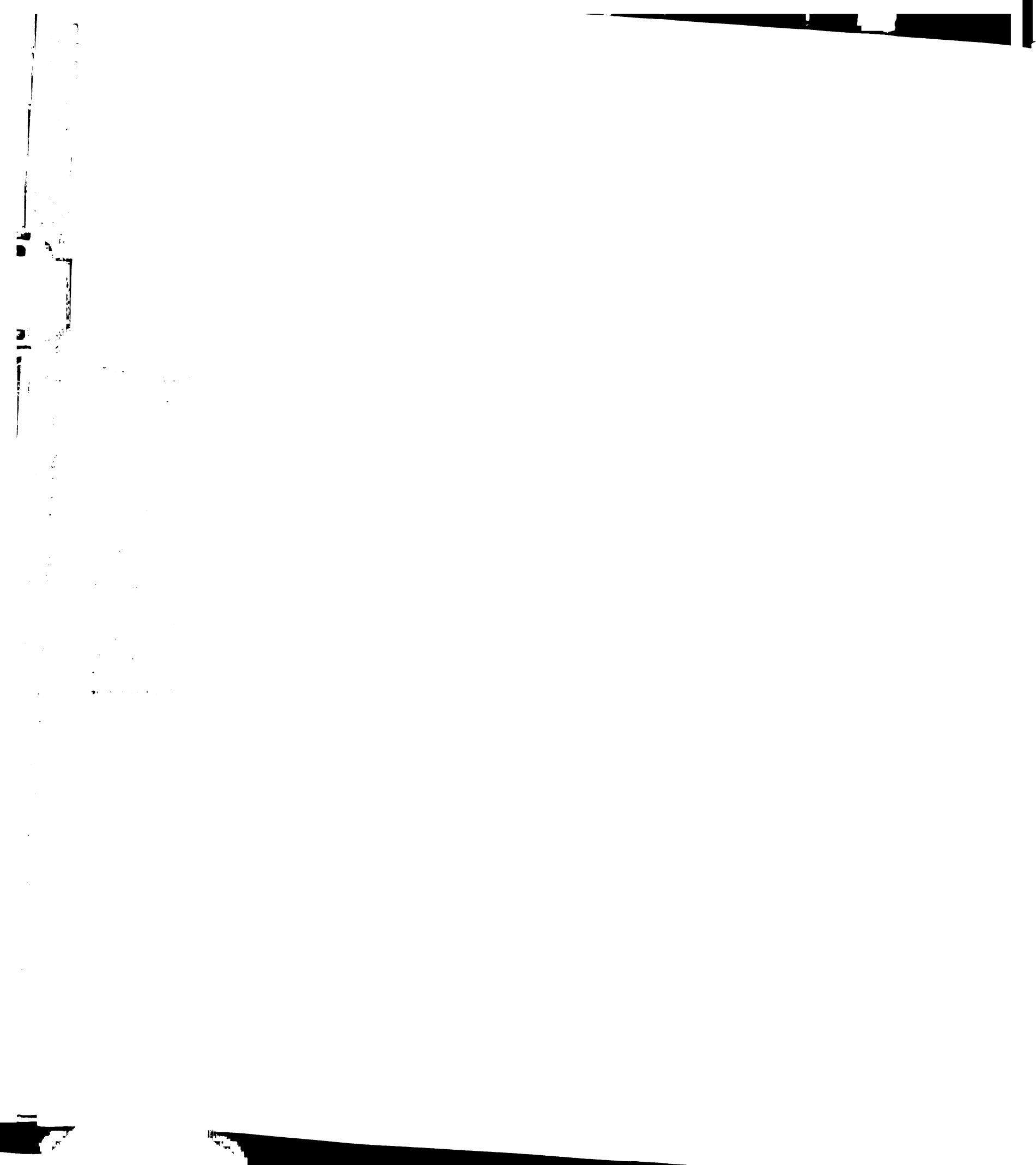
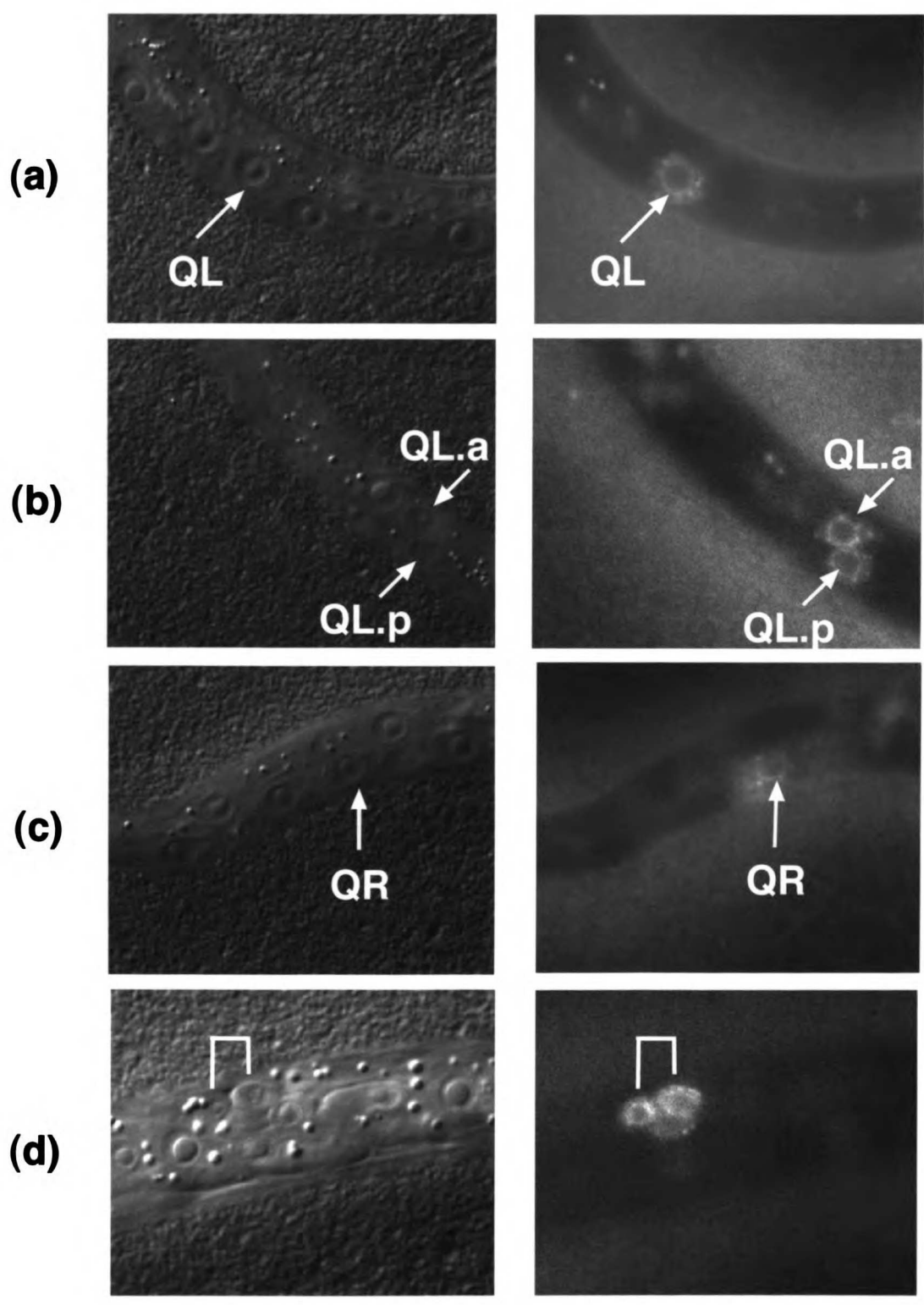


Figure 3-8. *mig-21* is expressed in QL and QR at the time of their migration. (a), (b) and (c): N-terminal *mig-21::GFP* construct. (d) C-terminal *mig-21::GFP* construct. For all panels, Nomarski (DIC) images are on the left, and corresponding fluorescent images are on the right. (a, c) Early L1 *mig-21* is expressed in QL (a) and QR (c) before and during their migrations. (b) *mig-21* can be seen in the plasma membrane of the Q.a and Q.p cells on the left (b) and right sides after the first Q division. (d) L2: *mig-21* is expressed in the developing postdereid. This line also had partial rescuing activity. Expression of the postdereid was also observed in the N-terminal *mig-21::GFP* construct (not shown).

migrations
ig-21::GFP
and the
ig-21 is
(b) early
s on the
sed in the
Expressor
nstruct (a



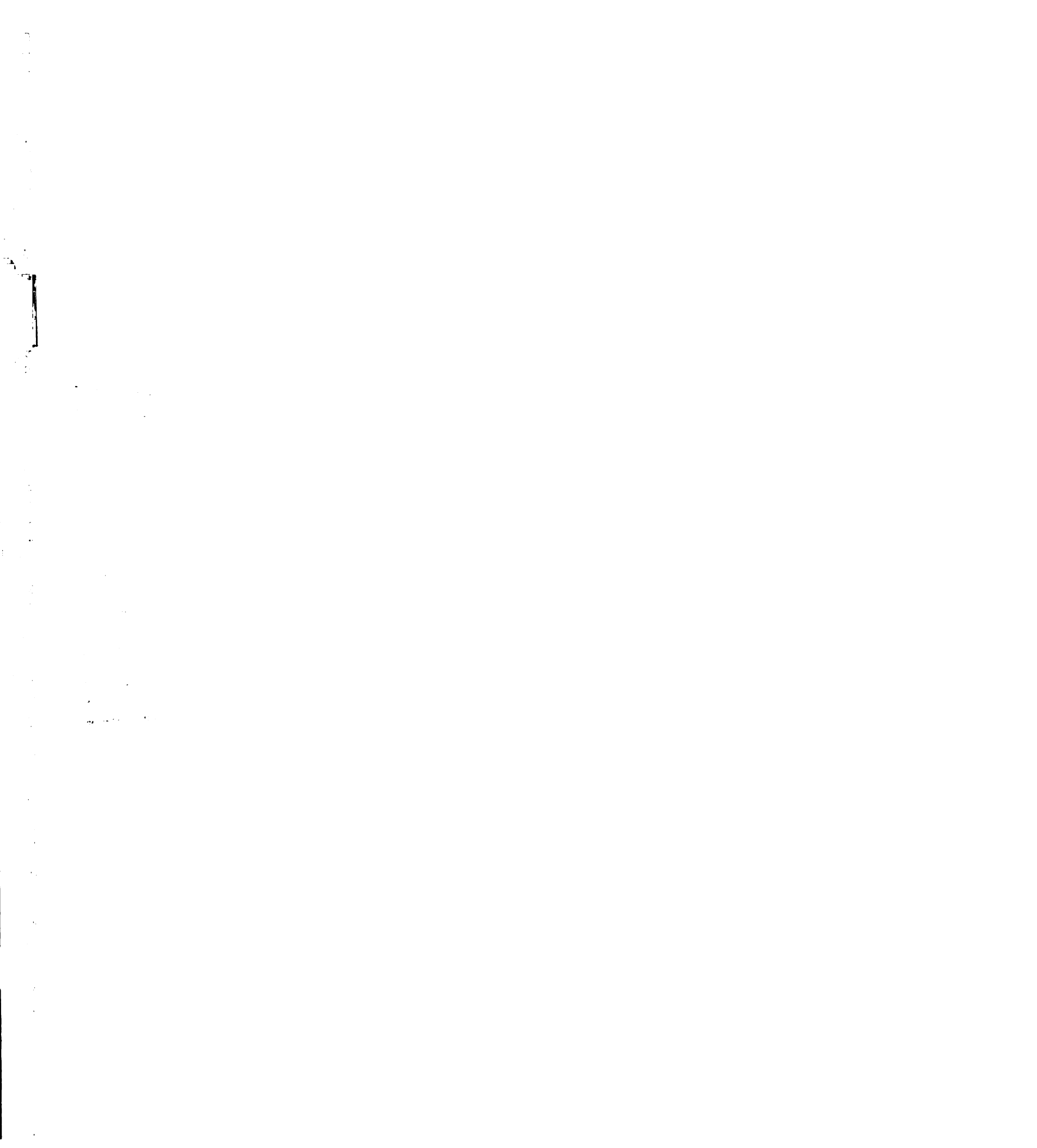
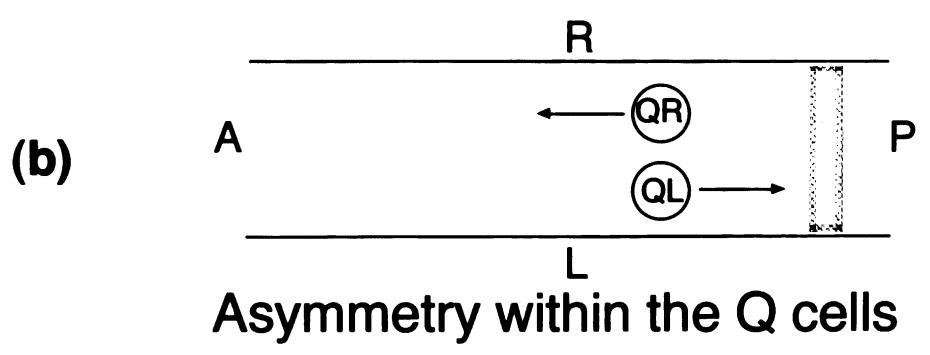
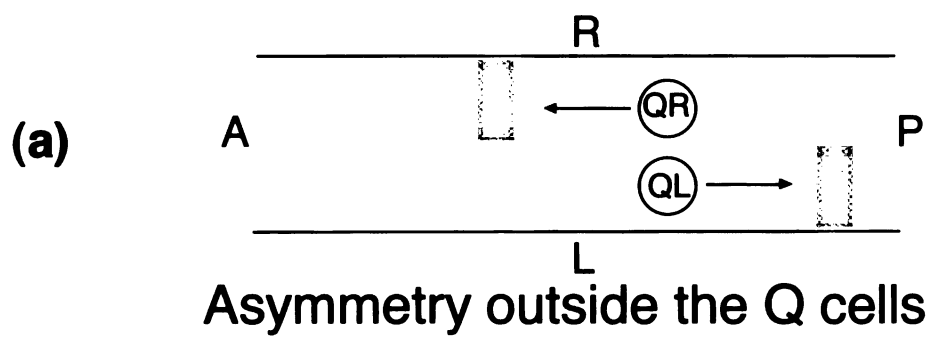


Figure 3-9. Models for the origin of asymmetry in Q cell migration.

Dorsal view of the animal, showing both QL and QR and the possible location of a polarization signal (a) Asymmetry outside the Q cells. In this model, the asymmetry arises from an asymmetric polarizing signal. Each Q cell responds similarly to the signal, using the same downstream signal response pathway. (b) Asymmetry within the Q cells. In this model, the polarizing signal is symmetrically localized. The Q cells respond differently to the signal, with one cell being attracted and the other cell being repelled.

cell migration.
of the possible loca
in this model, the
Each Q cell respon
response pathway
ing signal is
to the signal with



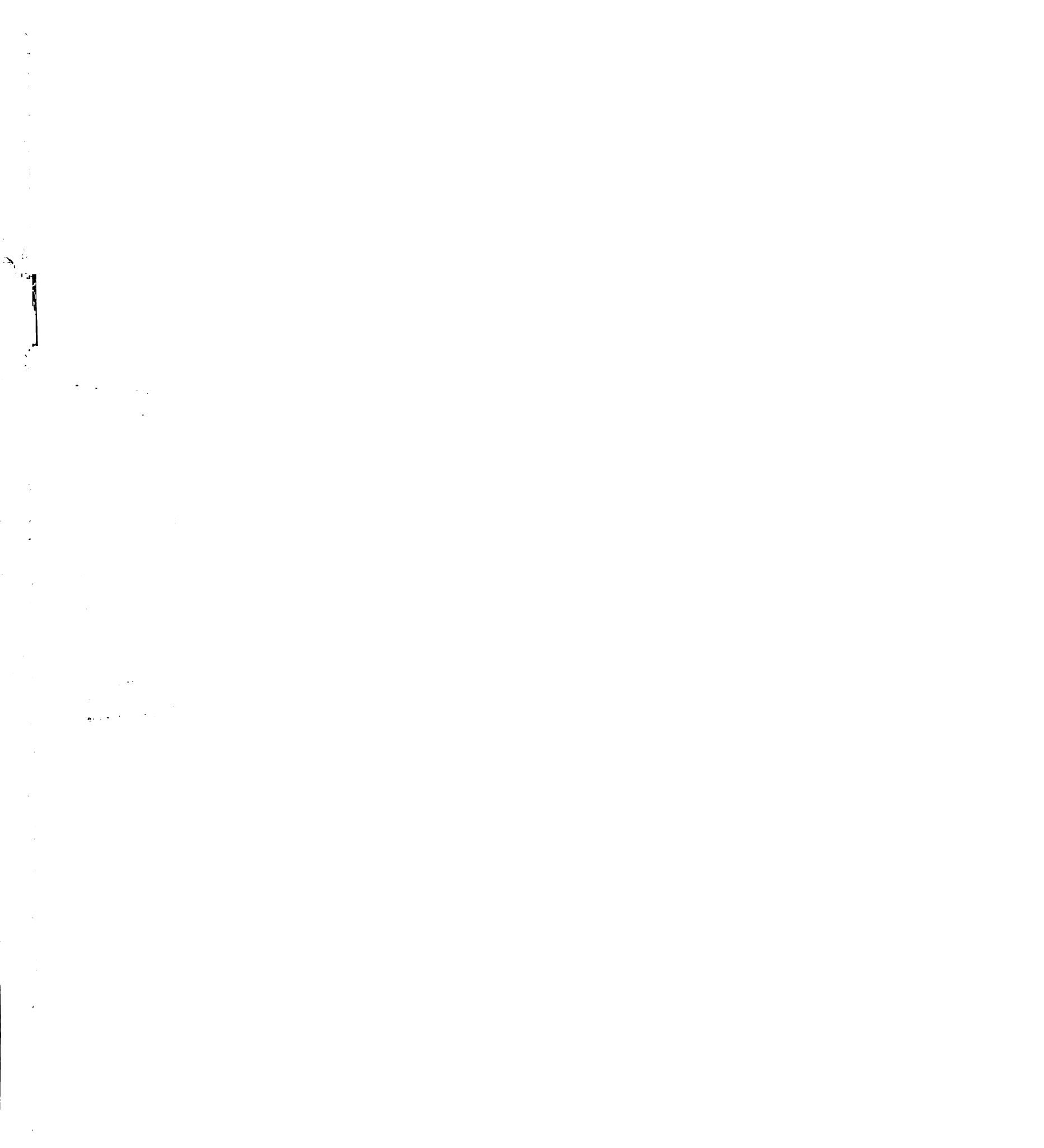
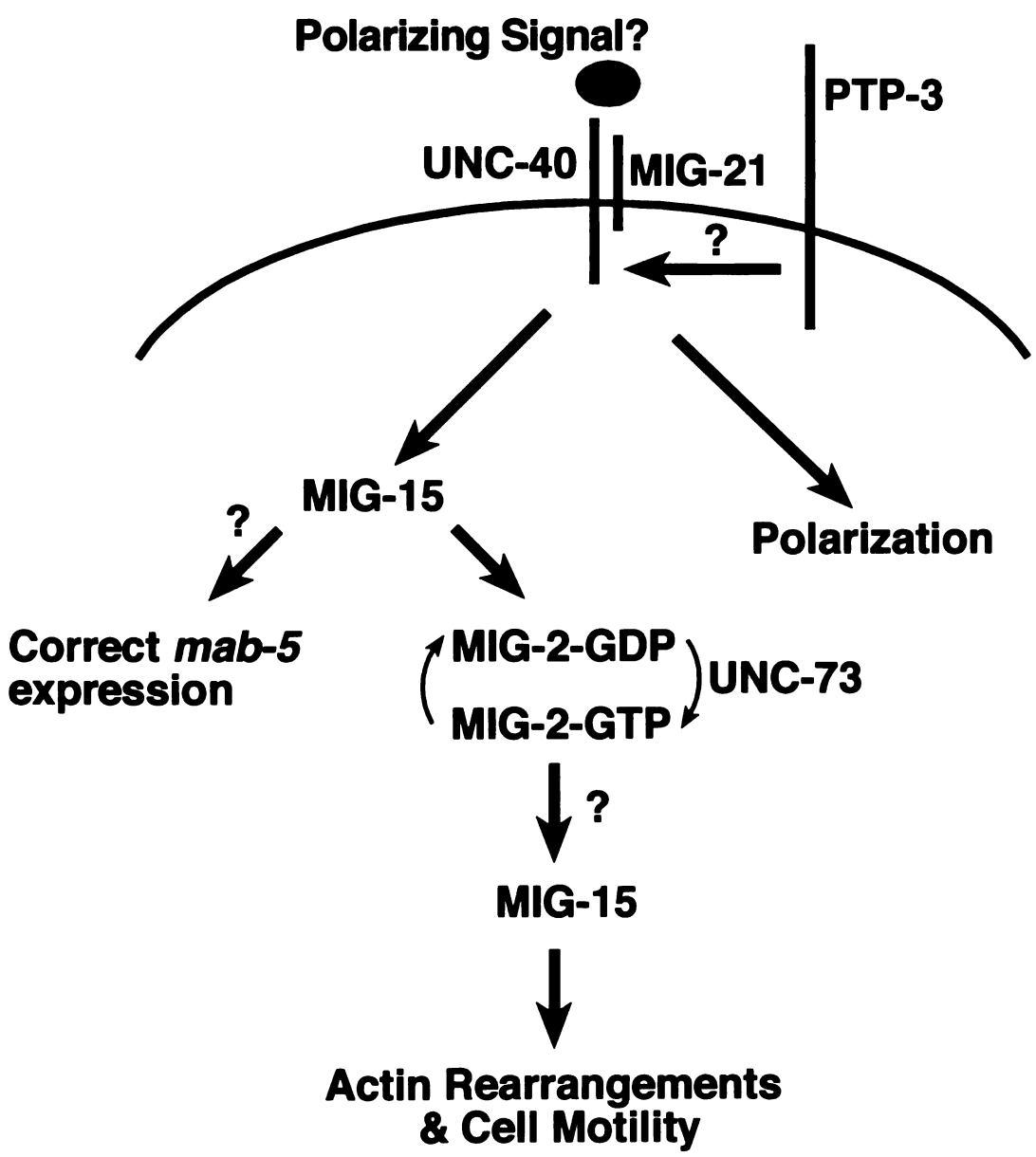


Figure 3-10. A model for the signal transduction pathway that controls Q neuroblast migration.

In this model, UNC-40 and MIG-21 act as co-receptors for the polarizing signal. PTP-3 may modulate the activity of UNC-40 and/or MIG-21. The signal is transduced downstream to the cell motility factors MIG-15, MIG-2 and UNC-73. MIG-15 is also required for *mab-5* expression in QL.

at controls Q
polarizing signal
The signal is
MIG-2 and UNC-73



REFERENCES

- Baker, M. W. and Macagno, E.** (2000). The Role of a LAR-like Receptor Tyrosine Phosphatase in Growth Cone Collapse and Mutual-Avoidance by Sibling Processes. *Journal of Neurobiology* **44**, 194-203.
- Bateman, J., Reddy, R. S., Saito, H. and Van Vactor, D.** (2001). The receptor tyrosine phosphatase Dlar and integrins organize actin filaments in the *Drosophila* follicular epithelium. *Current Biology* **11**, 1317-1327.
- Baum, P. D. and Garriga, G.** (1997). Neuronal Migrations and Axon Fasciculation Are Disrupted in *ina-1* Integrin Mutants. *Neuron* **19**, 51-62.
- Chalfie, M. and Sulston, J.** (1981). Developmental Genetics of the mechanosensory neurons of *Caenorhabditic elegans*. *Developmental Biology* **82**, 358-370.
- Chan, S. S., Zheng, H., Su, M. W., Wilk, R., Killeen, M. T., Hedgecock, E. M. and Culotti, J. G.** (1996). UNC-40, a *C. elegans* homolog of DCC (Deleted in Colorectal Cancer), is required in motile cells responding to UNC-6 netrin cues. *Cell* **87**, 187-95.
- Clandinin, T. R., Lee, C.-H., Herman, T., Lee, R. C., Yang, A. Y., Ovasapyan, S. and Zipursky, S. L.** (2001). *Drosophila* LAR Regulates R1-R6 and R7 Target Specificity in the Visual System. *Neuron* **32**, 237-248.
- Desai, C. J., Gindhart, J. G. J., Goldstein, L. S. B. and Zinn, K.** (1996). Receptor Tyrosine Phosphatases Are Required for Motor Axon Guidance in the *Drosophila* Embryo. *Cell* **84**, 599-609.



- Desai, C. J., Krueger, N. X., Saito, H. and Zinn, K. (1997).** Competition and cooperation among receptor tyrosine phosphatases control motoneuron growth cone guidance in *Drosophila*. *Development* **124**, 1941-1952.
- Du, H. and Chalfie, M. (2001).** Genes Regulating Touch Cell Development in *Caenorhabditis elegans*. *Genetics* **158**, 197-207.
- Frohman, M. A. (1993).** Rapid Amplification of Complementary DNA Ends for Generation of Full-Length Complementary DNAs: Thermal RACE. *Methods in Enzymology* **218**, 340-356.
- Frydman, H. M. and Spradling, A. C. (2001).** The receptor-like tyrosine phosphatase Lar is required for epithelial planar polarity and for axis determination within *Drosophila* ovarian follicles. *Development* **128**, 3209-3220.
- Garrity, P. A., Lee, C.-H., Salecker, I., Robertson, H. C., Desai, C. J., Zinn, K. and Zipursky, S. L. (1999).** Retinal Axon Selection in *Drosophila* Is Regulated by a Receptor Protein Tyrosine Phosphatase. *Neuron* **22**, 707-717.
- Gertler, F. B., Niebuhr, K., Reinhard, M., Wehland, J. and Soriano, P. (1996).** Mena, a Relative of VASP and *Drosophila* Enabled, Is Implicated in the Control of Microfilament Dynamics. *Cell* **87**, 227-239.
- Gu, T., Orita, S. and Han, M. (1998).** *Caenorhabditis elegans* SUR-5, a Novel but Conserved Protein, Negatively Regulates LET-60 Ras Activity during Vulval Induction. *Molecular and Cellular Biology* **18**, 4556-4564.
- Hamelin, M., Zhou, Y., Su, M. W., Scott, I. M. and Culotti, J. G. (1993).** Expression of the UNC-5 guidance receptor in the touch neurons of *C. elegans* steers their axons dorsally. *Nature* **364**, 327-30.
- Harrington, R. J., Gutch, M. J., Hengartner, M. O., Tonks, N. K. and Chisholm, A. D. (2002).** The *C. elegans* LAR-like receptor tyrosine phosphatase PTP-3 and

the CAB-1 Eph receptor tyrosine kinase have partly redundant functions in morphogenesis. *Development* **129**, 2141-2153.

Harris, J., Honigberg, L., Robinson, N. and Kenyon, C. (1996). Neuronal cell migration in *C. elegans*: regulation of Hox gene expression and cell position. *Development* **122**, 3117-31.

Hedgecock, E. M., Culotti, J. G. and Hall, D. H. (1990). The unc-5, unc-6, and unc-40 genes guide circumferential migrations of pioneer axons and mesodermal cells on the epidermis in *C. elegans*. *Neuron* **4**, 61-85.

Hobert, O., Moerman, D. G., Clark, K. A., Beckerle, M. C. and Ruvkun, G. (1999). A Conserved LIM Protein That Affects Muscular Adherens Junction Integrity and Mechanosensory Function in *Caenorhabditis elegans*. *Journal of Cell Biology* **144**, 45-57.

Honigberg, L. and Kenyon, C. (2000). Establishment of left/right asymmetry in neuroblast migration by UNC-40/DCC, UNC-73/Trio and DPY-19 proteins in *C. elegans*. *Development* **127**, 4655-68.

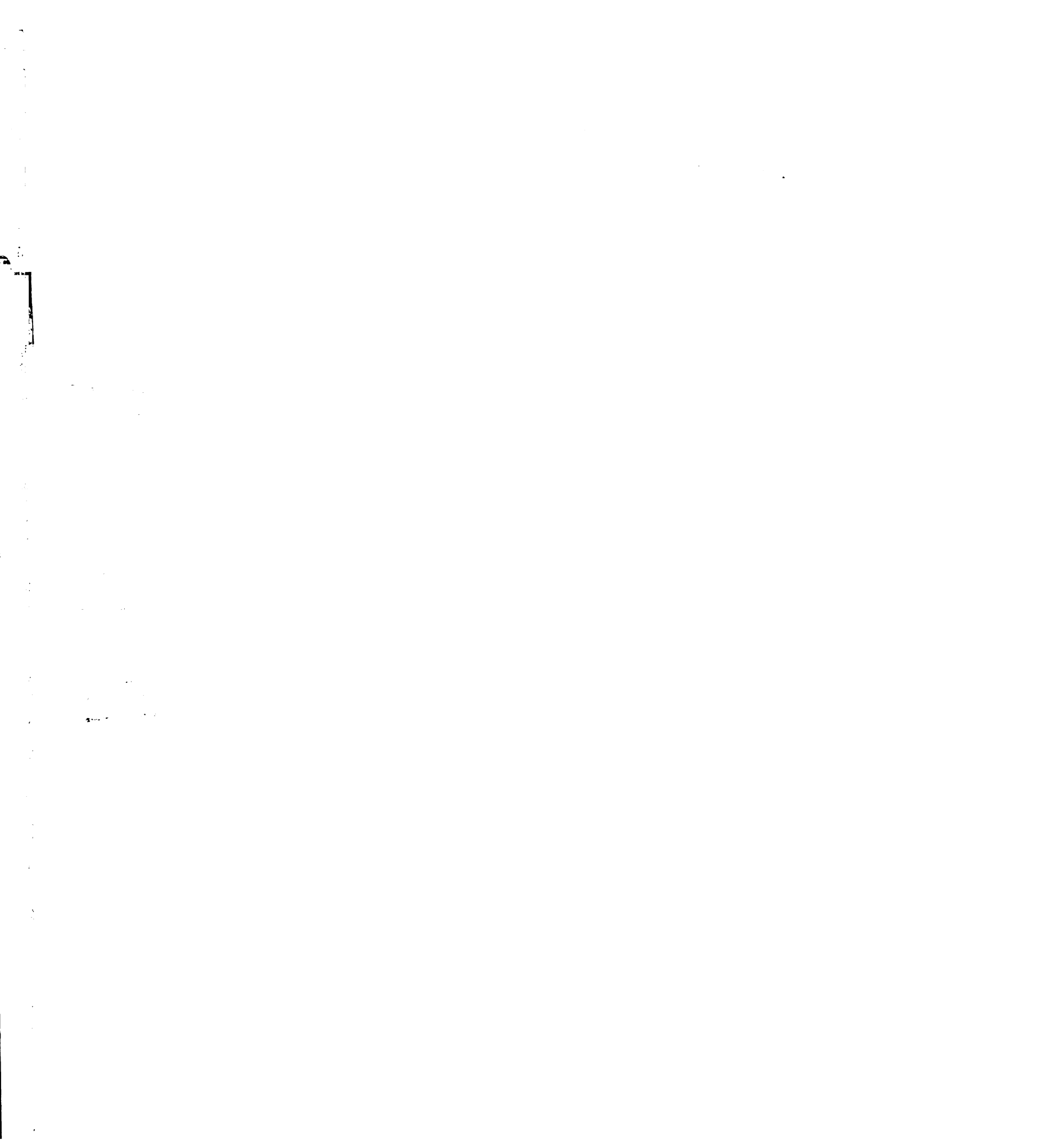
Ishii, N., Wadsworth, W. G., Stern, B. D., Culotti, J. G. and Hedgecock, E. M. (1992). UNC-6, a laminin-related protein, guides cell and pioneer axon migrations in *C. elegans*. *Neuron* **9**, 873-81.

Krueger, N. X., Van Vactor, D., Wan, H. I., Gelbart, W. M., Goodman, C. S. and Saito, H. (1996). The transmembrane tyrosine phosphatase DLAR controls motor axon guidance in *Drosophila*. *Cell* **84**, 611-22.

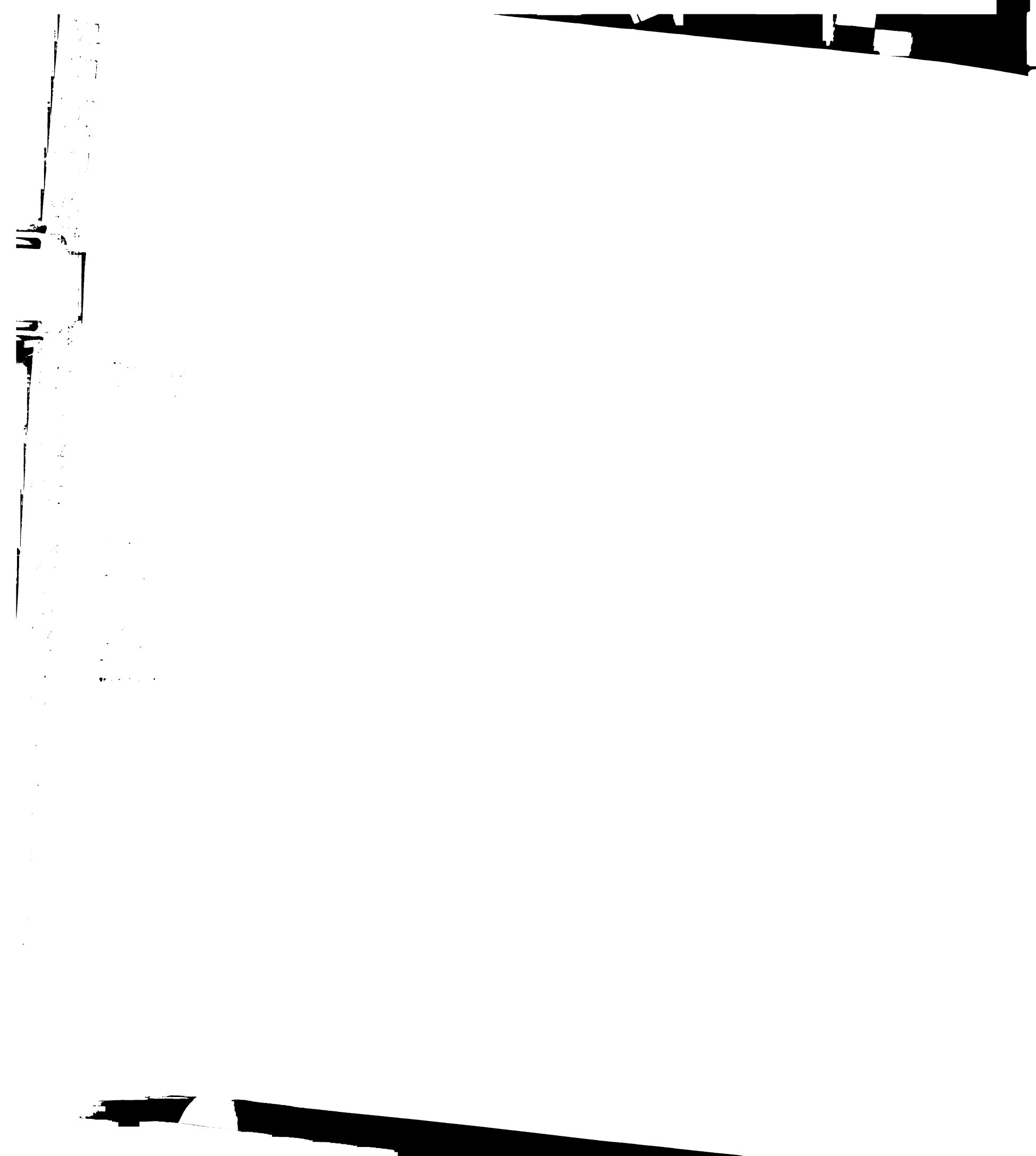
Leung-Hagesteijn, C., Spence, A. M., Stern, B. D., Zhou, Y., Su, M. W., Hedgecock, E. M. and Culotti, J. G. (1992). UNC-5, a transmembrane protein with immunoglobulin and thrombospondin type 1 domains, guides cell and pioneer axon migrations in *C. elegans*. *Cell* **71**, 289-99.



- Maurel-Zaffran, C., Suzuki, T., Gahmon, G., Treisman, J. E. and Dickson, B. J.** (2001). Cell-Autonomous and -Nonautonomous Functions of LAR in R7 Photoreceptor Axon Targeting. *Neuron* **32**, 22-235.
- Merz, D. C., Zheng, H., Killeen, M. T., Krizus, A. and Culotti, J. G.** (2001). Multiple Signaling Mechanisms of the UNC-6/netrin Receptors UNC-5 and UNC-40/DCC *in vivo*. *Genetics* **158**, 1071-1080.
- Poinat, P., De Arcangelis, A., Sookhareea, S., Zhu, X., Hedgecock, E. M., Labouesse, M. and Georges-Labouesse, E.** (2002). A Conserved Interaction between β 1 Integrin/PAT-3 and Nck-Interacting Kinase/MIG-15 that Mediates Commissural Axon Navigation in *C. elegans*. *Current Biology* **12**, 622-631.
- Renfranz, P. J. and Beckerle, M. C.** (2002). Doing (F/L)PPPPs: EVH1 domains and their proline-rich partners in cell polarity and migration. *Current Opinion in Cell Biology* **14**, 88-103.
- Rickert, P., Weiner, O. D., Wang, F., Bourne, H. R. and Servant, G.** (2000). Leukocytes navigate by compass: roles of PI3Kg and its lipid products. *Trends in Cell Biology* **10**, 466-473.
- Salser, S. J. and Kenyon, C.** (1992). Activation of a *C. elegans Antennapedia* homologue in migrating cells controls their direction of migration. *Nature* **355**, 255-8.
- Sulston, J. E. and Horvitz, H. R.** (1977). Post-embryonic cell lineages of the nematode, *Caenorhabditis elegans*. *Dev Biol* **56**, 110-56.
- Sulston, J. E., Schierenberg, E., White, J. G. and Thomson, J. N.** (1983). The embryonic cell lineage of the nematode *Caenorhabditis elegans*. *Dev Biol* **100**, 64-119.



- Sun, Q., Bahri, S., Schmid, A., Chia, W. and Zinn, K. (2000).** Receptor tyrosine phosphatases regulate axon guidance across the midline of the *Drosophila* embryo. *Development* **127**, 801-812.
- Tian, S.-S., Tsoulfas, P. and Zinn, K. (1991).** Three Receptor-Linked Protein-Tyrosine Phosphatases Are Selectively Expressed on Central Nervous System Axons in the *Drosophila* Embryo. *Cell* **67**, 675-685.
- Wadsworth, W. G., Bhatt, H. and Hedgecock, E. M. (1996).** Neuroglia and pioneer neurons express UNC-6 to provide global and local netrin cues for guiding migrations in *C. elegans*. *Neuron* **16**, 35-46.
- Wadsworth, W. G. and Hedgecock, E. M. (1996).** Hierarchical guidance cues in the developing nervous system of *C. elegans*. *BioEssays* **18**, 355-62.
- Wang, F., Herzmark, P., Weiner, O. D., Srinivasan, S., Servant, G. and Bourne, H. R. (2002).** Lipid products of PI(3)Ks maintain persistent cell polarity and directed motility in neutrophils. *Nature Cell Biology* **4**, 513-518.
- Weiner, O. D., Neilsen, P. O., Prestwich, G. D., Kirschner, M. W., Cantley, L. C. and Bourne, H. R. (2002).** A PtdInsP3- and Rho GTPase-mediated positive feedback loop regulates neutrophil polarity. *Nature Cell Biology* **4**, 509-512.
- Williams, B. D., Schrank, B., Huynh, C., Shownkeen, R. and Waterston, R. H. (1992).** A genetic mapping system in *Caenorhabditis elegans* based on polymorphic sequence-tagged sites. *Genetics* **131**, 609-24.
- Wills, Z., Bateman, J., Korey, C. A., Comer, A. and Van Vactor, D. (1999).** The Tyrosine Kinase Abl and Its Substrate Enabled Collaborate with the Receptor Phosphatase Dlar to Control Motor Axon Guidance. *Neuron* **22**, 301-312.
- Yang, X., Seow, K. T., Bahri, S. M., Oon, S. H. and Chia, W. (1991).** Two *Drosophila* Receptor-like Tyrosine Phosphatase Genes Are Expressed in a Subset



of Developing Axons and Pioneer Neurons in the Embryonic CNS. *Cell* **67**, 661-673.

Zhu, X. (1998). MIG-15, a NIK Ortholog of the STE-20 Family of Serine/Threonine Kinases, is Involved in Cell Migration and Cell Signaling in *C. elegans*, (ed., pp. 180. Baltimore: The Johns Hopkins University).



Chapter Four: Future Directions

OVERVIEW

This thesis presents the results of investigations into mutants in the left-right asymmetric migrations of the Q neuroblasts. This work included the following: the mapping and characterization of a set of mutants isolated in an extensive mutagenesis screen for genes involved in the migrations of the Q descendants; the characterization of two of these isolated genes, *mig-21* and *ptp-3*; and the cloning of *mig-21*. The characterization of the Q migration phenotype of the candidate gene, *mig-15*, is also presented here. The Q descendant migration phenotype of *mig-15* has been described previously (Zhu, 1998). The Q neuroblasts provide an opportunity to study many aspects of cell biology, from cell polarization to cell migration to left-right asymmetry to the control of Hox gene expression. The focus of this study was to elucidate further the mechanism by which the Q cells polarize and migrate.

The construction of a bright GFP marker expressed specifically in only six neurons in the nematode, two of which are Q descendants, allowed the rapid identification of mutants with defects in the final positions of the Q.pax cells. These mutants were presumed to have defects in the migrations of the cells. The mutants were classified according to the type of migration defect present – QL.pax misplaced, QR.pax misplaced, or both QL.pax and QR.pax misplaced. The class of mutants with defects in the migrations of the QL.pax cells was presented in Chapter 2. These mutants are principally involved in the activation

of *mab-5* in QL, since all but one also have defects in *mab-5* expression, which are responsible for the resultant QL.pax migration defects.

The class of mutants with defects in the migrations of the cells on both the left and right sides were candidates for mutants in which the earliest asymmetry of the Q cells is disrupted. Two of these mutants, *mig-21* and *ptp-3*, were characterized and found to have generally randomized phenotypes in the Q lineage: the asymmetry of the polarizations, migrations and *mab-5* expression were all disrupted in *mig-21* and *ptp-3* mutants. Double mutant analysis provided evidence that *mig-21* may act in parallel with *ptp-3* and the netrin receptor *unc-40* in directing the asymmetry of the Q cells. *mig-21* and *ptp-3* act upstream of *mab-5* in the control of Q migration, since removing *mab-5* activity prevents any of the cells from remaining in the posterior, on both left and right sides of the animal. *mig-21* was found to encode a novel transmembrane protein expressed specifically in the migrating Q cells. Therefore, MIG-21, perhaps along with UNC-40, could be a receptor for an unidentified external signal which directs the polarizations and migrations of the Q cells. *ptp-3*, a LAR-like receptor protein tyrosine phosphatase, is also required for the early asymmetry, acting in parallel with *mig-21* and perhaps *unc-40*.

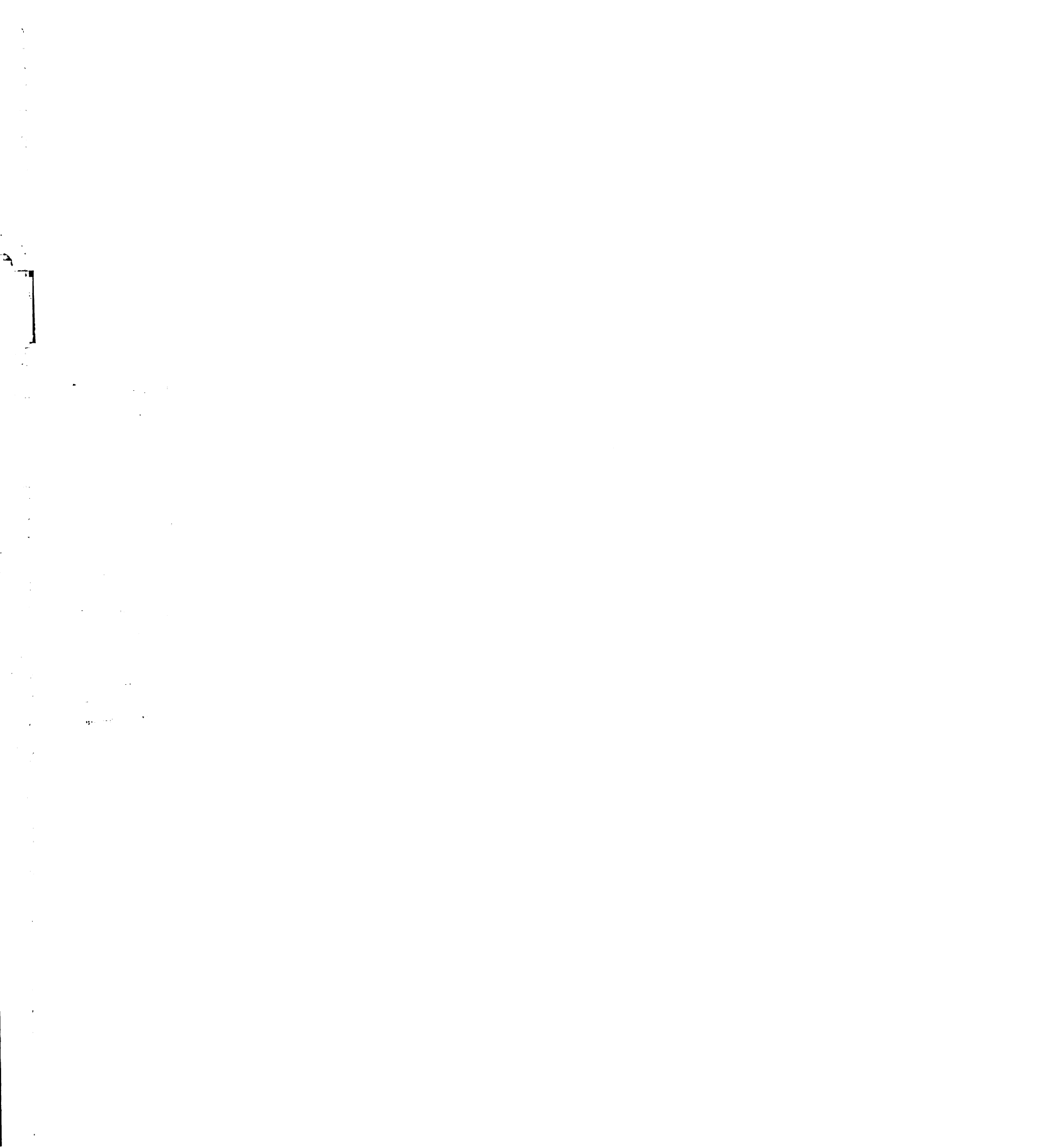
mig-15 was identified as a candidate for the initial Q migrations since mutations in the gene displayed a migration defect on both sides of the animal. Characterization of *mig-15* mutants revealed that MIG-15 is required for the motility of the Q cells, but not for the early asymmetry. MIG-15 may function with the integrins INA-1 and PAT-3, the small GTPase MIG-2, and its activator, UNC-73, in the regulation of actin cytoskeletal dynamics and cell adhesion in order to allow the Q cells to move.

FUTURE DIRECTIONS

What and where is the Q polarization signal?

As a pathway controlling Q neuroblast migration is beginning to emerge, many fascinating questions have been raised. First and foremost, the polarizing signal remain elusive. This signal will hopefully be the key to determining exactly where the left-right asymmetry lies. Is it in the signal itself, or in the response of the Q cells to a symmetric signal? Anatomically, *C. elegans* is largely left-right symmetric. There are a few left-right asymmetries: the gonad arms; intestine; the position of the migratory M cell in the early larva; the positions of the coelomocytes; and the paths of the circumferentially directed motoneuron axons all display a left-right asymmetry (Wood, 1997). The M cell is dispensable for the asymmetry of Q cell migration (J. Austin, L. Honigberg, and C. Kenyon, unpublished data), and so is not a candidate for the source of an asymmetric signal. Attempts to ablate commissural axon precursors in the embryo have not been successful (L. Yang, personal communication), thus the possibility that these axons provide a polarizing signal remains. Specifically, the DA6 motoneuron sends an axon which passes close to QL, and the DB6 motoneuron sends out an axon close to QR (Chalfie and White, 1988; Sulston et al., 1988), providing a tantalizing clue that these projections may contain a Q migration signal. MIG-13, a transmembrane protein required for the anterior migrations of QR, is localized in commissural axons, demonstrating that the Q cells can respond to cues expressed in these cells.

The *mec-7::GFP* screen was not saturated, as indicated by the fact that many known Q migration genes were not isolated in the screen, and many of the genes described are represented by a single allele. A larger screen, including clonal screens to identify essential genes, and F3 screens to identify maternally rescued genes, may identify further factors required for the early asymmetry of the Q cells, including the presumptive signal. The screen was successful in identifying a number of previously unknown genes with roles in Q migration, thus a more thorough screen may well yield more factors. Another approach for finding the polarization signal is a direct biochemical approach. Either UNC-40 and/or MIG-21 acts as the receptor for this signal, therefore, a direct search for proteins which interact with their extracellular domains may yield the putative signal. A yeast two hybrid system, in which the extracellular domains of MIG-21 and UNC-40 act as the bait, or a GST pull-down experiment followed by mass-spectrometric analysis of interacting partners, are straightforward experiments which may identify potential ligands for MIG-21 and UNC-40. The *in vivo* significance of any potential binding partner can be assayed by RNAi of the corresponding gene. Analysis of the endogenous expression pattern could well be informative in this regard, and would also provide information about the left-right asymmetry in Q cell migration. If the signal is left-right symmetrically localized, presumably the Q cells respond asymmetrically, with one cell being attracted and one cell being repelled. To date, all mutations that affect the early asymmetry of the cells affect both left and right sides, suggesting that a common signal response pathway is used by both cells. However, since no signal has been identified, one formal possibility is that the two cells are each responding to one



of two different signals. This latter model could also be supported or discarded by experiments designed to isolate an UNC-40 and/or MIG-21 ligand(s).

The netrin UNC-6 is required for almost all UNC-40 signaling functions. However, there are a few UNC-6-independent UNC-40 functions: the migrations of the Q neuroblasts do not require *unc-6*, and mutations in *unc-40*, but not *unc-6*, suppress SLT-1 gain-of-function defects in AVM guidance and *sax-3* loss-of-function defects in the nerve ring (Honigberg and Kenyon, 2000; Yu et al., 2002). Why do the Q cells not respond to the ventral source of UNC-6? Are the cells physically too far removed from the guidance cue? It would be interesting to test whether misexpression of UNC-6, either dorsally or laterally, could induce the Q cells to respond inappropriately. If the cells cannot be induced to polarize or migrate towards (or away from) UNC-6, the further question would be raised: what is masking that response? Since the Q cells express UNC-40, it is conceivable that they should be able to respond to UNC-6. Perhaps some component of the Q migration pathway blocks the ability of the Q cells to respond to the UNC-6 cue, allowing the cells to respond instead to another polarizing signal. Alternatively, perhaps the Q cells may simply lack some critical component of the UNC-6 downstream response pathway, rendering them insensitive to UNC-6 signaling.

How do MIG-21 and UNC-40 interact?

mig-21 and *unc-40* show a modest genetic interaction: there is a distinct anterior shift in the positions of the QL.pax and QR.pax cells that is more pronounced in the double mutant than that seen in either of the single mutants.

1

2
3
4
5
6
7
8
9
10
11
12
13
14
15
16
17
18
19
20
21
22
23
24
25
26
27
28
29
30
31
32
33
34
35
36
37
38
39
40
41
42
43
44
45
46
47
48
49
50
51
52
53
54
55
56
57
58
59
60
61
62
63
64
65
66
67
68
69
70
71
72
73
74
75
76
77
78
79
80
81
82
83
84
85
86
87
88
89
90
91
92
93
94
95
96
97
98
99
100

How do these two receptors transduce the polarizing signal? Does UNC-40 function cell-autonomously for Q cell migration? This question can be answered by mosaic analysis to demonstrate where *unc-40* is required, or by using tissue-specific promoters to drive *unc-40* expression in the Q cells. The *egl-17::GFP* is expressed in the Q cells during their early migrations (Branda and Stern, 2000), although attempts to obtain rescue by driving gene expression under the *egl-17* promoter for genes presumed to act cell-autonomously have not been successful (L. Yang, personal communication). This suggests that *egl-17* may not be switched on sufficiently early for it to be useful in these experiments. Another promising promoter is the *scm* promoter, which is expressed in the lateral seam cells along the hypodermis during embryonic and larval development (S. Alper and J. Kasmir, personal communication). A drawback to using this promoter is that it also drives expression in the seam cells adjacent to the Q cells, thus rendering any positive rescue results somewhat ambiguous. Although *unc-40* is not normally expressed in the seam cells (Chan et al., 1996), ectopic expression in these cells could conceivably influence Q cell migration if *unc-40* is capable of acting cell-non-autonomously.

Do MIG-21 and UNC-40 function as receptor and co-receptor, by analogy with UNC-5 and UNC-40? The cytoplasmic domain of UNC-5 is sufficient to convert netrin-mediated attraction into repulsion in *Xenopus* spinal axons (Hong et al., 1999). The cytoplasmic domains of UNC-5 and UNC-40 interact directly *in vitro*, but this interaction is repressed in the full-length proteins (Hong et al., 1999). It is possible that MIG-21 and UNC-40 heterodimerize upon ligand binding, in which case it may be difficult to detect a direct interaction without knowing the identity of the ligand. Alternatively, the receptors may exist

endogenously as a heterodimer, and be activated upon ligand binding. The direct interaction of the two cytoplasmic domains, or of the two extracellular domains, could be determined by co-IP experiments. A yeast two hybrid experiment using one or other of the cytoplasmic domains may yield the other protein if there is a physical interaction. The MIG-21 cytoplasmic domain is relatively small, and contains no known signaling or binding motifs, suggesting that the role of MIG-21 may be in ligand binding rather than signal transduction. If this is the case, the MIG-21 cytoplasmic domain may be dispensable for Q migration. Injection of truncated constructs into mutant backgrounds may begin to address this question. For example, injection of the MIG-21 cytoplasmic domain into *mig-21* mutants may partially rescue the Q migration defect.

The enhancement of the Q phenotype observed in the *unc-40; mig-21* double mutant also suggests that either receptor may retain some signaling function in the absence of the other. If this is the case, overexpression of *unc-40* may partially rescue *mig-21* defects and *vice versa*. Another pertinent observation is that the double mutant phenotype results in virtually all cells migrating to the anterior. This suggests that there may be a default pathway for anterior Q migration in the absence of the signaling system. This "default" pathway is presumably a result of a complete failure to switch on *mab-5* in the double mutant. The link between early Q cell asymmetry and *mab-5* activation is still somewhat unclear. All known mutations that disrupt early asymmetry also disrupt *mab-5* expression, suggesting that the appropriate expression of *mab-5* in QL is dependent upon the correct Q cell polarization and migration.

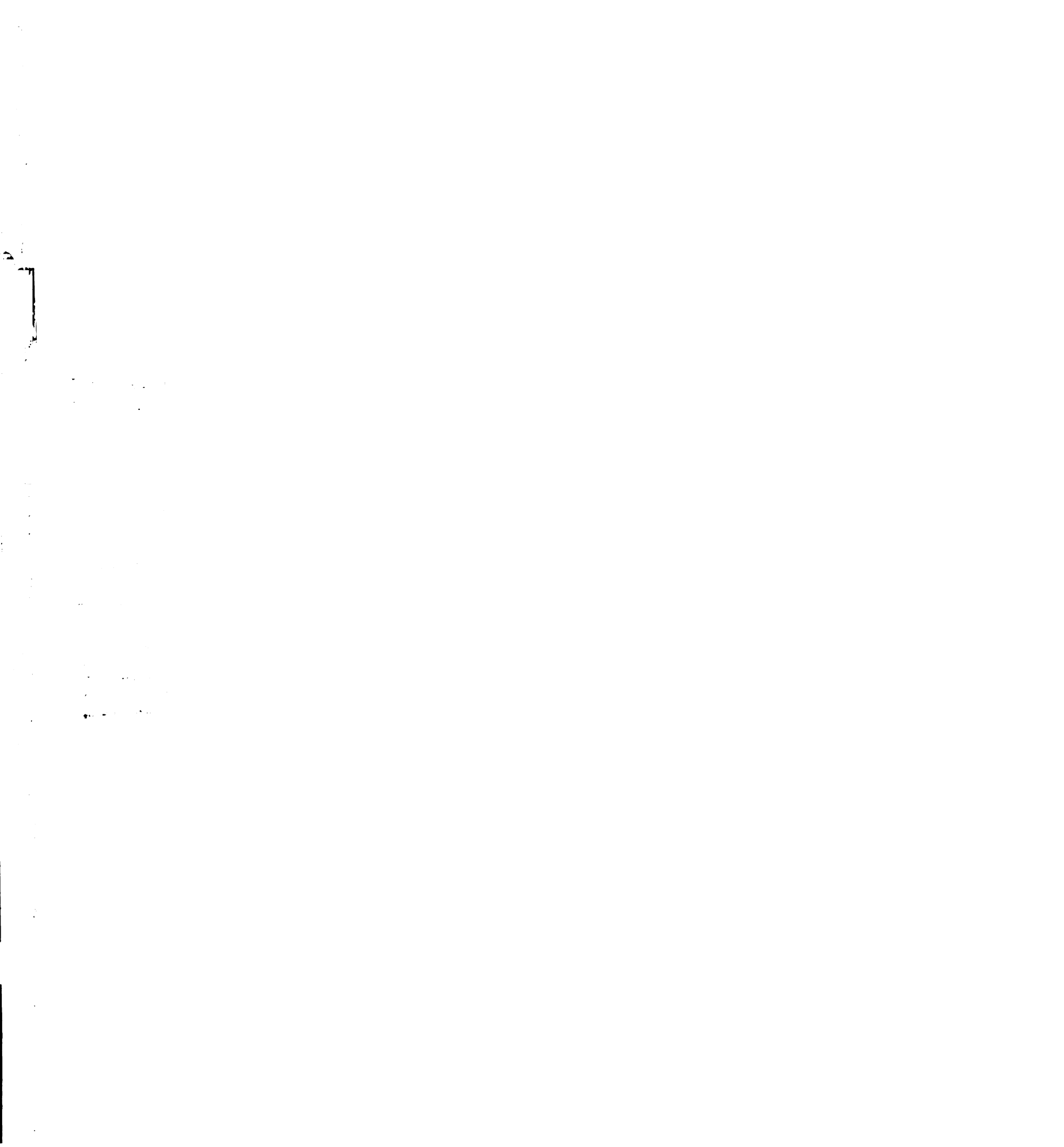
The role of PTP-3 in guiding the Q cells

The role of kinases and phosphatases in signal transduction has been well described. LAR-like receptor tyrosine phosphatases have a variety of roles in cellular processes ranging from axon guidance to embryonic morphogenesis, and can act cell-autonomously or cell-nonautonomously (Bateman et al., 2001; Desai et al., 1996; Desai et al., 1997; Frydman and Spradling, 2001; Garrity et al., 1999; Harrington et al., 2002; Krueger et al., 1996; Wills et al., 1999). Several models can therefore be envisaged for the role of *ptp-3* in Q cell migration, depending on its mode of action. Simply determining where *ptp-3* functions in the context of Q cell migration would therefore further our understanding of its role in the signal transduction pathway. Mosaic analysis of *ptp-3* mutants is not trivial, due to the relatively low penetrance of the Q migration phenotype. Mosaics in which the Q cells are mutant would always be informative, yielding information about where *ptp-3* does *not* function, however, mosaics in which the Q cells are in their wild-type positions would only be informative if many animals of that mosaic class could be isolated. While this is possible, it is not practical, and other approaches to determining the site of action of *ptp-3* are recommended. Tissue-specific promoter fusions, as described above using the *egl-17* and/or *scm* promoters, may generate meaningful results. *ptp-3* is expressed in the Q cells and also in the adjacent seam cells (data not shown), so the question of autonomy may not be resolved with the *scm* promoter.

If *ptp-3* is acting cell-autonomously, which appears to be the most parsimonious model, what are its direct downstream targets? UNC-40 and MIG-21 both contain intracellular tyrosine residues, indicating that either of the

receptors may be PTP-3 targets. This could be resolved by a simple *in vitro* dephosphorylation assay (Wills et al., 1999). What is the effect of dephosphorylation of the PTP-3 targets? Previous work suggests that the principle role of PTP-3 may be to regulate cellular adhesion, and Dlar, the *Drosophila* ortholog of *ptp-3*, binds directly to the Abl kinase and the actin regulator Ena (Wills et al., 1999). The *C. elegans* homolog of Ena is *unc-34* (M. Dell and G. Garriga, personal communication, and while *unc-34* has a modest posterior shift in the QR.pax cells, the Q phenotype is not suggestive of a role of *unc-34* in the early asymmetry of the Q cells (data not shown and M. Sym and C. Kenyon, unpublished data). Thus, the downstream effectors linking *ptp-3* to the actin cytoskeleton are still waiting to be discovered.

The genetic interaction observed between *ptp-3* and *mig-21* is compelling. The final positions of the Q.pax cells appear to be completely randomized, a phenotype not previously observed in any other left-right asymmetry mutant. Does this represent a complete loss of signaling function early in Q cell polarization? It would be revealing to examine the phenotype of *unc-40; ptp-3* double mutants, and *unc-40; ptp-3; mig-21* triple mutants. However, there appears to be a synthetic lethal interaction between *unc-40* and *ptp-3*, making the direct construction of the double mutant impossible. While it may be possible to build a balanced strain, the lethality appears to occur during embryogenesis or early larval development – before the Q cells have completed their migrations (data not shown). An alternative method of investigating the phenotype of the double mutant is RNA-mediated interference (RNAi). RNAi can be used to significantly reduce gene function, and RNAi-induced phenotypes often phenocopy those of loss-of-function mutants (Kamath et al., 2000; Timmons et al., 2001). However,

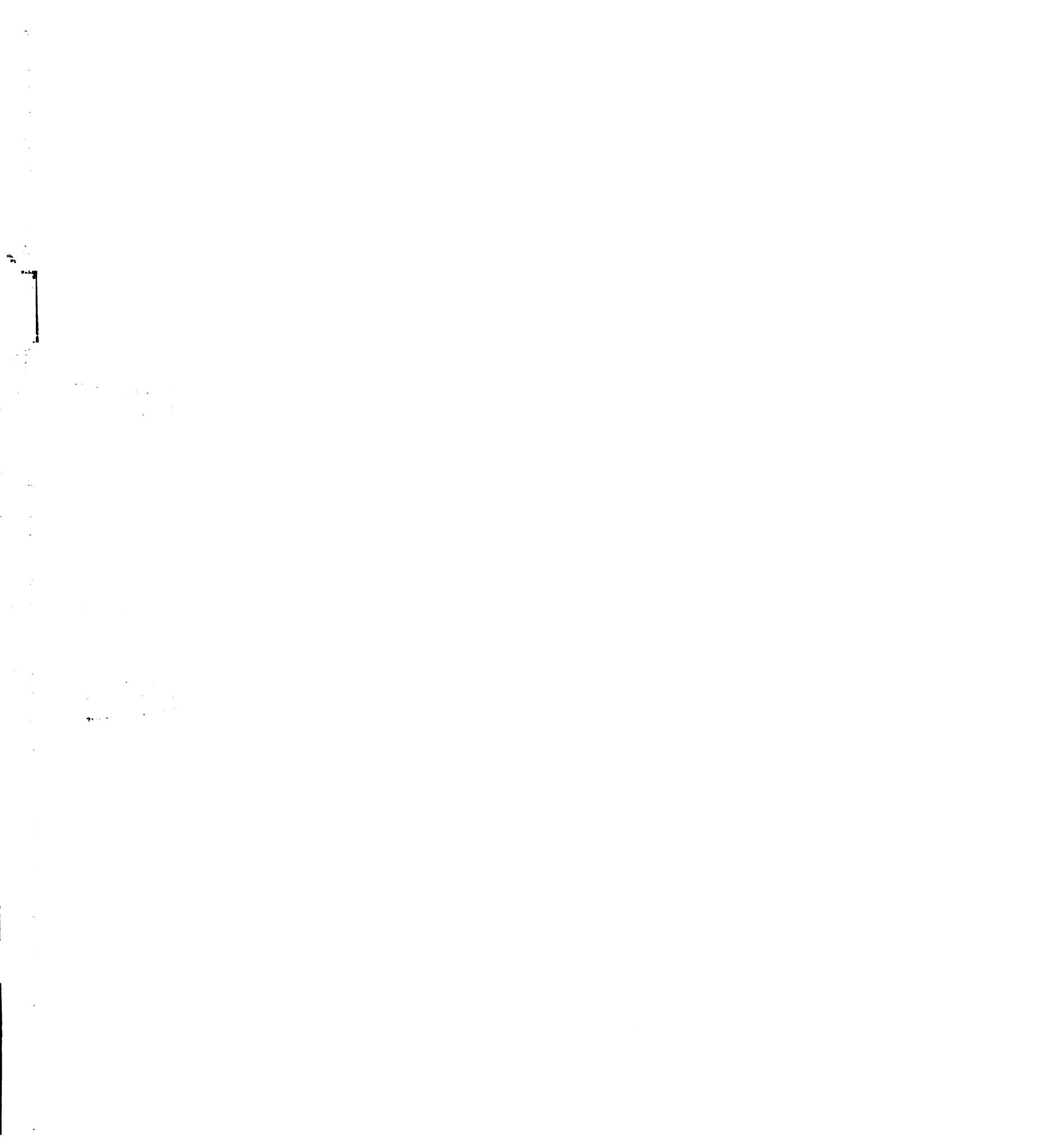


this method has proved somewhat troublesome for neuronal phenotypes, and RNAi-induced Q migration phenotypes are invariably weaker than mutant phenotypes for the corresponding gene. Nonetheless, RNAi of *unc-40* in a *ptp-3(mu256); rrf-3(pk1426)* mutant background may be informative. *rrf-3* is a mutation that renders neurons more sensitive to the effects of RNAi. Similarly, RNAi of *unc-40* in a *ptp-3(mu256); mig-21(mu238); rrf-3(pk1426)* mutant background may provide a clue to the phenotype of the *unc-40; ptp-3; mig-21* triple mutant.

***mig-15*, cellular motility and the control of *mab-5* expression**

mig-15 was identified by a candidate gene approach, and was discovered to have a defect in the motility of the Q cells, whereas the polarizations are unaffected, both in direction and extent. The principle function of *mig-15* appears to be in regulating cellular adhesion, thereby controlling cellular motility. This is achieved by interaction with, and presumably signaling through, the integrins *ina-1* and *pat-3*.

One important question that remains unanswered is whether *mab-5* is ectopically expressed in QR in *mig-15* mutants. This could be tested by *mab-5::lacZ* staining using the available *muIs3* construct. Results to date suggest that the principle Q migration defect, apart from motility, is in the incompletely penetrant failure of QL to express *mab-5*, but it is also possible that *mab-5* expression is partially randomized in *mig-15* mutants. The pattern of *mig-15* expression is unchanged in *unc-40* and *mig-5* mutant backgrounds (Zhu, 1998), suggesting that the *mig-15* functions independently of *unc-40* and *mig-5*. It may



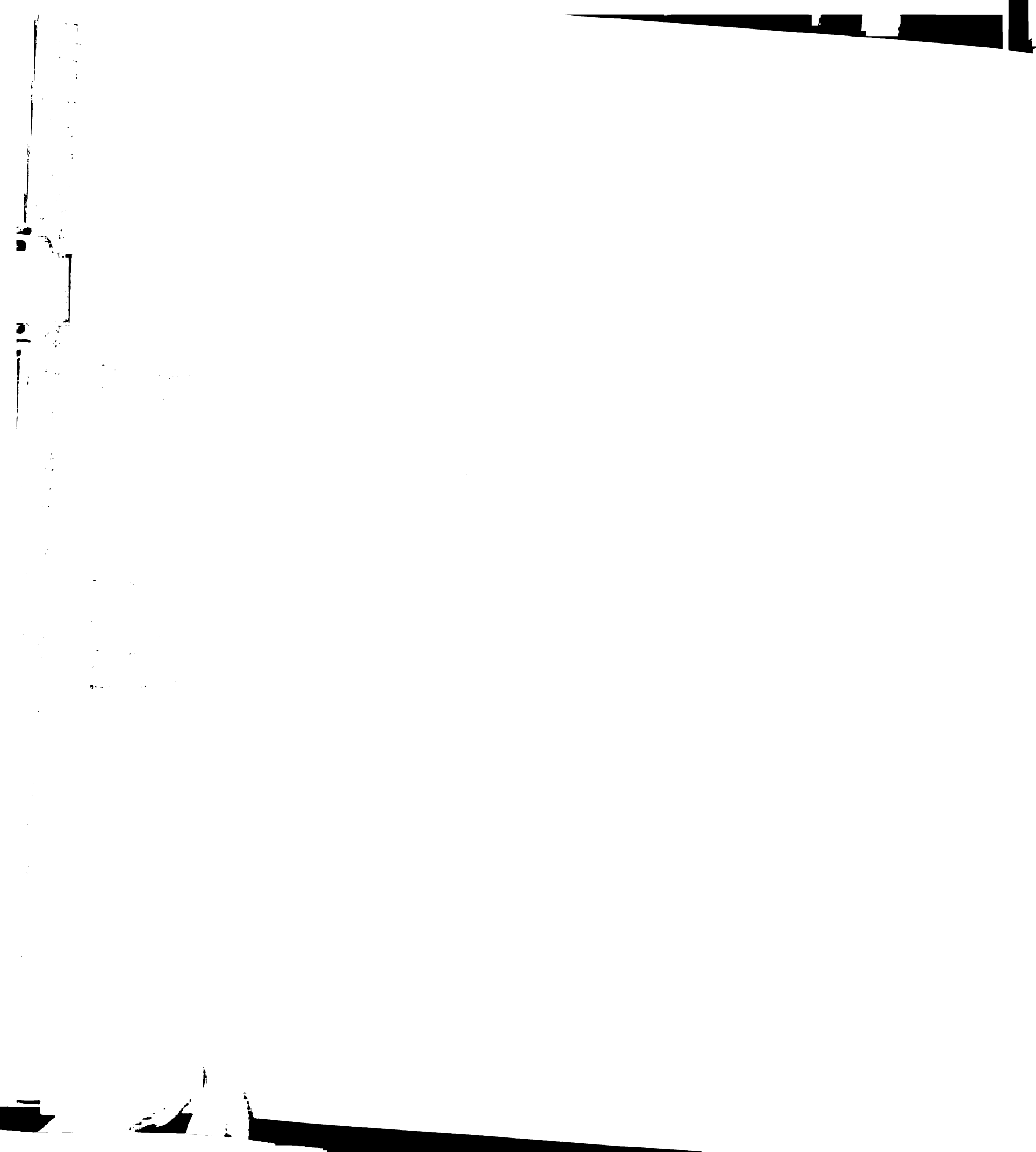
be informative to check the expression and localization of *mig-15* in a *mig-21* mutant background to determine whether *mig-21* influences the targeting of *mig-15* to focal adhesions during Q cell migration. A strong possibility is that *mig-15* activity is regulated by the binding of a small GTPase. *mig-15* interacts genetically with *mig-2*, *ced-10* and *rac-2*, and STE20/NIK family kinases are known to be regulated by binding to small GTPases. Therefore, MIG-15 may be activated by the binding of one of the small GTPases to its regulatory domain. An *in vitro* assay to test the ability of the MIG-15 regulatory domain to bind to MIG-2, CED-10, or RAC-2 may begin to test this idea. If an interaction is observed, its functional significance may be tested by an *in vitro* phosphorylation assay.

It is not known whether *mig-15* acts upstream or downstream of *ina-1* – overexpression of *mig-15* in an *ina-1* mutant background did not suppress the *ina-1* axon fasciculation phenotype, but rather, it enhanced the phenotype (Poinat et al., 2002). These results are difficult to interpret, since the same overexpression construct introduced in a *mig-15* mutant background does not produce the same effect. Integrins can regulate, and be regulated by, small GTPases (Schwartz and Shattil, 2000). For example, PAK activity is activated by the binding of fibroblasts to fibronectin, via activation of Cdc42, and Rac is activated by cell adhesion (Schwartz and Shattil, 2000). There are therefore several possible models for the position of *mig-15* in the pathway – it may be acting upstream or downstream of the integrins, and upstream or downstream of the small GTPase(s). If *mig-2* is acting downstream of the integrins – that is, integrins are signaling to the GTPases via *mig-15*, then the subcellular localization of MIG-15 may be dependent on the presence of functional integrins. If this is the case, the

expression pattern and/or localization of MIG-15 may be altered in *ina-1* or *pat-3* mutant backgrounds.

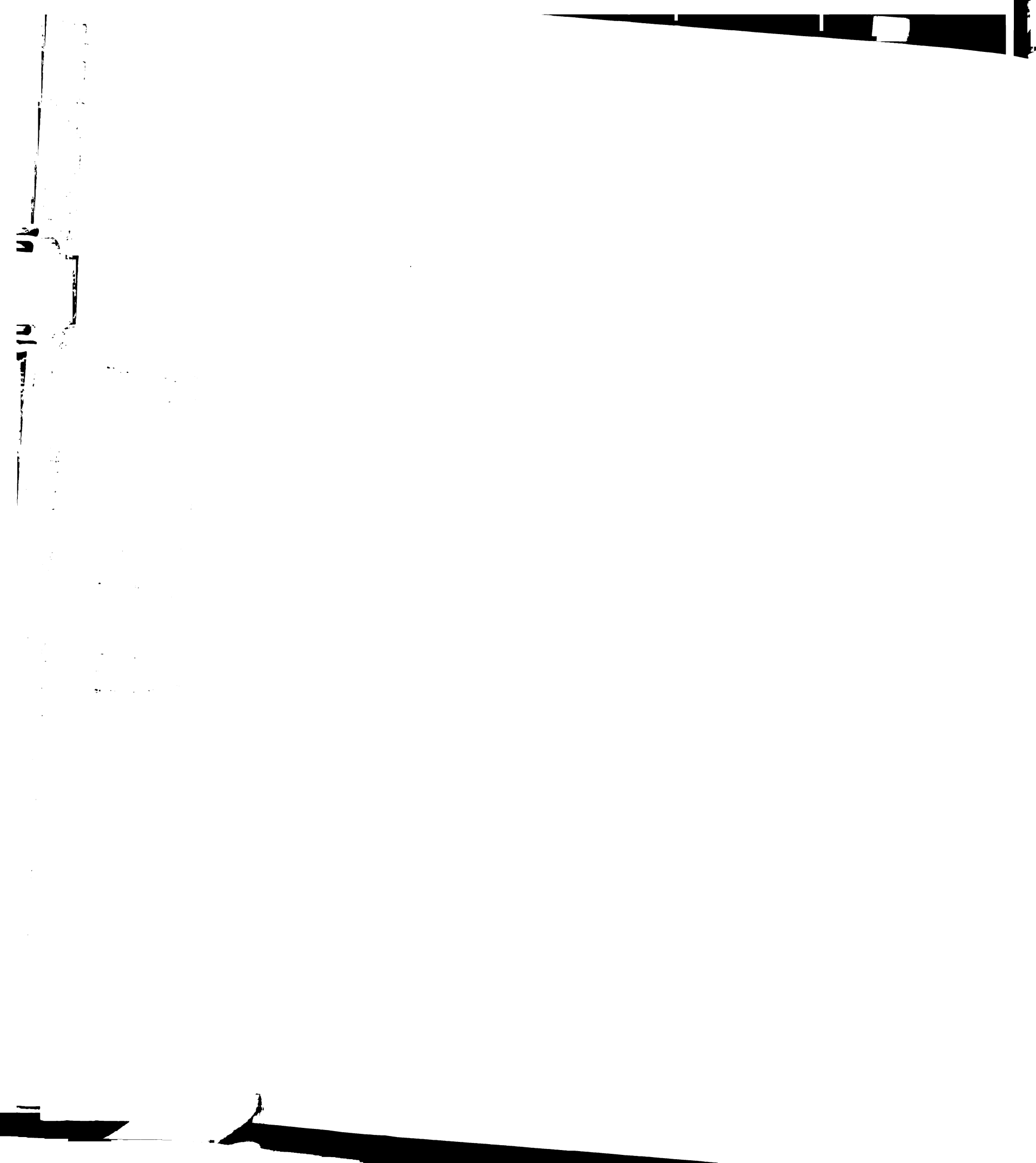
CONCLUDING REMARKS

While many of the molecular details of the signaling pathway guiding the polarizations and migrations of the Q cells remain unknown, this work has revealed a number of key elements of such a pathway. Most notably, the putative signal remains elusive, but candidate receptors, some downstream effectors, and cytoskeletal regulators have been identified. Future experiments as outlined in this chapter would begin to answer the remaining questions, and would shed light on the origins of left-right asymmetry and cell migration in this system.

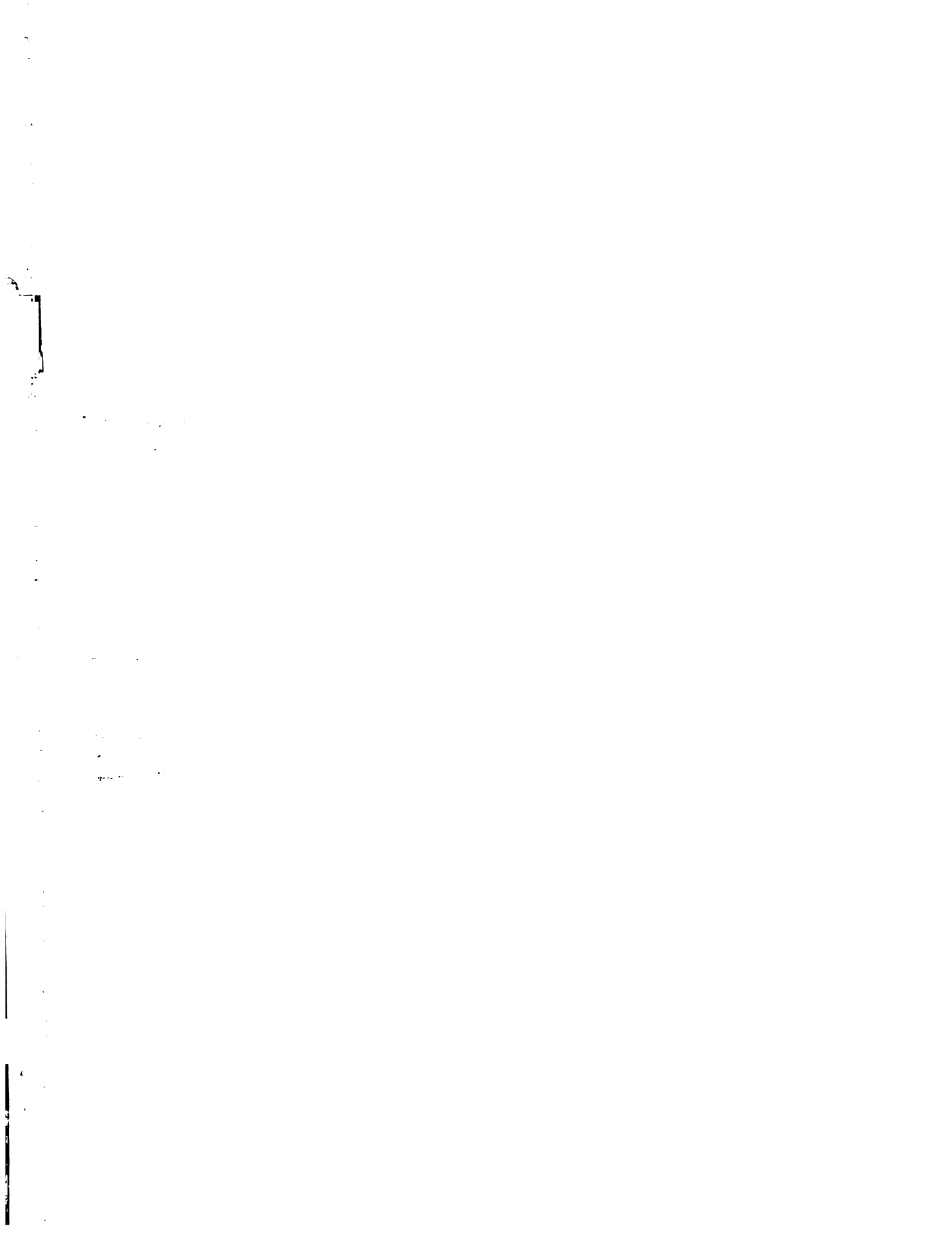


REFERENCES

- Bateman, J., Reddy, R. S., Saito, H. and Van Vactor, D.** (2001). The receptor tyrosine phosphatase Dlar and integrins organize actin filaments in the *Drosophila* follicular epithelium. *Current Biology* **11**, 1317-1327.
- Branda, C. S. and Stern, M. J.** (2000). Mechanisms Controlling Sex Myoblast Migration in *Caenorhabditis elegans* Hermaphrodites. *Developmental Biology* **226**, 137-151.
- Chalfie, M. and White, J.** (1988). The Nervous System. In *The Nematode Caenorhabditis elegans*, (ed. W. B. Wood), pp. 337-391. New York: Cold Spring Harbor Laboratory Press.
- Chan, S. S., Zheng, H., Su, M. W., Wilk, R., Killeen, M. T., Hedgecock, E. M. and Culotti, J. G.** (1996). UNC-40, a *C. elegans* homolog of DCC (Deleted in Colorectal Cancer), is required in motile cells responding to UNC-6 netrin cues. *Cell* **87**, 187-95.
- Desai, C. J., Gindhart, J. G. J., Goldstein, L. S. B. and Zinn, K.** (1996). Receptor Tyrosine Phosphatases Are Required for Motor Axon Guidance in the *Drosophila* Embryo. *Cell* **84**, 599-609.
- Desai, C. J., Krueger, N. X., Saito, H. and Zinn, K.** (1997). Competition and cooperation among receptor tyrosine phosphatases control motoneuron growth cone guidance in *Drosophila*. *Development* **124**, 1941-1952.



- Frydman, H. M. and Spradling, A. C.** (2001). The receptor-like tyrosine phosphatase Lar is required for epithelial planar polarity and for axis determination within *Drosophila* ovarian follicles. *Development* **128**, 3209-3220.
- Garrity, P. A., Lee, C.-H., Salecker, I., Robertson, H. C., Desai, C. J., Zinn, K. and Zipursky, S. L.** (1999). Retinal Axon Selection in *Drosophila* Is Regulated by a Receptor Protein Tyrosine Phosphatase. *Neuron* **22**, 707-717.
- Harrington, R. J., Gutch, M. J., Hengartner, M. O., Tonks, N. K. and Chisholm, A. D.** (2002). The *C. elegans* LAR-like receptor tyrosine phosphatase PTP-3 and the CAB-1 Eph receptor tyrosine kinase have partly redundant functions in morphogenesis. *Development* **129**, 2141-2153.
- Hong, K., Hinck, L., Nishiyama, M., Poo, M. M., Tessier-Lavigne, M. and Stein, E.** (1999). A ligand-gated association between cytoplasmic domains of UNC5 and DCC family receptors converts netrin-induced growth cone attraction to repulsion. *Cell* **97**, 927-41.
- Honigberg, L. and Kenyon, C.** (2000). Establishment of left/right asymmetry in neuroblast migration by UNC-40/DCC, UNC-73/Trio and DPY-19 proteins in *C. elegans*. *Development* **127**, 4655-68.
- Kamath, R. S., Martinez-Campos, M., Zipperlen, P., Fraser, A. G. and Ahringer, J.** (2000). Effectiveness of specific RNA-mediated interference through ingested double-stranded RNA in *Caenorhabditis elegans*. *Genome Biology* **2**, 1-10.
- Krueger, N. X., Van Vactor, D., Wan, H. I., Gelbart, W. M., Goodman, C. S. and Saito, H.** (1996). The transmembrane tyrosine phosphatase DLAR controls motor axon guidance in *Drosophila*. *Cell* **84**, 611-22.
- Poinat, P., De Arcangelis, A., Sookhareea, S., Zhu, X., Hedgecock, E. M., Labouesse, M. and Georges-Labouesse, E.** (2002). A Conserved Interaction



between $\beta 1$ Integrin/PAT-3 and Nck-Interacting Kinase/MIG-15 that Mediates Commissural Axon Navigation in *C. elegans*. *Current Biology* **12**, 622-631.

Schwartz, M. A. and Shattil, S. J. (2000). Signaling networks linking integrins and Rho family GTPases. *Trends in Biological Sciences* **388**, 388-391.

Sulston, J., Horvitz, H. R. and Kimble, J. (1988). Cell Lineage. In *The Nematode Caenorhabditis elegans*, (ed. W. B. Wood), pp. 457-489. New York: Cold Spring Harbor Laboratory Press.

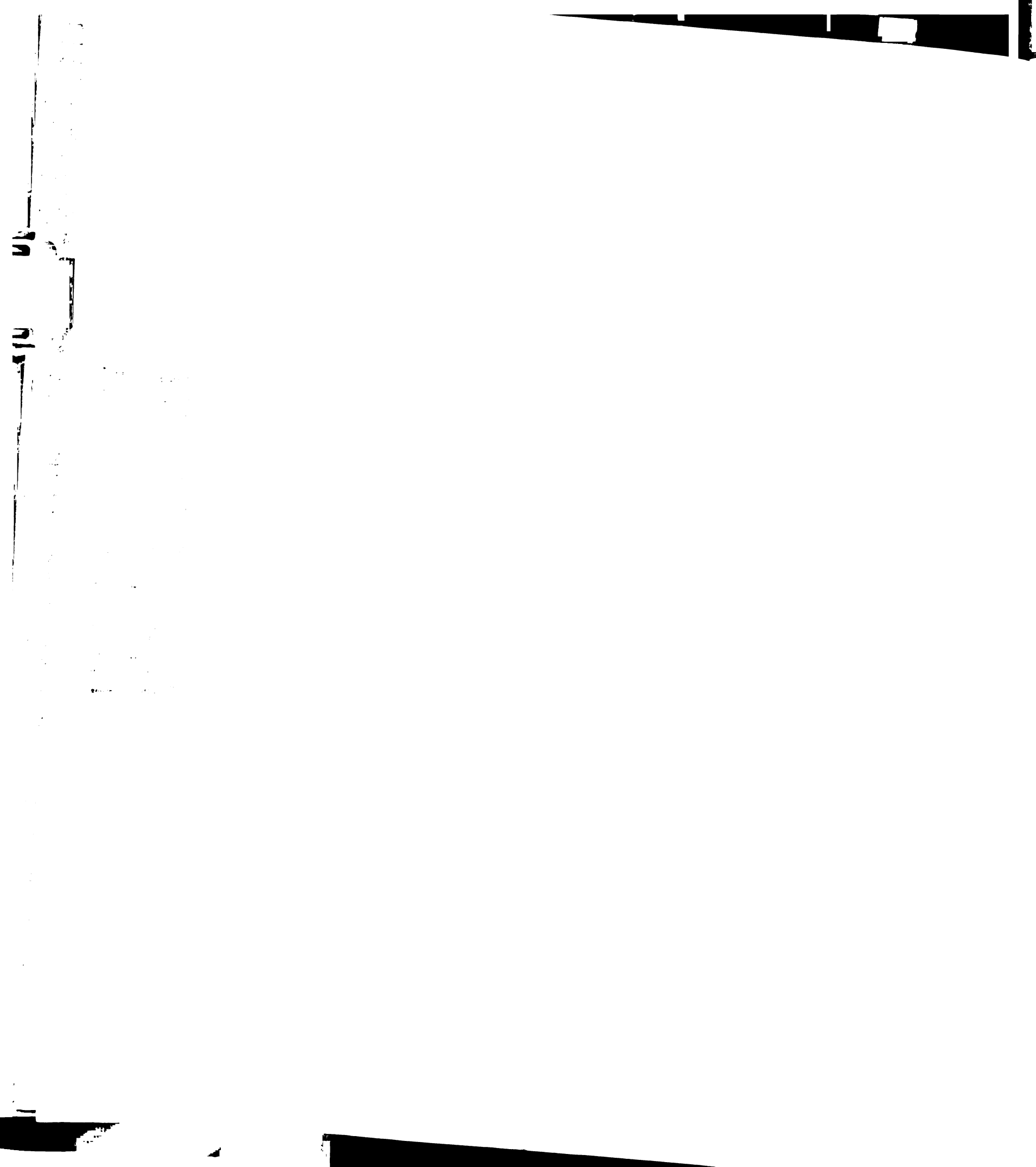
Timmons, L., Court, D. L. and Fire, A. (2001). Ingestion of bacterially expressed dsRNAs can produce specific and potent genetic interference in *Caenorhabditis elegans*. *Gene* **263**, 103-112.

Wills, Z., Bateman, J., Korey, C. A., Comer, A. and Van Vactor, D. (1999). The Tyrosine Kinase Abl and Its Substrate Enabled Collaborate with the Receptor Phosphatase Dlar to Control Motor Axon Guidance. *Neuron* **22**, 301-312.

Wood, W. B. (1997). Left-Right Asymmetry in Animal Development. *Annu. Rev. Cell Dev. Biol.* **13**, 53-82.

Yu, T. W., Hao, J. C., Lim, W., Tessier-Lavigne, M. and Bargmann, C. I. (2002). Shared receptors in axon guidance: SAX-3/Robo signals via UNC-34/Enabled and a Netrin-independent UNC-40/DCC function. *Nature Neuroscience* **5**, 1147-1154.

Zhu, X. (1998). MIG-15, a NIK Ortholog of the STE-20 Family of Serine/Threonine Kinases, is Involved in Cell Migration and Cell Signaling in *C. elegans*, (ed., pp. 180. Baltimore: The Johns Hopkins University).



Not to be taken
from the room.

For reference

7230603



3 1378 00723 0603

